



**Flanders**  
State of  
the Art

15\_068\_13  
FHR reports

# Modelling Belgian Coastal zone and Scheldt mouth area

Sub report 13  
Scaldis-Coast model  
Model setup and validation of the wave propagation model

DEPARTMENT  
**MOBILITY &  
PUBLIC  
WORKS**

[www.flandershydraulicsresearch.be](http://www.flandershydraulicsresearch.be)

# Modelling Belgian Coastal zone and Scheldt mouth area

## Sub report 13: Scaldis-Coast model – Model setup and validation of the wave propagation model

Wang, L.; Kolokythas, G.; Fonias, S.; De Maerschalck, B.; Vanlede, J.; Mostaert, F.

### Legal notice

Flanders Hydraulics Research is of the opinion that the information and positions in this report are substantiated by the available data and knowledge at the time of writing.  
 The positions taken in this report are those of Flanders Hydraulics Research and do not reflect necessarily the opinion of the Government of Flanders or any of its institutions.  
 Flanders Hydraulics Research nor any person or company acting on behalf of Flanders Hydraulics Research is responsible for any loss or damage arising from the use of the information in this report.

### Copyright and citation

© The Government of Flanders, Department of Mobility and Public Works, Flanders Hydraulics Research 2021  
 D/2021/3241/068

This publication should be cited as follows:

**Wang, L.; Kolokythas, G.; Fonias, S.; De Maerschcalck, B.; Vanlede, J.; Mostaert, F.** (2021). Modelling Belgian Coastal zone and Scheldt mouth area: Sub report 13: Scaldis-Coast model – Model setup and validation of the wave propagation model. Version 4.0. FHR Reports, 15\_068\_13. Flanders Hydraulics Research: Antwerp

Reproduction of and reference to this publication is authorised provided the source is acknowledged correctly.

### Document identification

Customer:	Vlaams-Nederlandse Scheldecommissie (VNSC)	Ref.:	WL2021R15_068_13
Keywords (3-5):	Coastal modelling, Complex Project Kustvisie, TELEMAT, TOMAWAC, Wave modelling		
Knowledge domains:	Hydraulics and sediment > Hydrodynamics > Waves > Numerical modelling		
Text (p.):	53	Appendices (p.):	12
Confidential:	<input checked="" type="checkbox"/> No	<input checked="" type="checkbox"/> Available online	

Author(s):	Wang, L.; Kolokythas, G.; Fonias, S.; De Maerschcalck, B.
------------	---

### Control

	Name	Signature
Reviser(s):	Vanlede, J.	Getekend door: Jons Vanlede (Signature) Getekend op: 2021-05-31 16:24:06 +02:00 Reden: lk keur dit document goed 
Project leader:	De Maerschcalck, B.	Getekend door: Bart De Maerschcalck (Sig) Getekend op: 2021-05-19 10:31:55 +02:00 Reden: lk keur dit document goed 

### Approval

Head of Division:	Mostaert, F.	Getekend door: Frank Mostaert (Signatur) Getekend op: 2021-05-17 16:32:47 +02:00 Reden: lk keur dit document goed 
-------------------	--------------	--



## Abstract

With the increasing awareness of sea level rise, the Flemish Authorities initiated the *Complex Project Kustvisie* (CPKV) in order to start together with all involved stakeholders to define the overall long-term coastal defence strategy for the Belgian Coast. In order to analyze the impact of sea level rise on the morphology of the coast and to assess mitigation measures on their efficiency the need for a flexible coastal model for the Belgian coast and Scheldt mouth area was revealed.

Therefore, in 2015 it was decided to build an integral coastal model within the TELEMAC-MASCARET model suite. The present report describes the setup and validation of the two-dimensional TOMAWAC wave propagation model. Together with the TELEMAC2D hydrodynamic model, the wave propagation model forms the basis of the final goal: the morphodynamic model. The hydrodynamic and the TOMAWAC spectral wave propagation model will be coupled to the SISYPHE sediment transport and bed update model.

The wave model is driven at the boundaries by the wave direction, height- and wave period measurements at *Meetnet Vlaamse Bank* measurement station Westhinder. The modelled wave propagation was validated against the wave buoy measurements from the Broersbank project for a selected period including two storms, one from the South-West and one from the North.

Two version of the model are available:

- A stand-alone TOMAWAC wave propagation model. Only the vertical effect of the tide, i.e. the water level, is considered in a schematised way: the water level is only temporally varying and spatially uniform in the entire domain.
- A coupled current-wave interaction version of the model. In this version both tidal currents as wave-induced currents are considered. Since the wave driven currents have a significant contribution of the sediment transport near-shore and onshore, this is the version that will be coupled to the sediment transport model.

Before, it was only possible to couple TOMAWAC wave propagation models to TELEMAC tidal models and SISYPHE sediment transport models, when all models have the same domain outline and identical grids. However, due to the nature of the models, a shallow water solver often requires different grid properties than a wave model. Often, a lower resolution is sufficient for the wave transport model than for the hydrodynamics and sediment transport model. Also, parts of the model domain that are limited influenced by waves, like upstream the estuary and the Eastern Scheldt, it is not necessary to include them in the wave model. Since the wave propagation model often is the bottle neck with respect to computational cost for long term morphodynamic modelling, it was decided to develop a new routine, TEL2TOM, which allows to couple the wave and the hydrodynamic models in an efficient way running the models on different grids with a different resolution and different domain. For the fully coupled morphodynamic model, the implementation of TEL2TOM reduced the total computation time with a factor two without loss of accuracy.

The wave propagation models are available at the Flanders Hydraulics Research model repository: [https://wl-subversion.vlaanderen.be/#!/#repoSpNumMod/view/head/TELEMAC/Scaldis-Kust/15\\_068%20Complex%20Model%20Kustvisie%202021/2\\_WAVEMODELS](https://wl-subversion.vlaanderen.be/#!/#repoSpNumMod/view/head/TELEMAC/Scaldis-Kust/15_068%20Complex%20Model%20Kustvisie%202021/2_WAVEMODELS).



# Contents

Abstract .....	III
Contents .....	V
List of tables.....	VI
List of figures .....	VII
1 Introduction.....	1
2 Data availabilities.....	6
2.1 Waves .....	6
2.2 Wind .....	7
2.3 Tidal data: water levels.....	9
3 Model setup.....	10
3.1 Model Bathymetry and mesh .....	10
3.2 Boundary conditions.....	14
3.3 Model parameters.....	14
3.4 Simulation period .....	15
4 Model results.....	16
4.1 Selection of boundary conditions.....	16
4.2 Sensitivity tests.....	21
4.3 Computation time and parallelization performance.....	33
4.4 Coupled simulation of TELEMAC2D and TOMAWAC.....	35
4.4.1 Coupled with water level only.....	35
4.4.2 Coupled with water level and current velocity both.....	41
5 TEL2TOM .....	45
5.1 Method .....	45
5.2 Schematised coastal model testcase.....	46
5.3 Implementation of TEL2TOM in the Scaldis-Coast model.....	49
6 Conclusions.....	52
References.....	53
Appendix A. Paper presented at the TELEMAC User Conference 2019 (TUC 2019).....	A1
Introduction.....	A1
Description of the code development.....	A2
Test Cases .....	A4
User Manual .....	A11
Summary and Conclusions .....	A12
References.....	A12

## List of tables

Table 1 – List of delivered FHR reports (R) and memos (M) within project 15_068.....	2
Table 2 – Conference proceedings/presentations .....	5
Table 3 – Summary of model parameters .....	14
Table 4 – Simulation cases of the idealized model using the TEL2TOM functionality.....	47

## List of figures

Figure 1 – Location of the observation stations of the Broersbank project.....	6
Figure 2 – Location of the measurement point Westhinder (WHIDW1, red cross) and grid points of ERA5 data (circles); .....	7
Figure 3 – Snapshot of wind field from space-varying ERA5 data.....	8
Figure 4 – Wind speed at 10 m height and direction observed at the measurement station Westhinder .....	9
Figure 5 – Model layout of the Scaldis-Coast wave propagation model.....	11
Figure 6 – Wave model bathymetry .....	11
Figure 7 – Grid of the hydrodynamic Scaldis-Coast model .....	12
Figure 8 – Detail of the Scaldis Coast wave propagatino model (blue) and the hydrodynamics model (black) at Wenduine .....	12
Figure 9 – Grid resolution of the TOMAWAC wave grid.....	13
Figure 10 – Grid resolution of the TELEMAC2D hydrodynamic mesh.....	13
Figure 11 – Observed significant wave height and mean wave direction during the simulation period.....	15
Figure 12 – Comparison of the significant wave height and peak wave period measured at Weshhinder and interpolated from ERA5 data to the Weshhinder measuement station .....	16
Figure 13 – Observed water level at the measurement station Westhinder November 2015.....	17
Figure 14 – Comparison of significant wave height between the observed data and modelled results (T010b) at measurement stations, with boundary directional factor 10 for JONSWAP spectrum. ....	18
Figure 15 – Comparison of significant wave height between the observed data and modelled results (T010c) at measurement stations, with boundary directional factor 4 for JONSWAP spectrum. ....	19
Figure 16 – Comparison of significant wave height between the observed data and modelled results (T010f) at measurement stations, with boundary directional factor 2 for JONSWAP spectrum. ....	20
Figure 17 – Observed and modelled power spectral density (PSD) at the storm wave from north in the simulation period .....	21
Figure 18 – Comparison of significant wave height between the observed data and modelled results (T009c1) at measurement stations, with Thornton and Guza model (1983) for DEPTH-INDUCED BREAKING DISSIPATION .....	22
Figure 19 – Comparison of peak wave period between the observed data and modelled results (T009c1) at measurement stations, with Thornton and Guza model (1983) for DEPTH-INDUCED BREAKING DISSIPATION .....	23
Figure 20 – Comparison of significant wave height between the observed data and modelled results (T009c2) at measurement stations, with Roelvink model (1993) for DEPTH-INDUCED BREAKING DISSIPATION .....	24
Figure 21 – Comparison of peak wave period between the observed data and modelled results (T009c2) at measurement stations, with Roelvink model (1993) for DEPTH-INDUCED BREAKING DISSIPATION .....	25
Figure 22 – Comparison of significant wave height between the observed data and modelled results (T009c3) at measurement stations, with Izumiya and Horikawa model (1984) for DEPTH-INDUCED BREAKING DISSIPATION .....	26

Figure 23 – Comparison of peak wave period between the observed data and modelled results (T009c3) at measurement stations, with Izumiya and Horikawa model (1984) for DEPTH-INDUCED BREAKING DISSIPATION .....	27
Figure 24 – RMSE0 of different models for DEPTH-INDUCED BREAKING DISSIPATION at measurement stations, upper: significant wave height, lower: peak wave period.....	28
Figure 25 – Comparison of significant wave height between the observed data and modelled results (T009c4) at measurement stations, with WAM cycle 4 formula for WIND GENERATION, and Komen et al. (1984) and Janssen (1991) for WHITE CAPPING DISSIPATION.....	29
Figure 26 – Comparison of peak wave period between the observed data and modelled results (T009c4) at measurement stations, with WAM cycle 4 formula for WIND GENERATION, and Komen et al. (1984) and Janssen (1991) for WHITE CAPPING DISSIPATION.....	30
Figure 27 – Comparison of significant wave height between the observed data and modelled results (T009c5) at measurement stations, with WAM cycle 3 formula for WIND GENERATION, and Komen et al. (1984) and Janssen (1991) for WHITE CAPPING DISSIPATION.....	31
Figure 28 – Comparison of peak wave period between the observed data and modelled results (T009c5) at measurement stations, with WAM cycle 3 formula for WIND GENERATION, and Komen et al. (1984) and Janssen (1991) for WHITE CAPPING DISSIPATION.....	32
Figure 29 – RMSE0 of different combination for WIND GENERATION and WHITE CAPPING DISSIPATION at measurement stations, upper: significant wave height, lower: peak wave period. ....	33
Figure 30 – Computational time versus the number of cores utilized for the parallel test runs.....	34
Figure 31 – Speedup ( $S_p$ ) versus the number of cores (left figure) and Performance( $\alpha_p$ ) versus the number of cores utilized for the parallel test runs.....	34
Figure 32 – Comparison of significant wave height between the observed data and modelled results (HSW005g) at measurement stations, coupled with water level only.....	36
Figure 33 – Comparison of significant wave height between the observed data and modelled results (W002b) at measurement stations, stand-alone wave model with water level inputs.....	37
Figure 34 – Comparison of water depth derivative respect to time between the coupled and stand-alone simulations, with original wrong code in the routine cormar.f for coupled simulation. ....	38
Figure 35 – Comparison of water depth derivative respect to time between the coupled and stand-alone simulations, with fixed code in the routine cormar.f for coupled simulation. ....	39
Figure 36 – Comparison of significant wave height between the observed data and modelled results (HSW005s) at measurement stations, with fixed code in the routine cormar.f for coupled simulation.....	40
Figure 37 – Comparison of significant wave height between the observed data and modelled results (HSW009f) at measurement stations, coupled with water level and current velocity both. ....	42
Figure 38 – Comparison of significant wave height between the observed data and modelled results (HSW009I) at measurement stations, coupled with water level and current velocity both but without consideration of energy transfer between frequencies due to accelerating and decelerating currents. ....	43
Figure 39 – Comparison of mean wave period between the observed data and modelled results (HSW009I) at measurement stations, coupled with water level and current velocity both but without consideration of energy transfer between frequencies due to accelerating and decelerating currents. ....	44
Figure 40 – Zoom of the TELEMAC2D and TOMAWAC gid with local node numbers.....	46
Figure 41 – TOMAWAC domain and mesh for test case C1. TELEMAC2D domain area is indicated with black solid line.....	47

Figure 42 – Snapshot of the velocity magnitude after 12d 16.5h of full simulation of tides and waves for test case C3.....	48
Figure 43 – Cross-shore profiles (section indicated with black solid line in Figure 42) of the velocity magnitude within fractions of one tidal cycle for test cases C1 (black solid line), C2 (blue dashed line) and C3 (red dash-dotted line).....	48
Figure 44 – Timeseries of velocity magnitude at a specific location 370 m far from the coastal boundary of TELEMAC2D domain) for test cases C1 (black solid line), C2 (blue dashed line) and C3 (red dash-dotted line). .....	49
Figure 45 – Comparison of significant wave height for the fully coupled TELEMAC2D-TOMWAC model with (A003) and without TEL2TOM (HSW009).....	50
Figure 46 – Comparison of mean wave period for the fully coupled TELEMAC2D-TOMWAC model with (A003) and without TEL2TOM (HSW009). In blue is the observed mean wave period.....	51
Figure 47 – Mesh for TELEMAC and SIYPHE (red) and TOMAWAC (green) for the littoral drift test case.....	A5
Figure 48 – Calculated significant wave height on a transect perpendicular to the beach for the fine and the coarse model. ....	A6
Figure 49 – Calculated velocity profile on a transect perpendicular to the beach for the fine and the coarse model.....	A6
Figure 50 – Calculated elevation of the free surface on a transect perpendicular to the beach for the fine and the coarse model.....	A6
Figure 51 – Locations of the field measurement stations of the Broersbank project.....	A7
Figure 52 – Computational domains and meshes for TOMAWAC (upper figure) and TELEMAC2D (lower figure) for the TEL2TOM simulation of the Scaldis-Coast model.....	A8
Figure 53 – Comparison of significant wave height between the observed data and modelled results at measurement stations, for a coupled TELEMAC2D-TOMAWAC case using TEL2TOM with a coarser TOMAWAC mesh. ....	A9
Figure 54 – Comparison of mean wave period between the observed data and modelled results at measurement stations, for coupled a TELEMAC2D-TOMAWAC case using TEL2TOM with a coarser TOMAWAC mesh. ....	A10
Figure 55 – Example showing the numbering convention for linear interpolation on a simple mesh when sending information from TELEMAC to TOMAWAC.....	A11



# 1 Introduction

Within the *Complex Project Kustvisie* (CPKV) all involved stakeholders participate in process of defining the overall design of the long-term coastal defence of the Belgian Coast. The project was formerly known as project *Vlaamse Baaien* (Flemish Bays). The *Vlaamse Baaien* project was initiated in 2014 by the Flemish Authorities with the goal to protect the Belgian Coast from (extreme) sea level rise and climate change on the horizon 2050 – 2100. The goal of the project is to create an attractive and natural coast that is climate change resilient with economic benefits like estuarine traffic and renewable energy.

Within this project a wide variety of mitigation strategies can be considered, ranging from extra beach and foreshore nourishments, dunes on beaches to artificial offshore barrier islands. The evaluation of these interventions on currents, waves and morphology revealed the need for a flexible, accurate and versatile global coastal model for the Belgian coast and Western Scheldt mouth area.

Up till 2015, the available models for the Belgian coast, mostly restricted to selective stretches of the coast or ports, built for specific projects and limited in offshore direction, mostly based on structured grids. Or on the other hand large scale continental shelf models with little focus on the near- and onshore coastal area.

Therefore, it was decided to build an integral coastal model within the TELEMAC-MASCARET model suite (G. Kolokythas *et al.*, 2021b). The model should be suitable to estimate morphological evolutions both on the short scale (days to a year) as on the mid-term scale (up to a decades) both in the tidally driven off-shore part as on the near-shore.

The present report describes the setup and validation of the TOMAWAC wave propagation model. TOMAWAC is a scientific software which models the changes, both in the time and in the spatial domain, of the power spectrum of wind-driven waves and wave agitation for applications in the oceanic domain, in the intracontinental seas as well as in the coastal zone. Notice that TOMAWAC is a transient model, the boundary conditions and forcing are time dependent. This is different from the SWAN model which, in morphodynamic simulation, calculates a steady state solution of the density directional spectrum at each node for each time instance. The transient character of the model will have an impact on the morphodynamic model approach, i.e. on the use of the morphological amplification factor (MORFAC) and wave input reduction. This will be described in detail in the morphodynamic model setup and validation report (G. Kolokythas *et al.*, 2021b)

The proposed model describes the propagation and transformation of the waves from the offshore boundary towards the coast under the influence of tides and wind. The waves have a major impact on the coastal morphology of the foreshore and beach. They drive the littoral transport through wave induced currents and have a steering up effect on the sediment. The wave asymmetry and wave-skewness, Stokes drift, undertow and surface rollers are the main mechanisms for cross-shore sediment transport. Therefore, an accurate wave propagation model is necessary in predicting the near- and on-shore morphodynamic behaviour, but also in the shallow parts of the off-shore, like *Vlakte van de Raan* the wave energy contributes to the sediment transport.

In order to include the effect of the tide on the wave propagation, the TOMAWAC model is coupled to the TELEMAC2D hydrodynamic model which provides the water depths and tidal currents (G. Kolokythas *et al.*, 2021a). The coupling is a two-way coupling so that TELEMAC2D on its turn can calculate the wave driven currents.

Not only should the wave propagation model be accurate, but also computationally efficient, particularly for long-term (decades) morphodynamic modelling. With respect to computation time, generally, the spectral wave propagation model is the most CPU demanding submodule of the morphodynamic models. Typically, the wave propagation model does not require the same numerical mesh specifications as the hydrodynamical and sediment transport models. However, so far it was only possible to couple models with identical grids.

Therefore, a new module has been developed which allows to couple models with different grid resolutions: TEL2TOM (Breugem *et al.*, 2019). By reducing the grid resolution of the wave model, the computational time of the morphodynamic model was reduced by a factor two without loss of accuracy.

A list of the preceding reports and memos delivered within project 15\_068 is given in Table 1.

Table 1 – List of delivered FHR reports (R) and memos (M) within project 15\_068.

Title	ID
Report: Modelling Vlaamse Baaien, Deelrapport 1: Hydrodynamische Modelling Scenario's Oostkust	WL2016R15_068_1
Report: Modelling Belgische Kustzone en Scheldemonding, Deelrapport 2: Morfologische analyse scenario's Vlaamse Baaien	WL2017R15_068_2
Report: Modelling Belgische Kustzone en Scheldemonding, Deelrapport 3: Modelling van de morfologische effecten na aanleg nieuwe Geul van de Walvischstaart	WL2017R15_068_3
Report: Modelling Belgische Kustzone en Scheldemonding, Rekennota: Berekening golfklimaat Vlaamse Baaien scenario's E4 en F1	WL2017R15_068_4
Report: Modelling Belgische Kustzone en Scheldemonding, Sub report 5: Progress report - Scenarios Vlaamse Baaien and model developments	WL2017R15_068_5
Report: Modelling Belgian Coastal zone and Scheldt mouth area: Sub report 6: Progress report 2 - Evaluation of numerical modelling tools and model developments	WL2018R15_068_6
Report: Modelling Belgian Coastal zone and Scheldt mouth area: Sub report 7: Progress report 3 – Model developments: Hydrodynamics, waves and idealized modelling	WL2018R15_068_7
Report: Modelling Belgian Coastal zone and Scheldt mouth area: Sub report 8: Progress report 4 – Model developments: Waves, idealized modelling and morphodynamics	WL2019R15_068_8
Report: Modelling Belgian Coastal zone and Scheldt mouth area: Sub report 9: Progress report 5 – Model developments: Waves, idealized modelling and morphodynamics	WL2019R15_068_9
Report: Modelling Belgian Coastal zone and Scheldt mouth area: Sub report 10 – Summary of the 2D TELEMAC morphodynamic model Scaldis-Coast: version 2020 developed for the Complex Projects Coastal Vision and Extra Container Capacity Antwerp	WL2020R15_068_10
Report: Modelling Belgian Coastal zone and Scheldt mouth area: Sub report 11: Progress report 6 – Model developments: Grid optimization, Morphodynamics, Dredging/dumping subroutines, Wave conditions	WL2020_R15_068_11

Report: Modelling Belgian Coastal zone and Scheldt mouth area: Sub report 12: Scaldis-Coast model – Model setup and validation of the 2D Hydrodynamic model	WL2021_R15_068_12
Report: Modelling Belgian Coastal zone and Scheldt mouth area: Sub report 13: Scaldis-Coast model – Model setup and validation of the wave propagation model	WL2021_R15_068_13
Report: Modelling Belgian Coastal zone and Scheldt mouth area: Sub report 14: Scaldis-Coast model – Model setup and validation of the morphodynamic model	WL2021_R15_068_14
Memo: Modelling Belgian Coastal zone and Scheldt mouth area	WL2016M15_068_1
Memo: Beschrijving scenario's Vlaamse Baaien: Oostkust	WL2016M15_068_2
Memo: Berekeningen golfklimaat scenario F1	WL2016M15_068_3
Memo: Gebruik van de rekencluster aMT voor Telemac berekeningen	WL2016M15_068_4
Memo: Modelling of bed morphology evolution at Knokke for a beach nourishment scenario (G2) by XBeach	WL2016M15_068_5
Memo: Berekeningen golfklimaat scenario E4	WL2016M15_068_6
Memo: Morfologische analyse scenario's Vlaamse Baaien	WL2016M15_068_7
Memo: Vlaamse Baaien: invloed eiland ten oosten van Zeebrugge op het Zwin	WL2016M15_068_8
Memo: Sediment transport formulation in XBeach and Delft3D	WL2016M15_068_9
Memo: Impact aanleg nieuwe vaargeul op de morfologie van de Schelde monding en estuarium: Een geïdealiseerde modelstudie	WL2016M15_068_10
Memo: Morfodynamische effecten aanleg nieuwe geul van de Walvischstaart	WL2016M15_068_11
Memo: Morfologische modellering m.b.v. TELEMAC - SISYPHE	WL2016M15_068_12
Memo: Geul van de Walvischstaart: samenvatting morfologisch onderzoek stabiliteit en baggerbeslag	WL2016M15_068_13
Memo: Artikel Tijdingen: Vlaamse Baaien	WL2016M15_068_14
Memo: Toelichting baggerbeslag Geul van de Walvischstaart	WL2017M15_068_15
Memo: Hydrodynamic modelling of 'Vlaamse Baaien' dunebelt scenarios I3 and I4	WL2017M15_068_16
Memo: Dunebelt scenario I4 – Scaldis vs Semi-circular Telemac3D	WL2017M15_068_17
Memo: Overview of existing Telemac hydrodynamic models: NSG-BCG and Scaldis	WL2017M15_068_18

Memo: CSM and ZUNO run of 2009 including 60, 90 and 200 cm sea level rise	WL2017M15_068_19
Memo: Sea level rise impact on Zeebrugge port accessibility - Telemac3D hydrodynamic modelling	WL2017M15_068_20
Memo: Bringing TELEMAC and Gmsh meshing tool closer	WL2017M15_068_21
Memo: Time step sensitivity analysis for TOMAWAC stand alone and TELEMAC3D-TOMAWAC coupled simulations	WL2017M15_068_22
Memo: Unstructured high resolution coastal model for the Belgian Coast and Scheldt Mouth: model requirements	WL2018M15_068_23
Memo: Telemac2D (and 3D) coupling with Sisyphe	WL2017M15_068_24
Memo: TOMAWAC test runs	WL2017M15_068_25
Memo: Bathymetry and Mesh Construction for ScaldisKust	WL2018M15_068_26
Memo: Scaldis-Coast model calibration: Bottom roughness tuning	WL2018M15_068_27
Memo: Preparing SDS wind file for CSM-ZUNO runs	WL2019M15_068_28
Memo: TELEMAC2D-TOMAWAC-SISYPHE coupled run for hydrodynamics and wave validation	WL2019M15_068_29
Memo: Nestor coupling with TELEMAC2D/SISYPHE and set-up	WL2019M15_068_30
Memo: Scaldis-Coast: Summary Coastal 2D TELEMAC morphodynamic model for the Belgian Coast and Scheldt mouth area (input CREST final report)	WL2019M15_068_31
Memo: Scaldis-Coast: Summary Coastal 2D TELEMAC morphodynamic model for the Belgian Coast and Scheldt mouth area for the Complex Project Coastal Vision	WL2020M15_098_32
Memo: Artikel tijdingen: Storm Ciara	WL2020M15_068_33
Memo: Suspended sediment transport using GAIA	WL2020M15_068_34
Memo: Test runs with new module GAIA in the TELEMAC-MASCARET system	WL2020M15_068_35
Memo: Memo: Mixed sediment transport by GAIA: Improvements and a Scaldis-Coast application	WL2020M15_068_37

Table 2 – Conference proceedings/presentations

XBeachX 2017	MORPHODYNAMIC ANALYSIS OF INTERVENTION SCENARIOS AT THE BELGIAN COAST UNDER THE MASTERPLAN 'FLEMISH BAYS'	XBeach X Conference
ICCE 2018	IMPACT OF SEA LEVEL RISE ON THE ACCESSIBILITY OF COASTAL PORTS: A CASE STUDY OF THE PORT OF ZEEBRUGGE (BELGIUM)	International Conference on Coastal Engineering
TUC 2018	Neumann (water level gradient) boundaries in TELEMAC 2D and their application to wave-current interaction (Conference proceedings)	Telemac User Conference
EGU 2019	SCALDIS-COAST: AN INTEGRATED NUMERICAL MODEL FOR THE SIMULATION OF THE BELGIAN COAST MORPHODYNAMICS	EGU General Assembly
TUC 2019	TEL2TOM: coupling TELEMAC and TOMAWAC on arbitrary meshes	Telemac User Conference
VLIZ 2019	Scaldis-Coast: An unstructured next generation integrated model for the Belgian Coastal Zone	VLIZ Marine Science Day
IAHR 2020	Simulating the morphological evolution of the Belgian coast by means of the integrated numerical model SCALDIS-COAST	IAHR Europe Congress

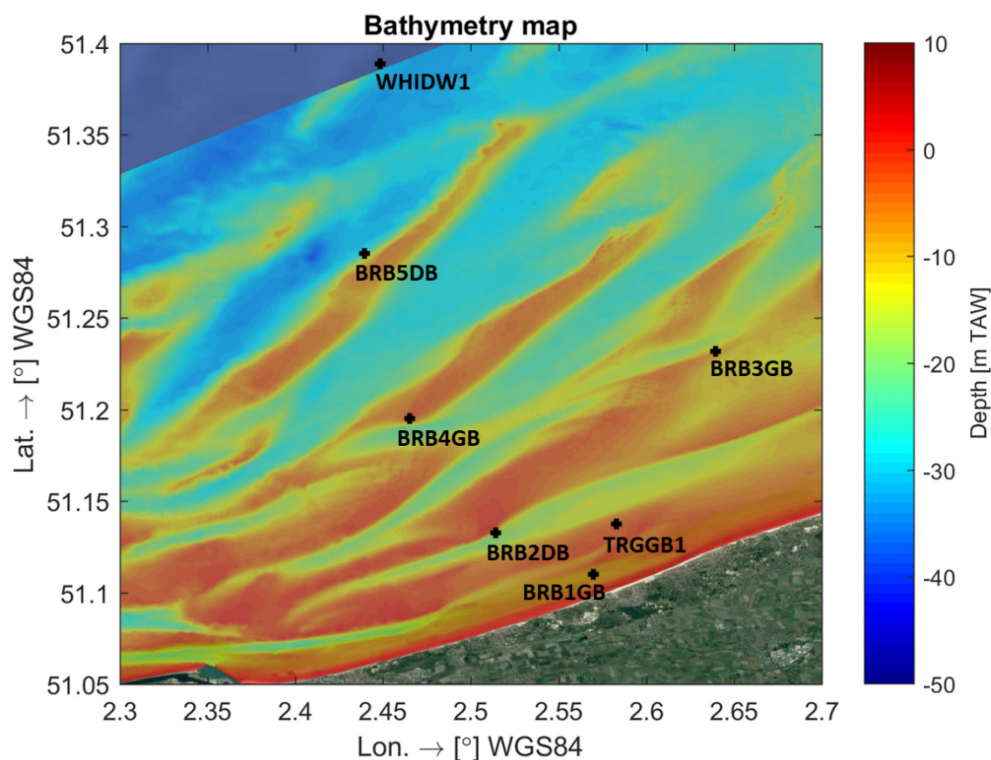
## 2 Data availabilities

### 2.1 Waves

Wave data can be used to calibrate/validate the model and provide boundary conditions to the model. In this study, two datasets are investigated: one dataset is collected at stationary measurement points within the context of the *Broersbank project* executed by the University of Leuven commissioned by Coastal Division (Komijani *et al.*, 2016). The other database is the ERA5 reanalysis provided by European Centre for Medium-Range Weather Forecasts (ECMWF). Both datasets contain spectral wave data.

In the Broersbank project, wave data was sampled at seven locations as below during the period between 2013 and 2017. The temporal resolution of the wave data reaches thirty minutes. The spectral wave data collected at the most offshore station “Westhinder” (code name WHIDW1) will be used as wave boundary condition for the model. Westhinder is a fixed measurement station part of the monitoring network Flemish Banks (*Meetnet Vlaamse Banken, MVB*). The other six stations are temporary wave buoys placed during the duration of the Broersbank project<sup>1</sup>. Since they are inside the model at different distances from the coast, they are particularly useful in validating the modelled wave propagation and transformation.

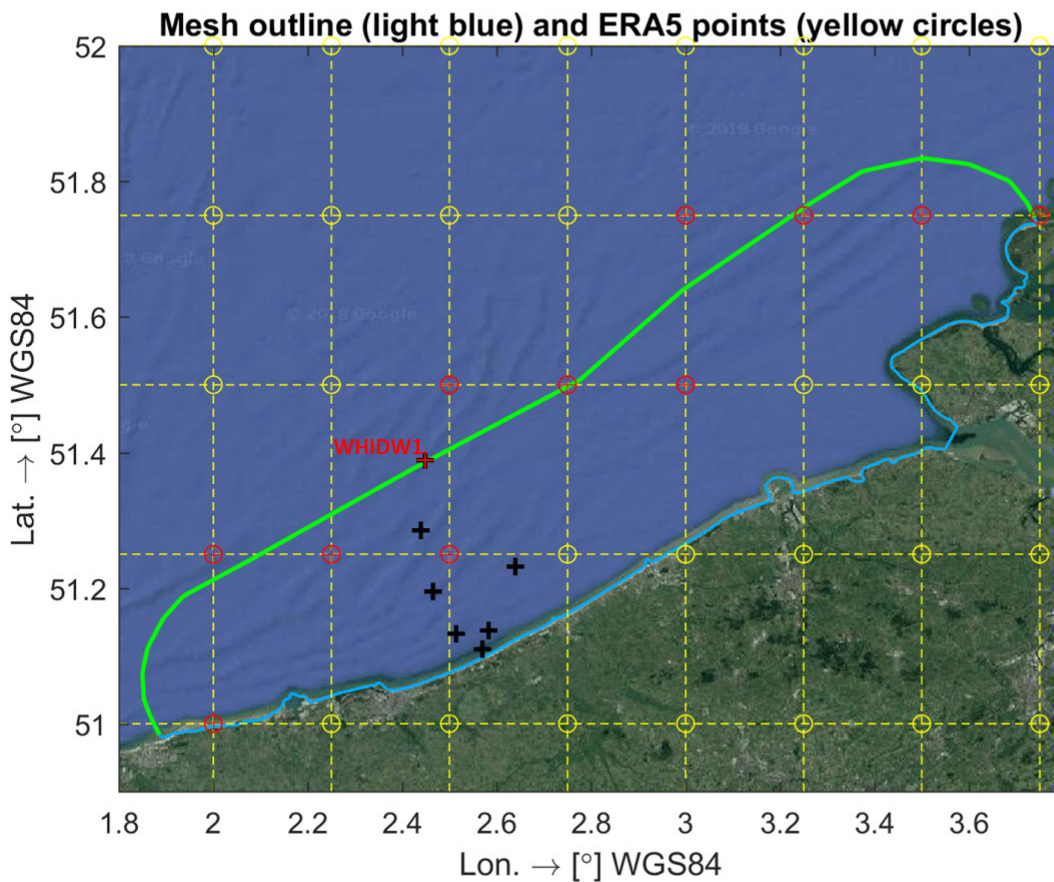
Figure 1 – Location of the observation stations of the Broersbank project



<sup>1</sup> Preliminary model results revealed that for strong wave conditions the original WHIDW1 data was wrongly processed. For the selected validation period of November 2015, the original wave data has been reprocessed by KU Leuven and provided to Flanders Hydraulics Research

The ERA5 is the fifth generation of ECMWF atmospheric reanalysis of the global climate. The reanalysis provides a numerical description of the recent climate by combining models with observations. Apart from wave output, it can also give meteorological outputs like wind and air pressure. These outputs are available for public use at one-hour temporal resolution and 0,25° spatial resolution (circles in Figure 2). Because of difficult interpolation for the space-varying spectral wave data, the wave boundaries of the model are extracted from the grid points nearest to local points on the model boundary (red circles in Figure 2).

Figure 2 – Location of the measurement point Westhinder (WHIDW1, red cross) and grid points of ERA5 data (circles); the offshore and land boundaries of the wave model are marked by green and blue solid lines respectively



## 2.2 Wind

The ERA5 reanalysis also includes wind output (Figure 3), which is available at the same temporal and spatial resolution as the wave output.

Also, the monitoring network Flemish Banks measures wind speed and direction at different off- and onshore measurement stations. The wind data is collected at Westhinder with a time resolution of 10 minutes.

The ERA5 is spatially varying data. However, due to the coarse resolution in the area of interest, the wind speeds can be underestimated in the nearshore due to interpolation between a *sea-node* and a *land-node*, when above land, the windspeed at 10 m height can drop and change direction easily. From Figure 4 it can also be observed that ERA5 is less accurate for the coastal zone. A reduced windspeed will affect directly the wave propagation near shore. Therefore, it was decided to use the Westhinder observed wind speeds and direction as forcing for the whole model domain.

Figure 3 – Snapshot of wind field from space-varying ERA5 data

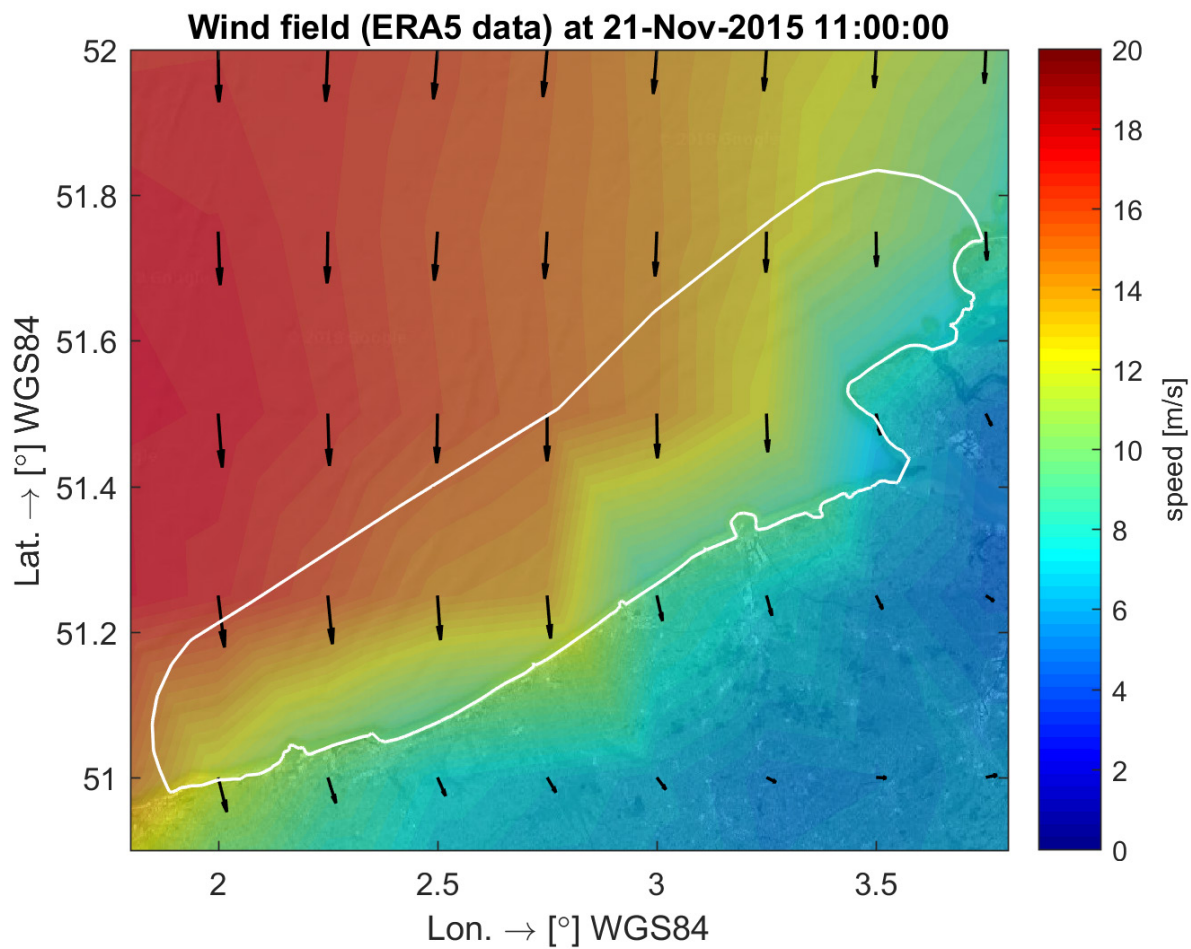
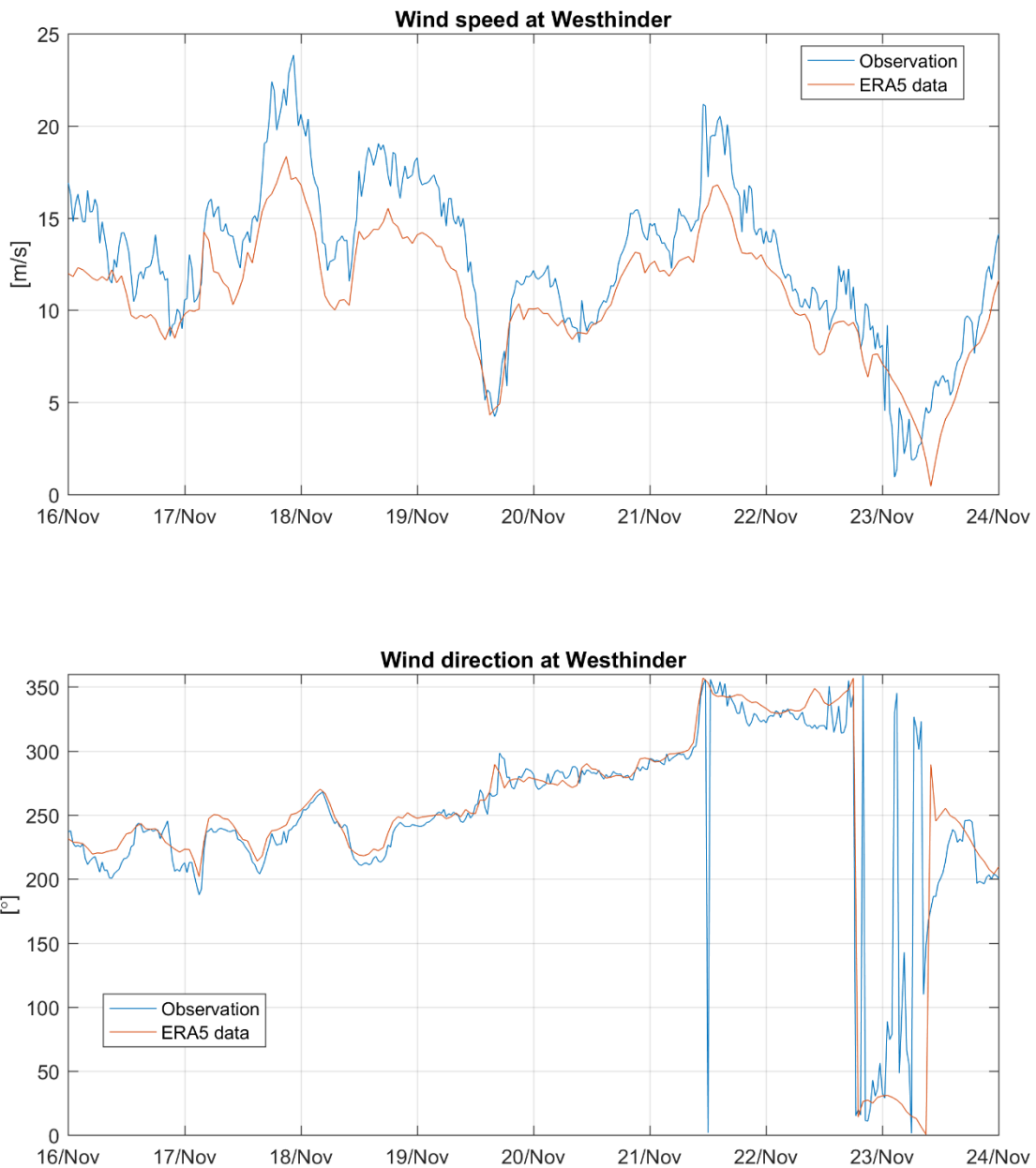


Figure 4 – Wind speed at 10 m height and direction observed at the measurement station Westhinder  
wind speed and direction derived from ERA5 data for the measurement station Westhinder



### 2.3 Tidal data: water levels

In a first phase the wave model will be forced by measured water levels. Data is available at different station of the monitoring network MVB. Whesthinder data with a temporal resolution of five minutes will be used. In the second phase, the model will be coupled with the validated hydrodynamical TELEMAC model to provide spatially varying water levels (G. Kolokythas *et al.*, 2021a). By two-way coupling wave setup and wave induced current are calculated by the TELEMAC model as well.

## 3 Model setup

### 3.1 Model Bathymetry and mesh

For the model grid an advanced grid generator GMSH (Geuzaine & Remacle, 2009) has been used. GMSH build in flexible which high-performance grid with automatic refinement based on geometric constraints, but also based on the gradient of the bathymetry. The same approach has been used as for the construction of the hydrodynamic model (Kolokythas *et al.*, 2021a). However, in order to run the wave model efficiently with respect to CPU time, the Eastern and Western Scheldt Estuaries have been removed from the model domain. Also, the resolution in the nearshore has been reduced to 50 meters, whereas the hydrodynamic model has a resolution of 25 meter. In the offshore part of the domain the grid resolution is comparable. For details on the grid generation and bathymetry, the reader is referred to Kolokythas *et al.* (2021a). The wave model mesh and bathymetry are presented in Figure 5 to Figure 6 below. The TOMAWAC wave transport grid counts 273 000 elements on 138 000 nodes

Before, coupling TELEMAC2D and TOMAWAC was only possible for identical grids. Therefore, all coupled runs in Section 4.4 are performed on the hydrodynamic grid, it has not only a higher resolution, but it also includes the Western and Eastern Scheldt estuaries. The full hydrodynamics mesh is shown in Figure 7. For more details on the hydrodynamic grid, the reader is referred to Kolokythas *et al.* (2021a). The original TELEMAC2D grid counts more than 500 000 triangular elements on almost 260 000 nodes.

However, since the wave and tidal model do not require the same resolution requirements, and since the Western and Eastern Scheldt Estuaries do not contribute to the coastal wave climate, within the project a new module, TEL2TOM, was developed to allow for coupling of the two models based on different domains and resolutions (Breugem *et al.*, 2019). Details of the TEL2TOM module is further in detail explained in Section 5, where the coarser wave grid is coupled to the finer and bigger hydrodynamics grid. A detail of the wave and hydrodynamic mesh is shown in Figure 8.

Figure 5 – Model layout of the Scaldis-Coast wave propagation model

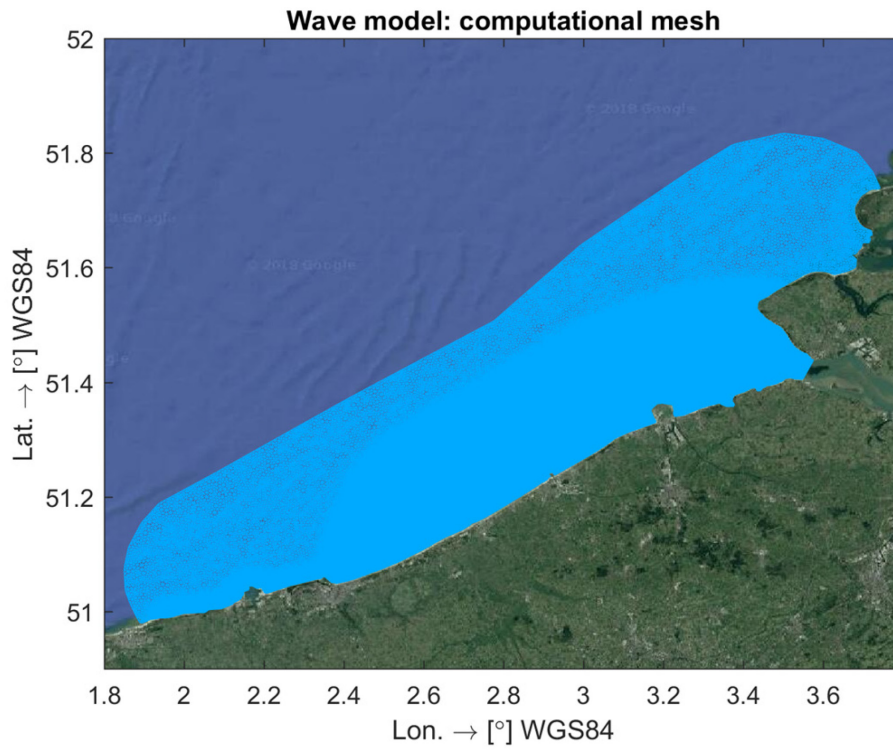


Figure 6 – Wave model bathymetry

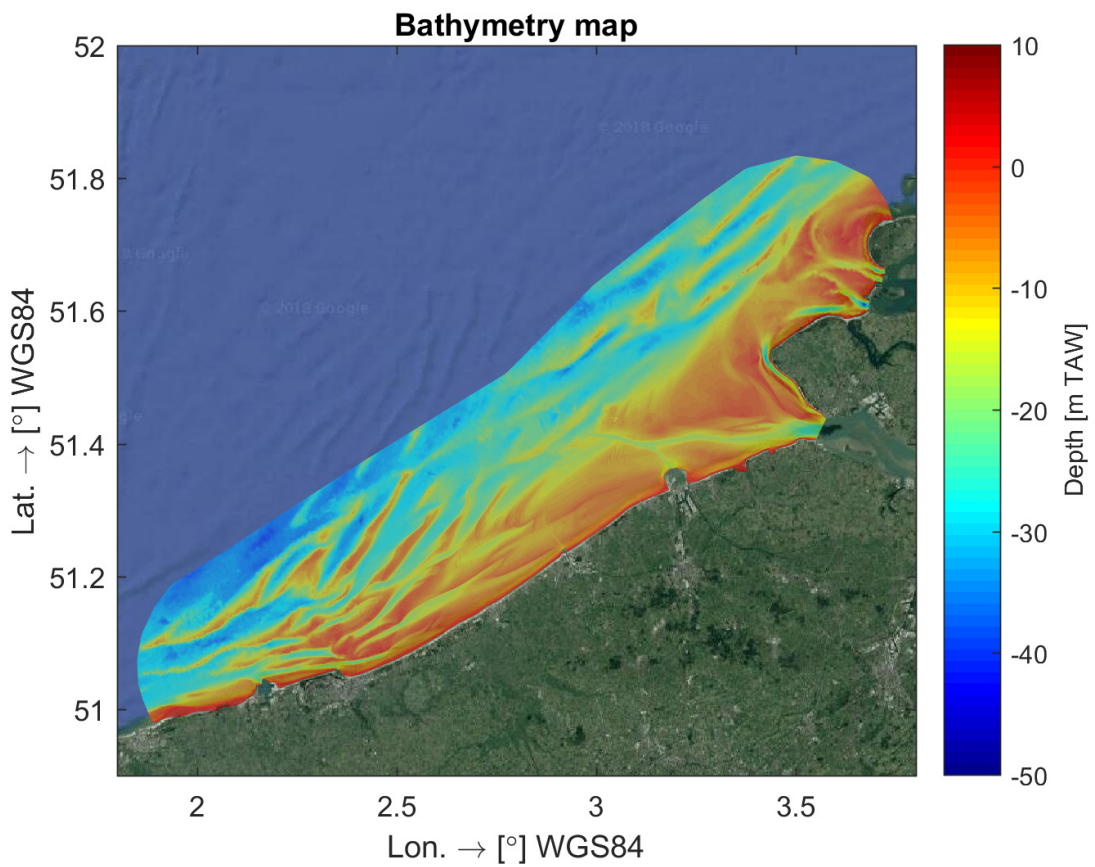


Figure 7 – Grid of the hydrodynamic Scaldis-Coast model

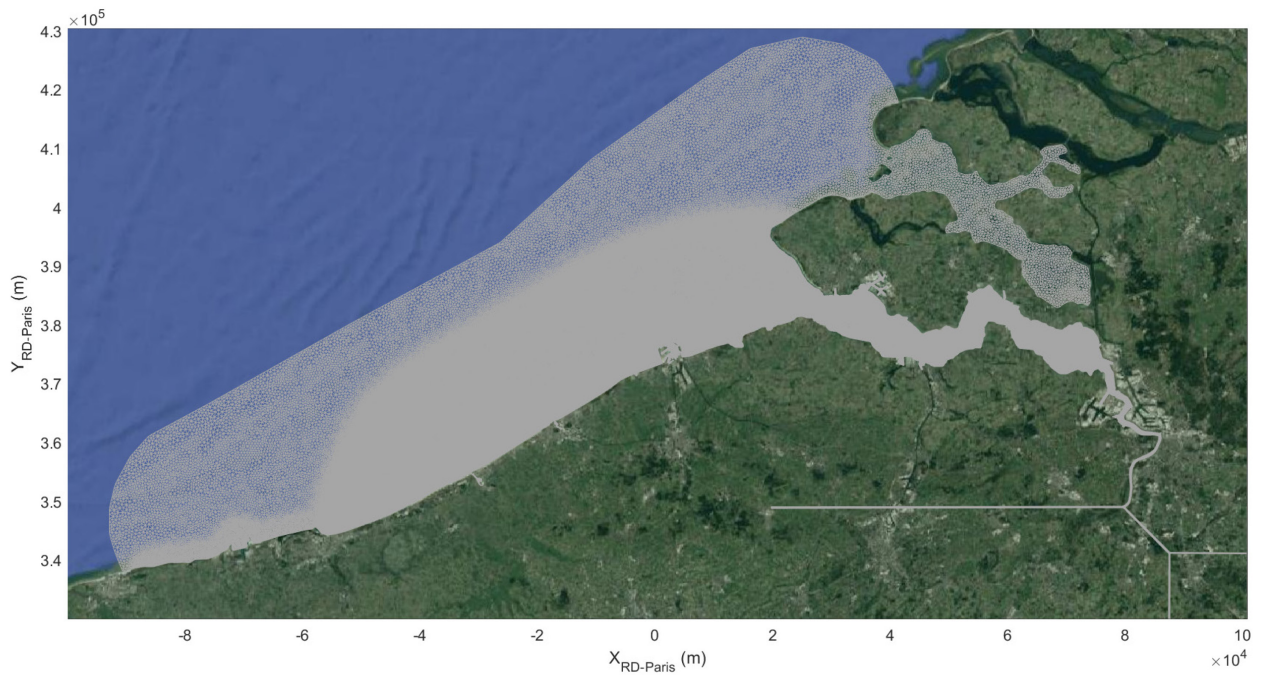


Figure 8 – Detail of the Scaldis Coast wave propagation model (blue) and the hydrodynamics model (black) at Wenduine

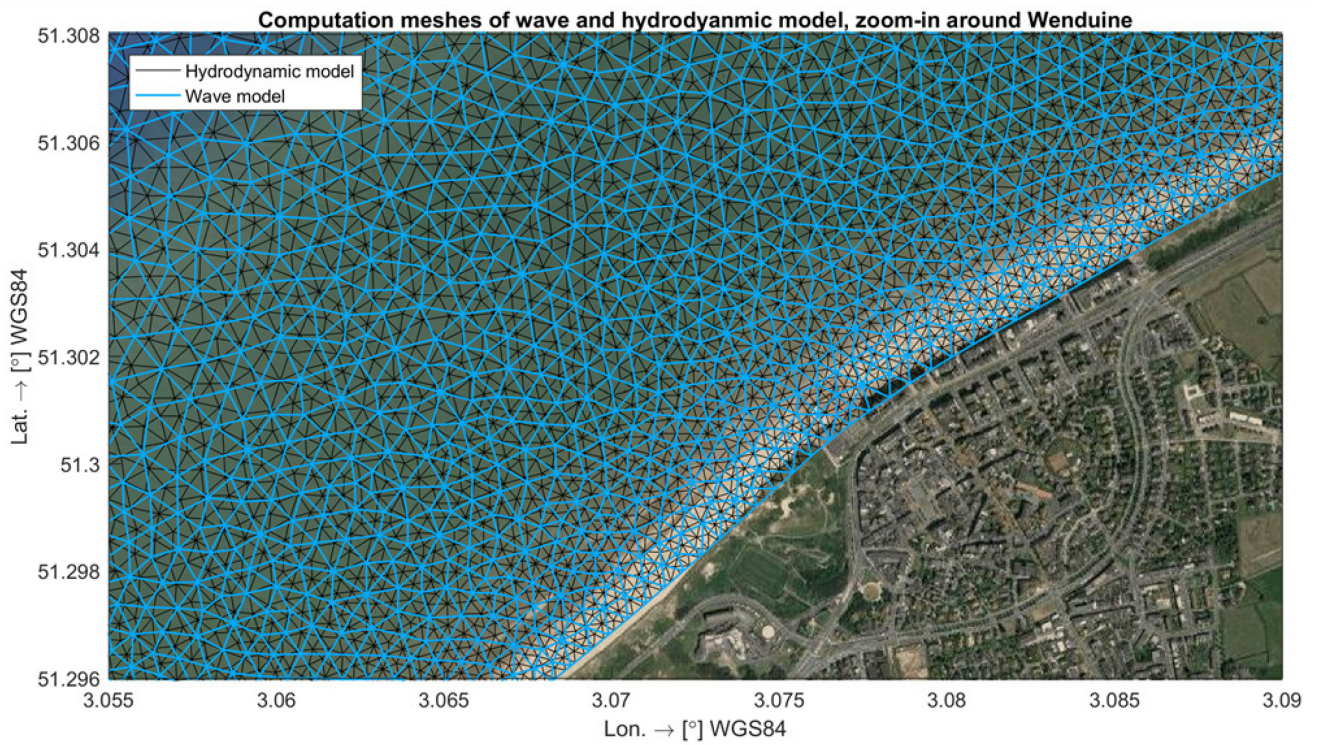


Figure 9 – Grid resolution of the TOMAWAC wave grid

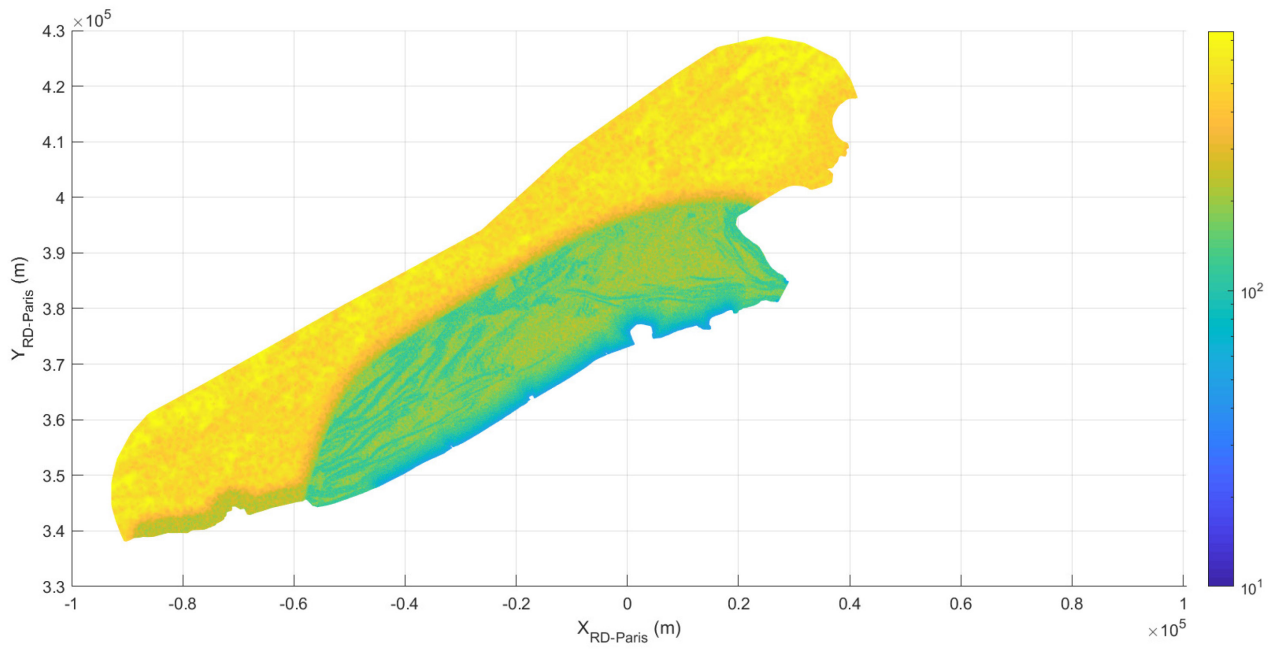
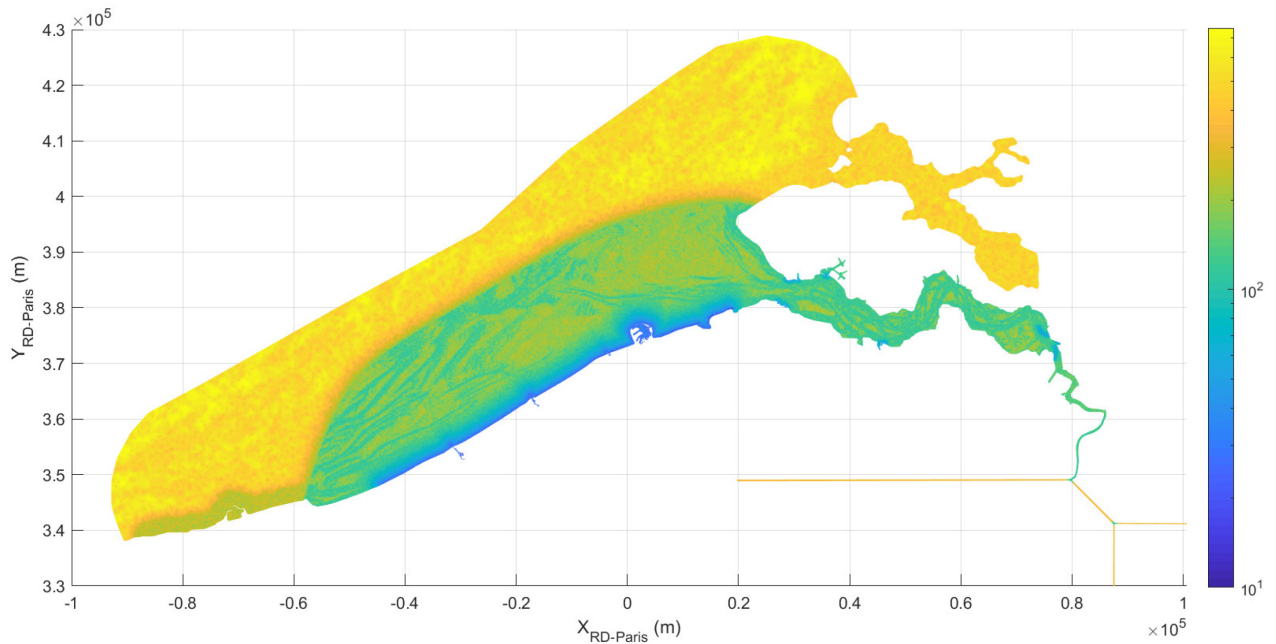


Figure 10 – Grid resolution of the TELEMAC2D hydrodynamic mesh



## 3.2 Boundary conditions

The boundary conditions of the wave model include wave conditions imposed at boundary points and wind conditions imposed within the whole model domain. As afore mentioned in the Section 2, the wave and wind data sources include observation at the station “Westhinder” and ERA5 reanalysis, both of which can be used to specify boundary conditions of the wave model.

In TOMAWAC spectral data can be applied directly to the boundary. However, from the perspective of long-term morphological modelling, the use of a JONSWAP spectrum based on timeseries of significant wave height, peak wave period and wave direction is a more practically approach. In the next sections the use of a JONSWAP spectrum will be compared to applying measured spectral wave data directly. Important to mention here is that the model only accepts absolute period on the boundaries, whereas the data only provides relative wave periods. It is advised to convert to absolute periods. However, the model results revealed that impact was rather limited.

## 3.3 Model parameters

In Kolokythas *et al.* (2018) the sensitivity of different model parameters has been tested extensively. It was found that, since in comparison to the SWAN model, TOMAWAC has no stationary mode, one must carefully select a proper time-step. It was suggested to use a maximum timestep of 120 seconds and a coupling period lower than 10 minutes. However, the latter is grid sensitive and later on also a bug fix seemed to have its relevance. Preliminary model results revealed that after the bug fix for the Scaldis-Coast model a coupling period of 30 minutes was still acceptable.

The other parameters are listed in the table below:

Table 3 – Summary of model parameters

TIME STEP (s)	120
COUPLIN INTERVAL (when coupling to TELEMAC2D) (s)	1800
NUMBER OF DIRECTIONS	36
MINIMAL FREQUENCY (1/s)	0.05
NUMBER OF FREQUENCIES	34
FREQUENTIAL RATIO	1.1
MINIMUM WATER DEPTH (m)	0.1
WIND GENERATION	Yan (1987)
LINEAR WAVE GROWTH	Cavaleri and Malanotte-Rizzoli (1981)
DEPTH-INDUCED BREAKING DISSIPATION	Battjes and Janssen model (1978)
WHITE CAPPING DISSIPATION	van der Westhuysen (2007)
NON-LINEAR TRANSFERS BETWEEN FREQUENCIES	Formula of WAM cycle 4 (DIA method)
BOTTOM FRICTION DISSIPATION	Formula of WAM cycle 4
TRIAD INTERACTIONS	OFF

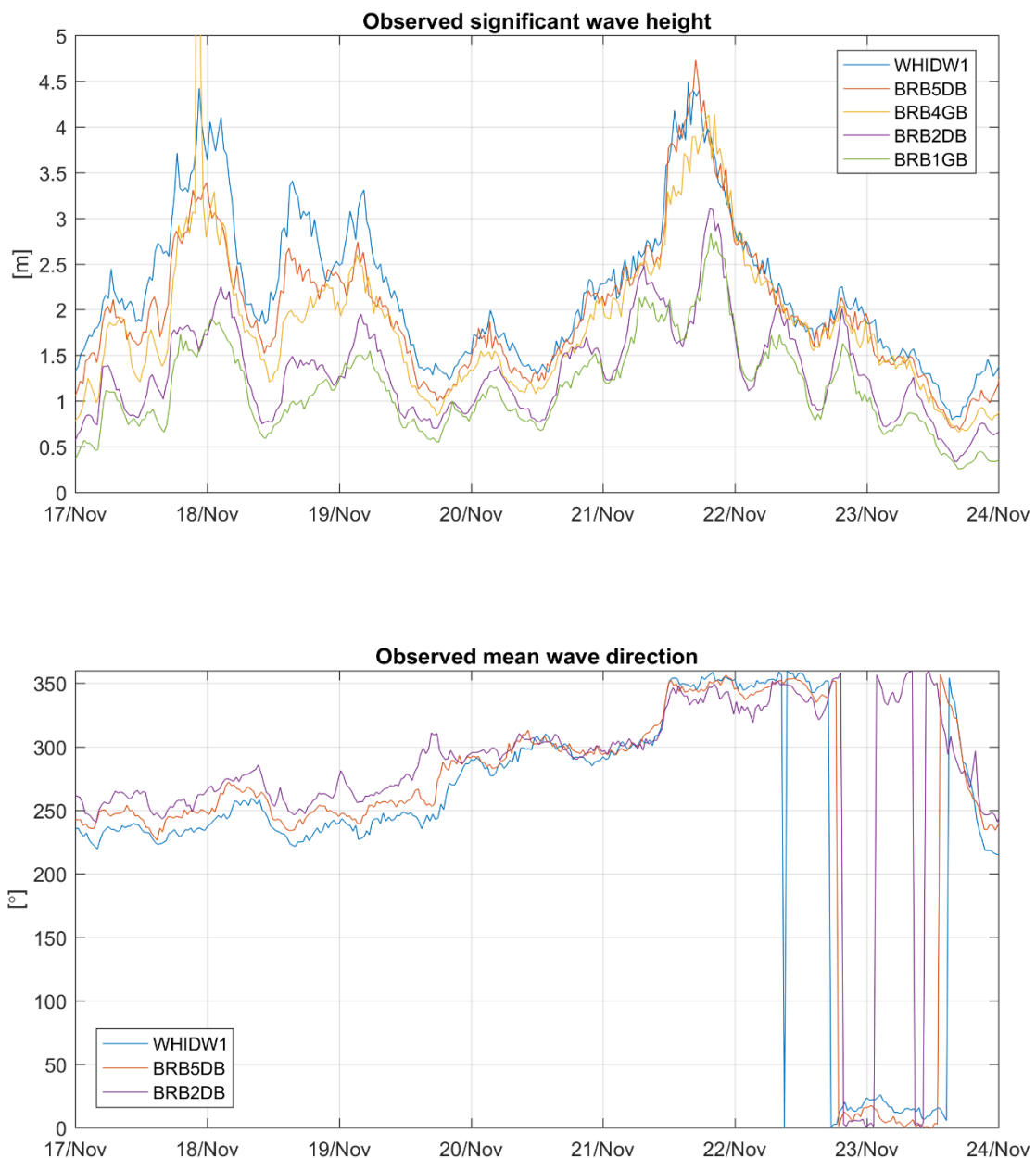
### 3.4 Simulation period

In this study, observed data from the Broersbank measurement project initiated by Coastal Division and executed by KU Leuven were utilized to estimate performance of the wave model (Komijani *et al.*, 2016).

In Figure 1 and Figure 2 and the locations of the observation stations have been marked by crosses. After exploration of the observed data, the simulation period has been selected between November 17 and November 24, 2015, during which one storm from Southwest took place around November 18 while the other one from the North on November 21 (Figure 11).

In general, the dissipation of energy can be observed in Figure 11 when the waves approach the coast. In the stations BRB2DB and BRB1GB the influence of the water level on the wave propagation can be observed.

Figure 11 – Observed significant wave height and mean wave direction during the simulation period



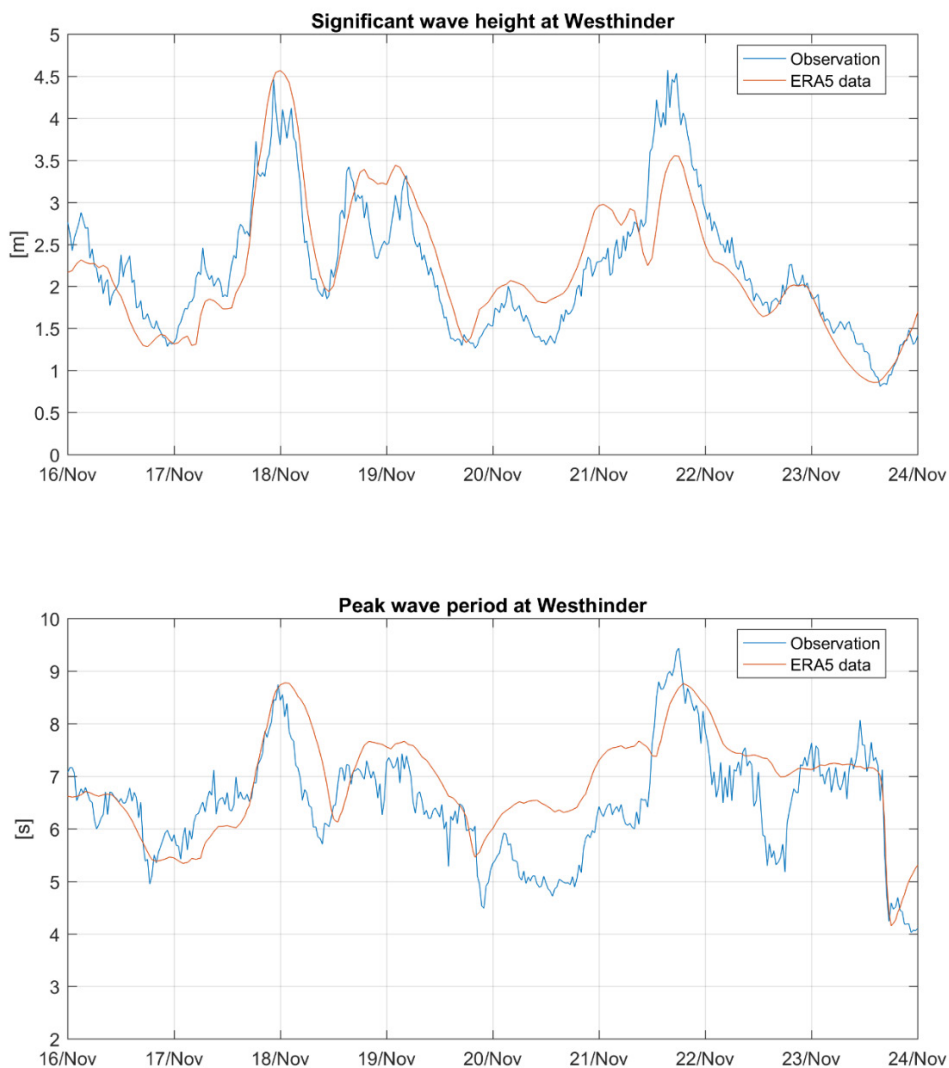
## 4 Model results

### 4.1 Selection of boundary conditions

As mentioned in Section 2.1, the boundary conditions of the wave model can be either derived from the space-varying ERA5 data or the observed data collected at the fixed measurement station Westhinder (WHIDW1) directly as spectral data or by a JONSWAP spectrum.

Figure 12 compares the ERA5 data interpolated to the Westhinder station location compared to the observed significant wave height and peak wave period. This is the TOMAWAC output at Westhinder when applying the wave spectra from *Meetnet Vlaamse Banken* and ERA5 at the boundary. Due to the temporal resolution, and the fact that the source of ERA5 data is large scale model data, the ERA5 data lacks accuracy at the model boundary. Nevertheless, the ERA5 data is spatially varying, it was decided to prefer the Westhinder observation data for the boundary condition.

Figure 12 – Comparison of the significant wave height and peak wave period measured at Westhinder and interpolated from ERA5 data to the Westhinder measurement station



It was already stated that from the perspective of long-term morphological modelling, the use of a JONSWAP spectrum based on timeseries of significant wave height, peak wave period and wave direction is a more practically approach.

A set of 3 tests with different boundary directional spreading values of 10, 4 and 2 were carried out, and the modelled significant wave heights were validated against the measured ones in Figure 14, Figure 15 and Figure 16 respectively. All the 3 tests are observed to produce quite equivalent results, which have a good agreement with the measured data. The factor 2 as default value gives the best results.

In the runs below, the model is not yet coupled to the hydrodynamic model for the tidal variation in water levels and currents. Instead the measured water levels at Westhinder, Figure 13, are imposed spatially constant through the whole domain.

Figure 13 – Observed water level at the measurement station Westhinder November 2015

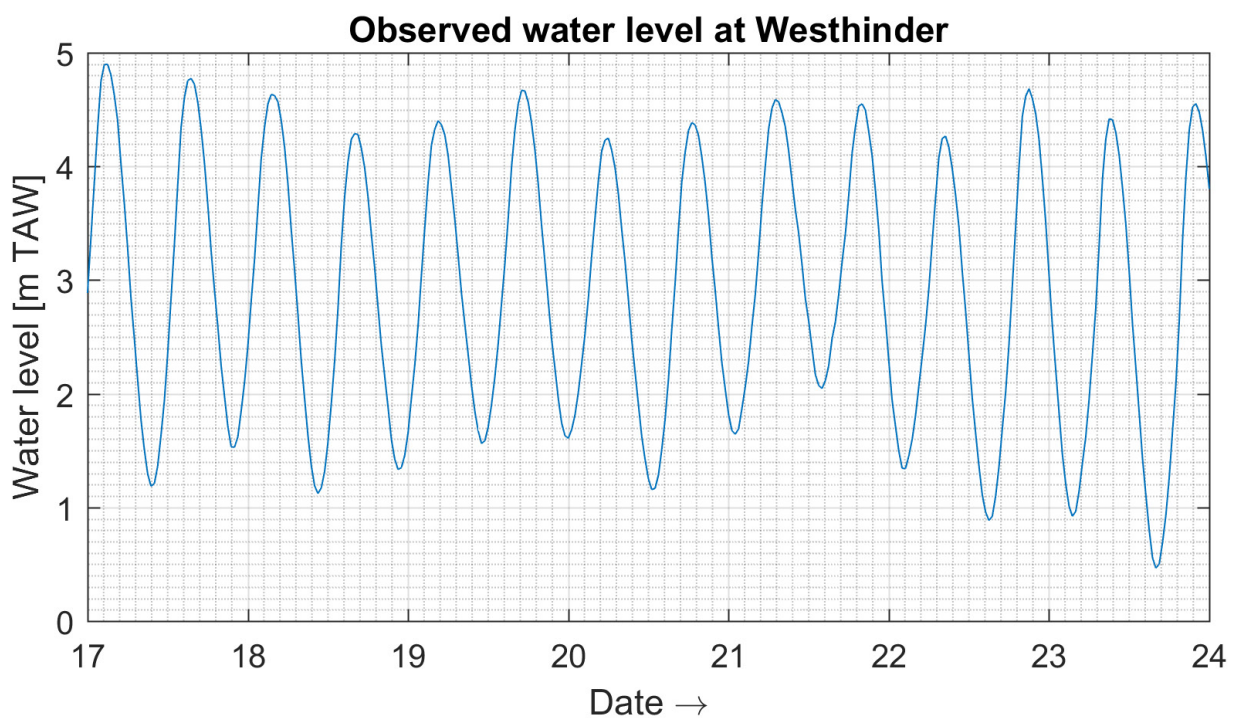


Figure 14 – Comparison of significant wave height between the observed data and modelled results (T010b) at measurement stations, with boundary directional factor 10 for JONSWAP spectrum.

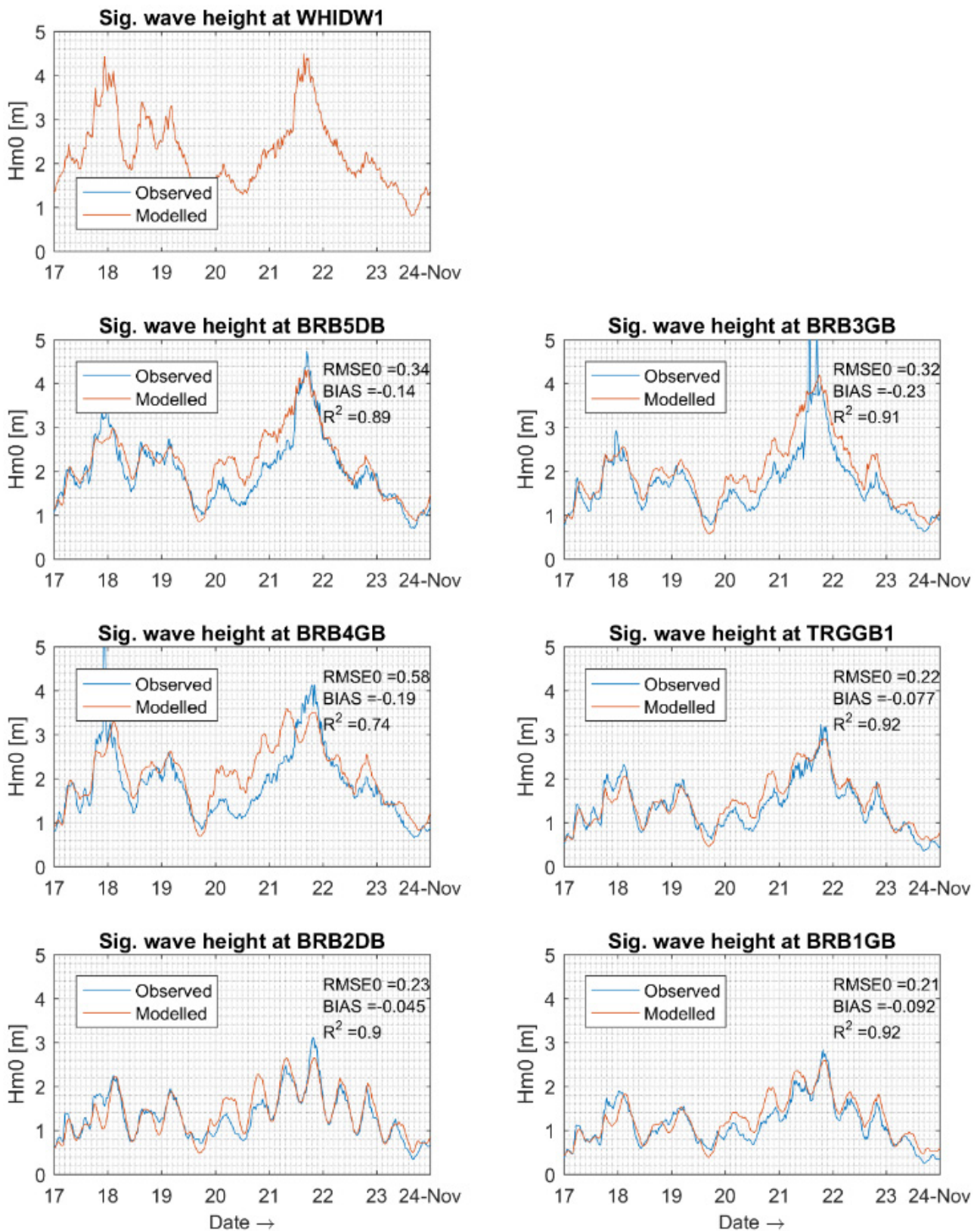


Figure 15 – Comparison of significant wave height between the observed data and modelled results (T010c) at measurement stations, with boundary directional factor 4 for JONSWAP spectrum.

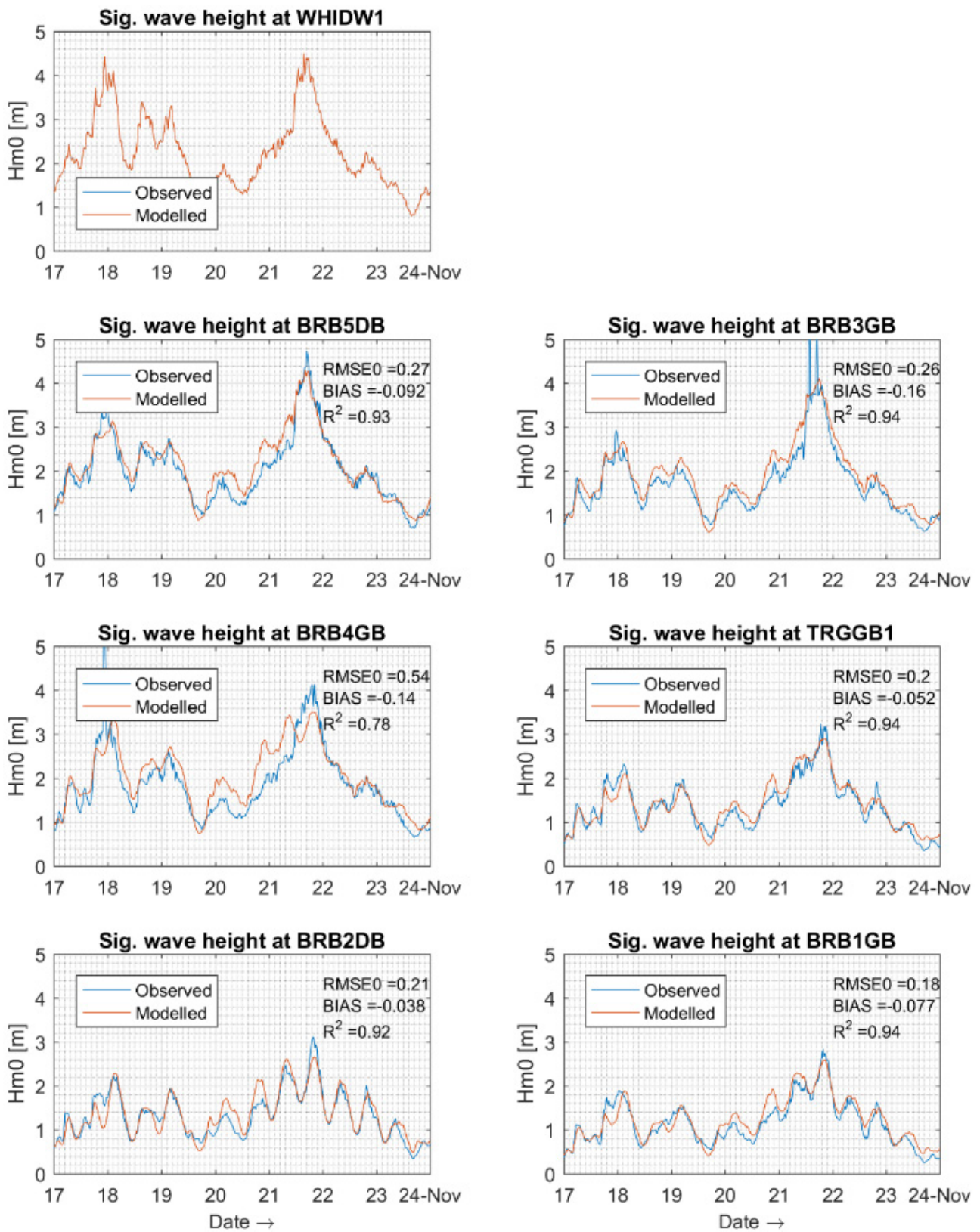


Figure 16 – Comparison of significant wave height between the observed data and modelled results (T010f) at measurement stations, with boundary directional factor 2 for JONSWAP spectrum.

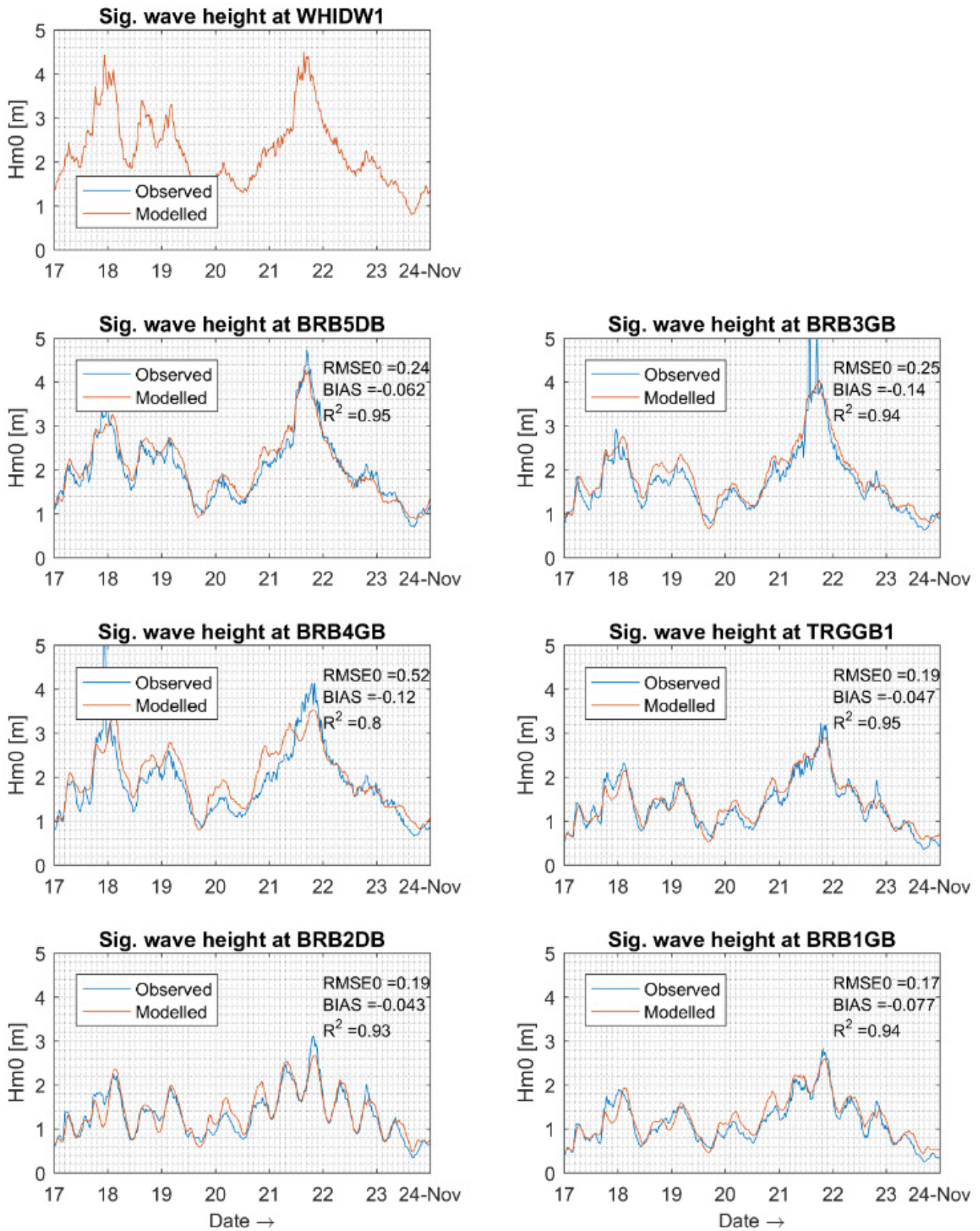
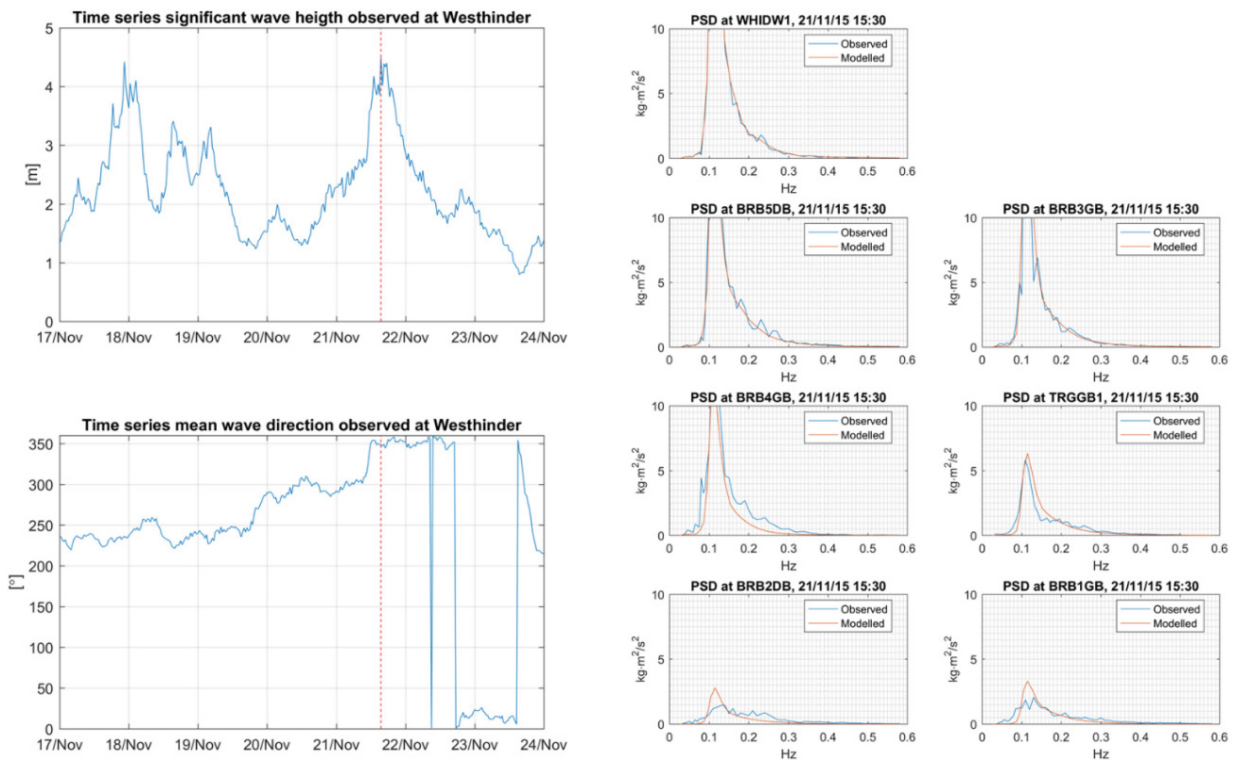


Figure 17 – Observed and modelled power spectral density (PSD) at the storm wave from north in the simulation period



## 4.2 Sensitivity tests

In addition to the options for the parameters listed in Table 3, other options for some of parameters were also tested in search of best performance for the wave model.

Firstly, the option for DEPTH-INDUCED BREAKING DISSIPATION was changed from Battjes and Janssen model (1978) to Thornton and Guza model (1983), Roelvink model (1993), and Izumiya and Horikawa model (1984) one after another. The modelled significant wave height and peak wave period of the sensitivity tests are presented Figure 18 to Figure 23. Compared to the original option Battjes and Janssen model (1978), the option Guza model (1983) produced much lower significant wave height, but a better agreement with observed peak wave period. The significant wave height produced by Roelvink model (1993) is also slightly lower than that produced by Battjes and Janssen model (1978). Nevertheless, the modelled results of Izumiya and Horikawa model are quite comparable with those from Battjes and Janssen model (1978).

Secondly, as a set of parameters, WIND GENERATION and WHITE CAPPING DISSIPATION were tested with new options. The option van der Westhuysen (2007) for WHITE CAPPING DISSIPATION was replaced by a new option Komen et al. (1984) and Janssen (1991), which has been combined with another two new options WAM cycle 3 and 4 formula respectively for WIND GENERATION. The modelled results produced by these two options are quite similar (Figure 25 ~ Figure 28). Compared to the original option van der Westhuysen (2007) combined with Yan (1987), the new options produce almost equivalent significant wave height and peak wave period.

Figure 18 – Comparison of significant wave height between the observed data and modelled results (T009c1) at measurement stations, with Thornton and Guza model (1983) for DEPTH-INDUCED BREAKING DISSIPATION

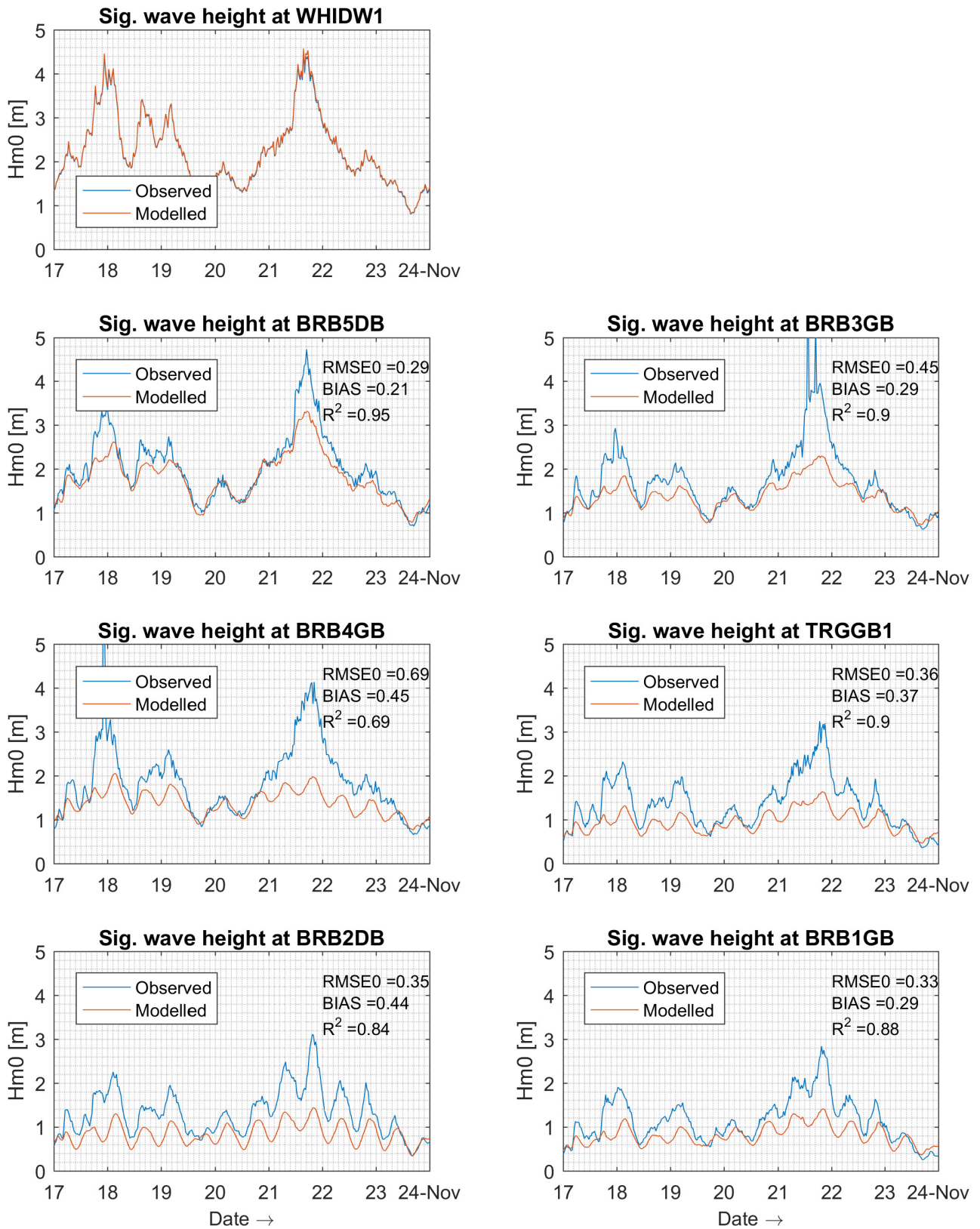


Figure 19 – Comparison of peak wave period between the observed data and modelled results (T009c1) at measurement stations, with Thornton and Guza model (1983) for DEPTH-INDUCED BREAKING DISSIPATION

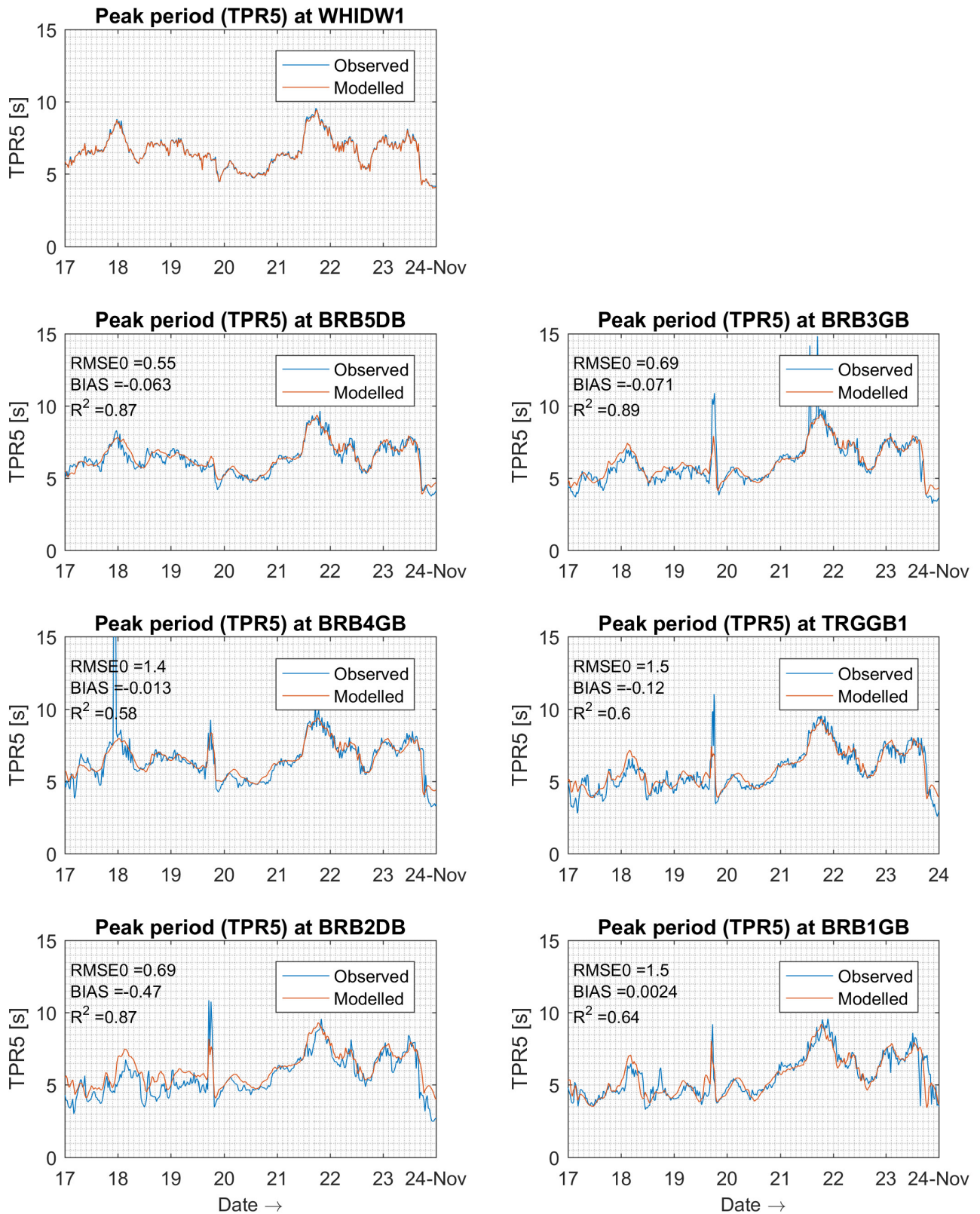


Figure 20 – Comparison of significant wave height between the observed data and modelled results (T009c2) at measurement stations, with Roelvink model (1993) for DEPTH-INDUCED BREAKING DISSIPATION

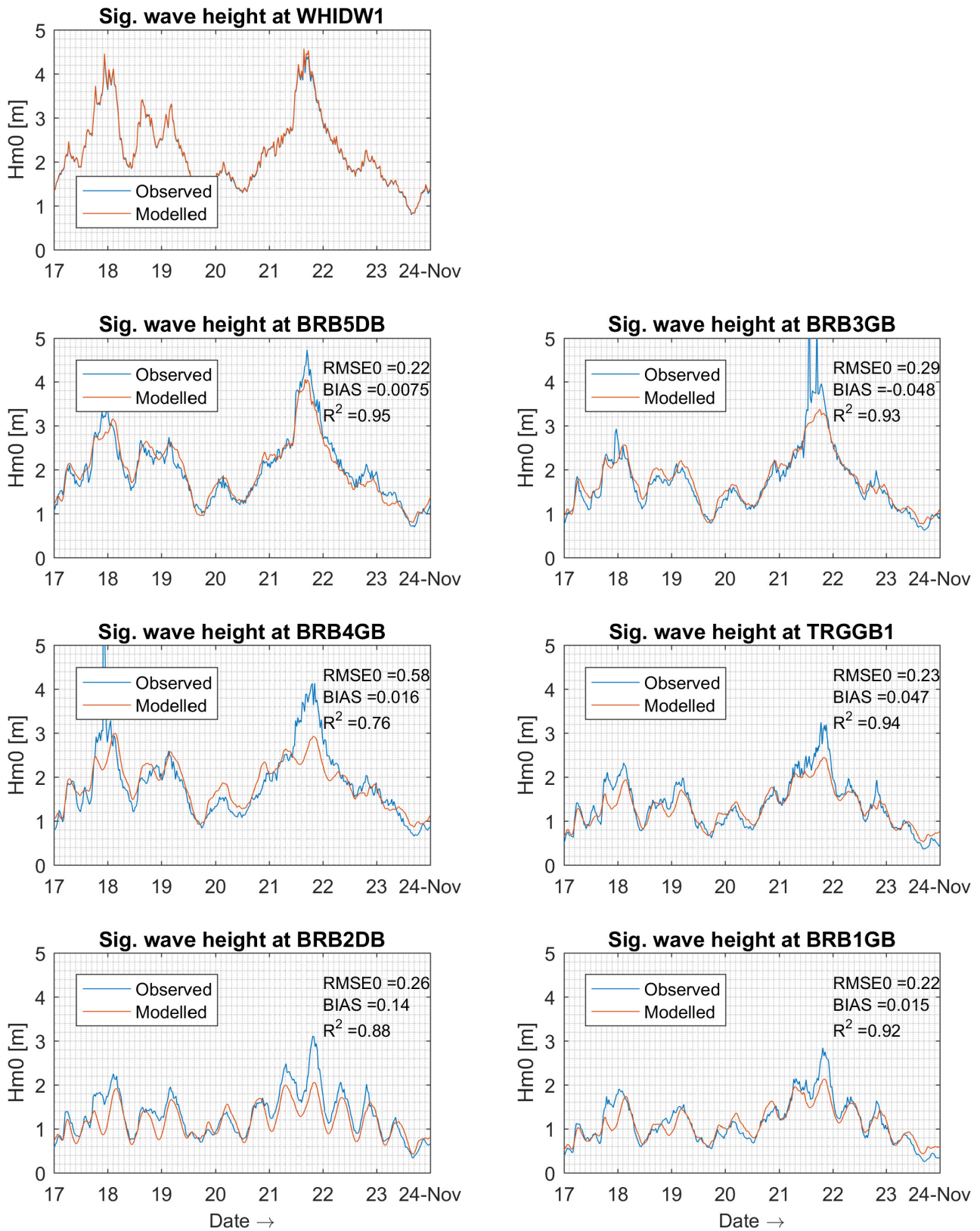


Figure 21 – Comparison of peak wave period between the observed data and modelled results (T009c2) at measurement stations, with Roelvink model (1993) for DEPTH-INDUCED BREAKING DISSIPATION

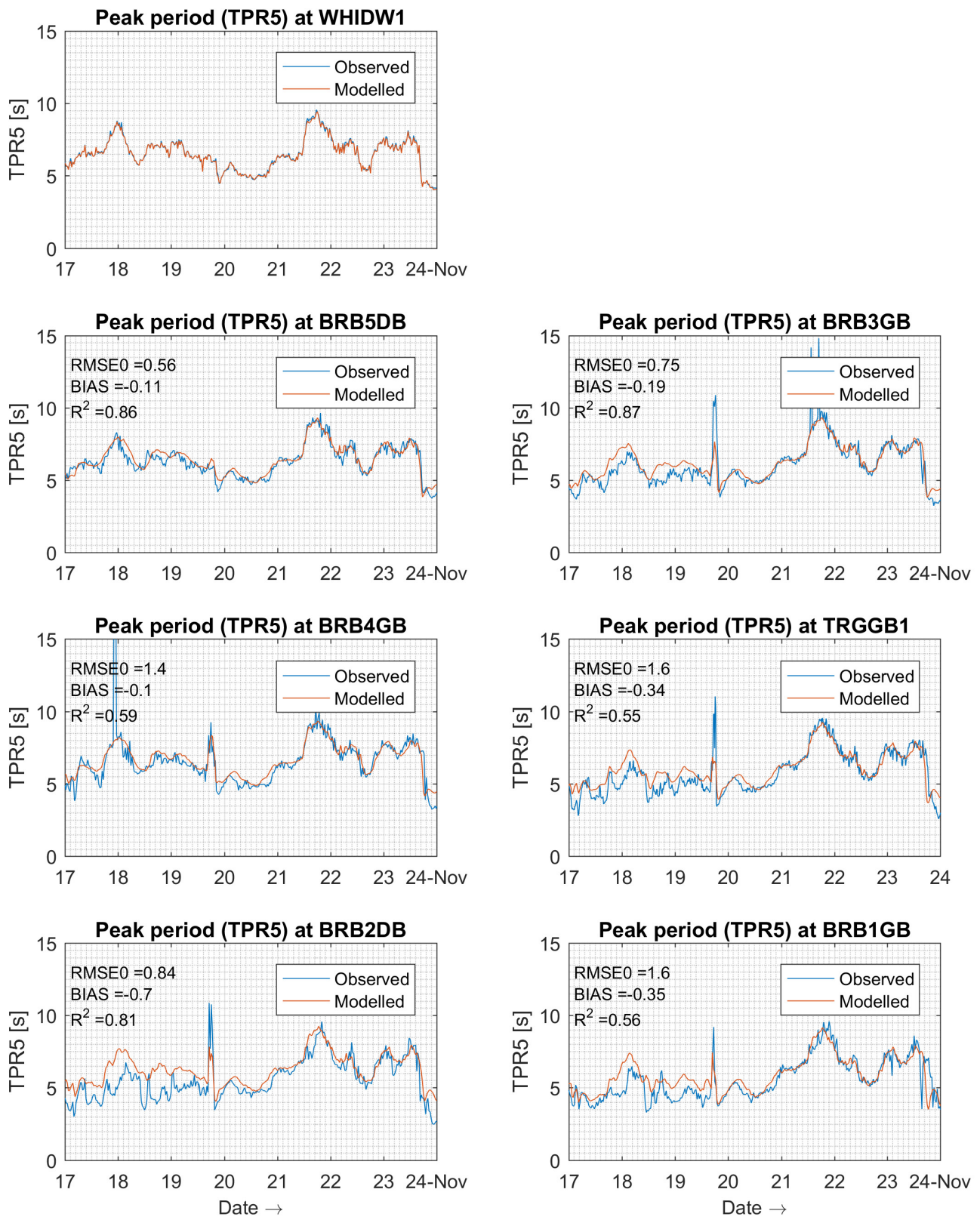


Figure 22 – Comparison of significant wave height between the observed data and modelled results (T009c3) at measurement stations, with Izumiya and Horikawa model (1984) for DEPTH-INDUCED BREAKING DISSIPATION

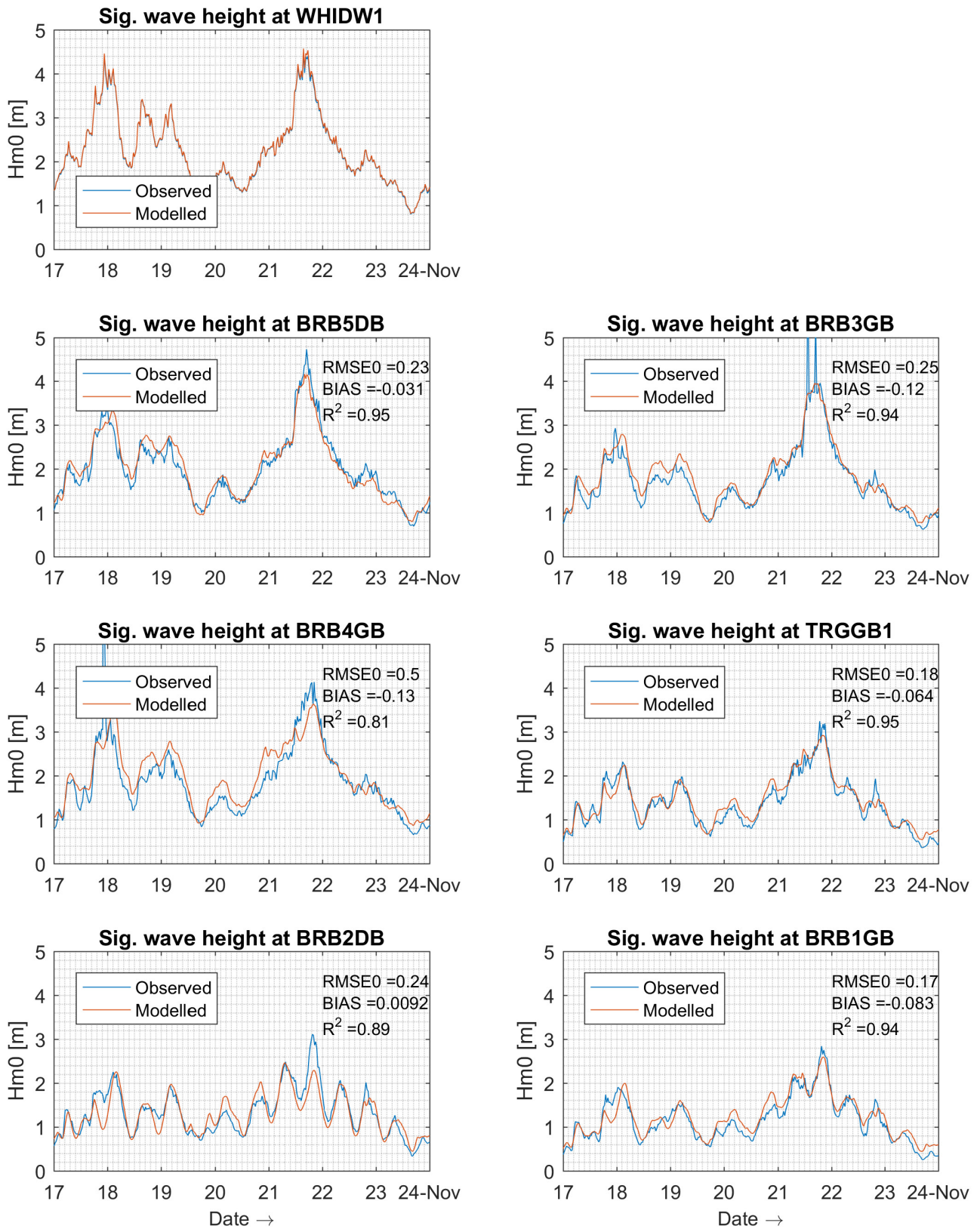


Figure 23 – Comparison of peak wave period between the observed data and modelled results (T009c3) at measurement stations, with Izumiya and Horikawa model (1984) for DEPTH-INDUCED BREAKING DISSIPATION

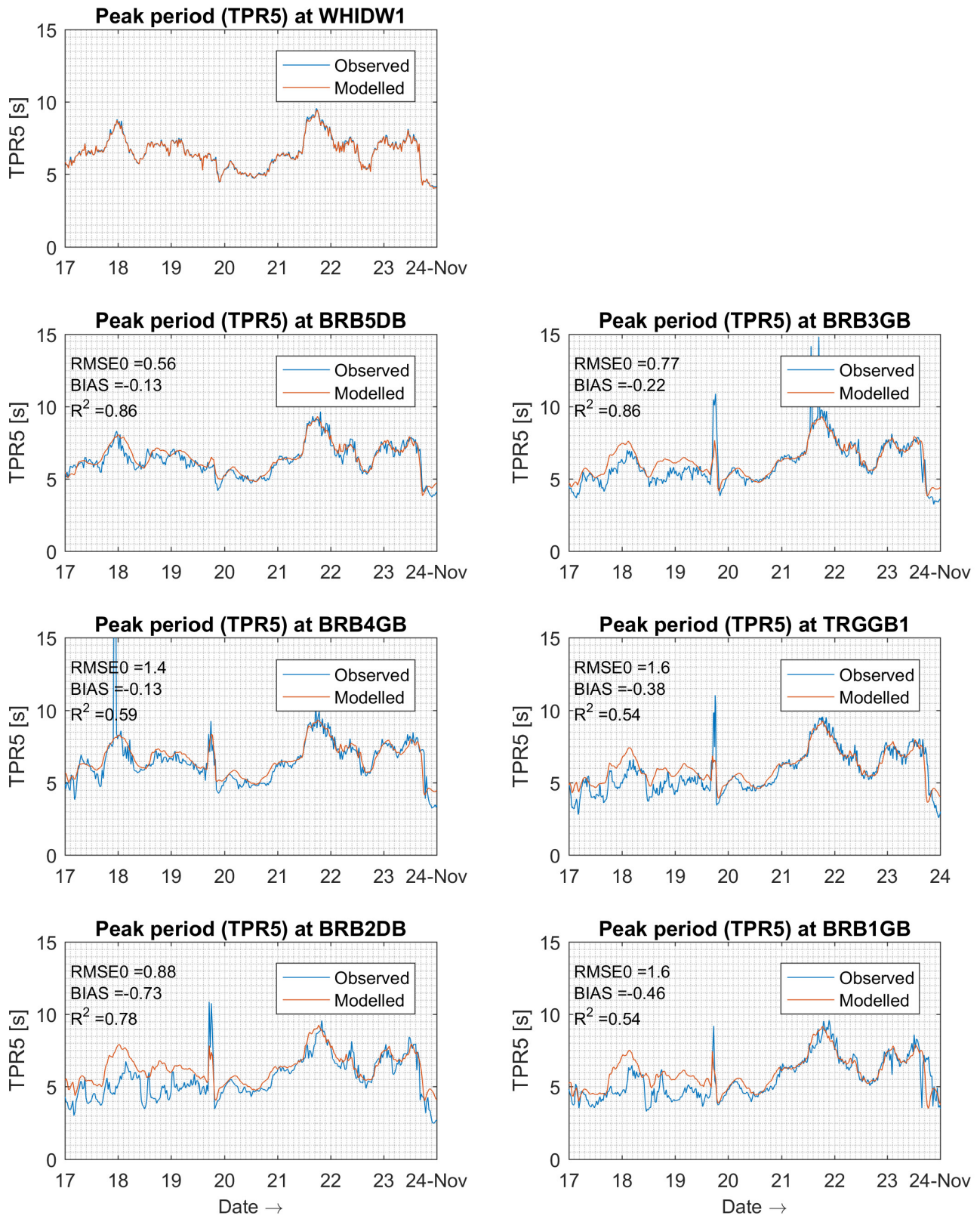


Figure 24 – RMSE0 of different models for DEPTH-INDUCED BREAKING DISSIPATION at measurement stations, upper: significant wave height, lower: peak wave period.

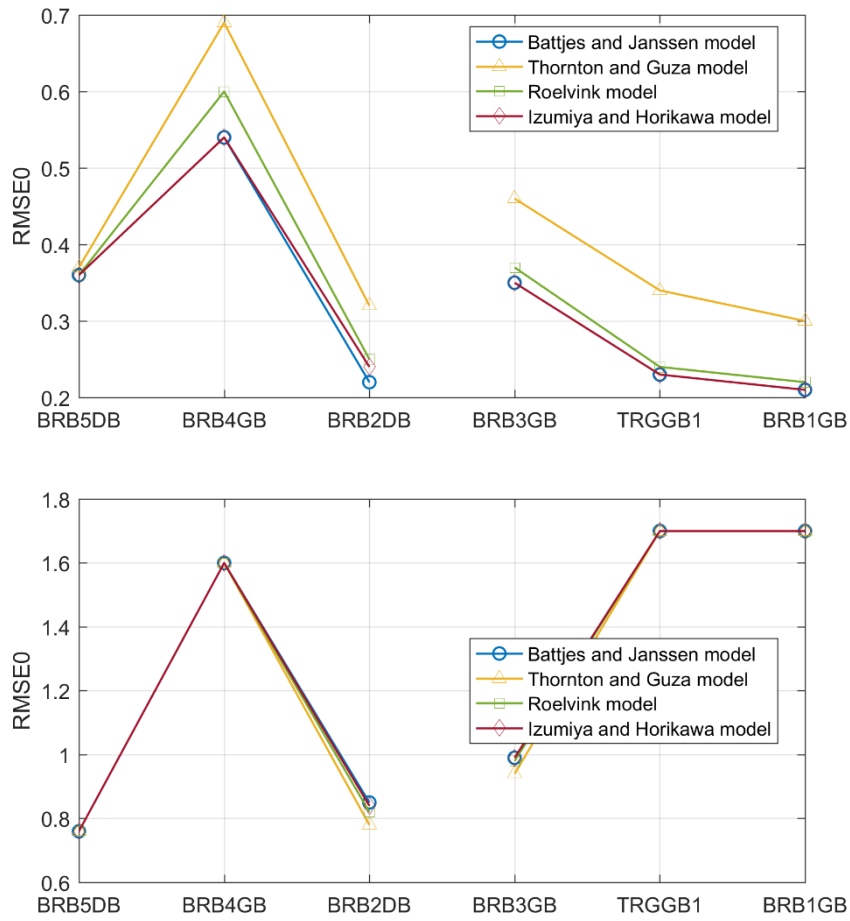


Figure 25 – Comparison of significant wave height between the observed data and modelled results (T009c4) at measurement stations, with WAM cycle 4 formula for WIND GENERATION, and Komen et al. (1984) and Janssen (1991) for WHITE CAPPING DISSIPATION

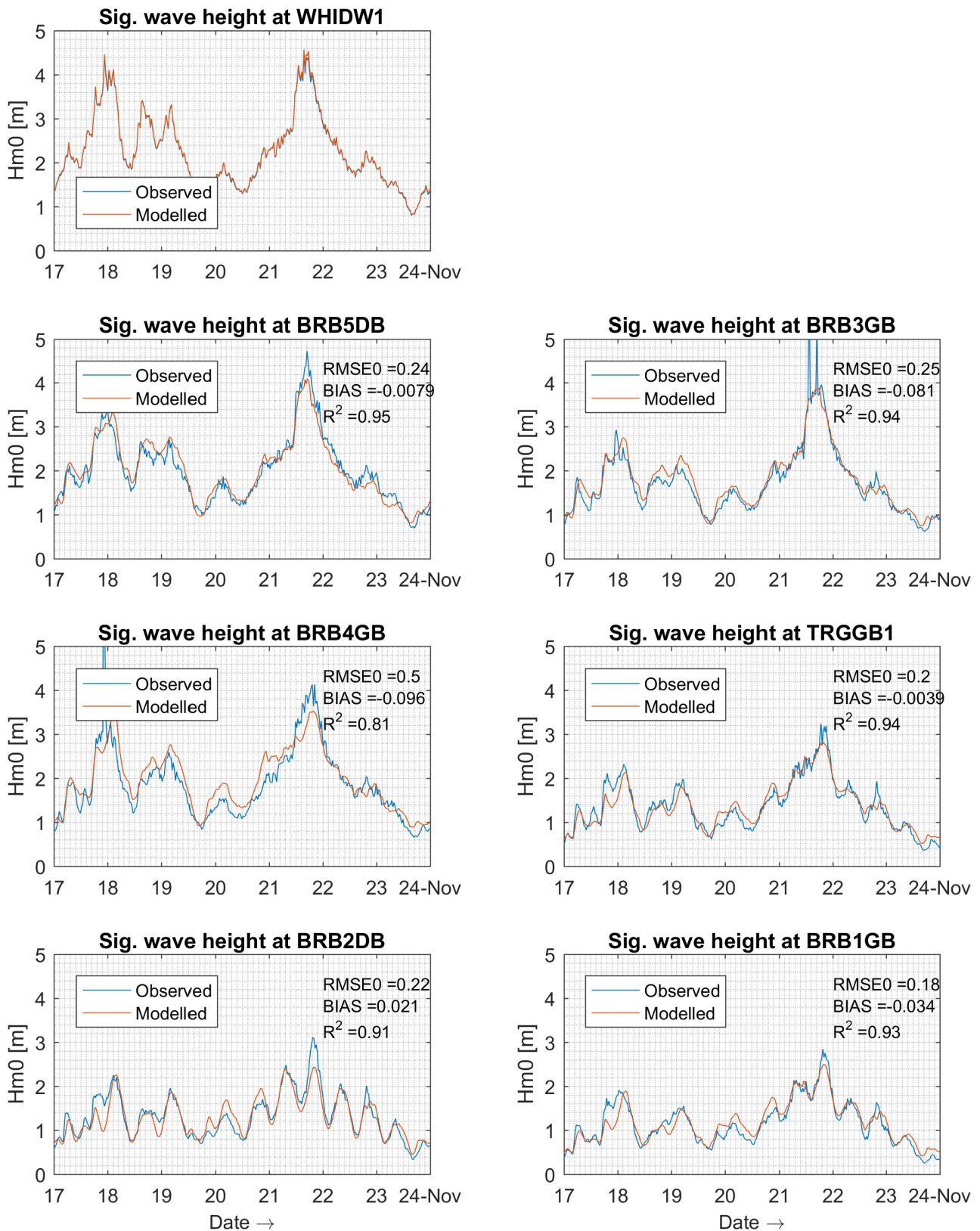


Figure 26 – Comparison of peak wave period between the observed data and modelled results (T009c4) at measurement stations, with WAM cycle 4 formula for WIND GENERATION, and Komen et al. (1984) and Janssen (1991) for WHITE CAPPING DISSIPATION

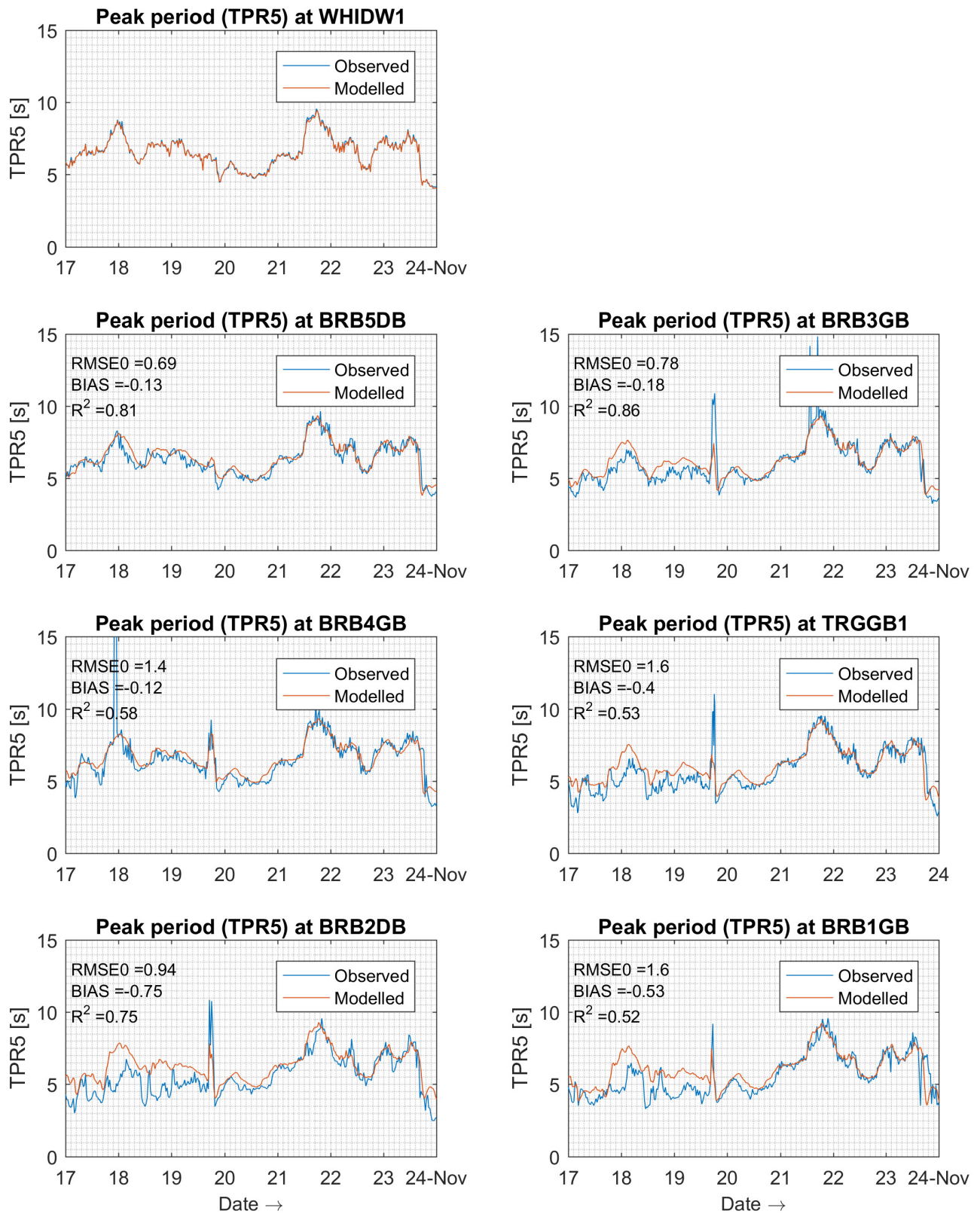


Figure 27 – Comparison of significant wave height between the observed data and modelled results (T009c5) at measurement stations, with WAM cycle 3 formula for WIND GENERATION, and Komen et al. (1984) and Janssen (1991) for WHITE CAPPING DISSIPATION

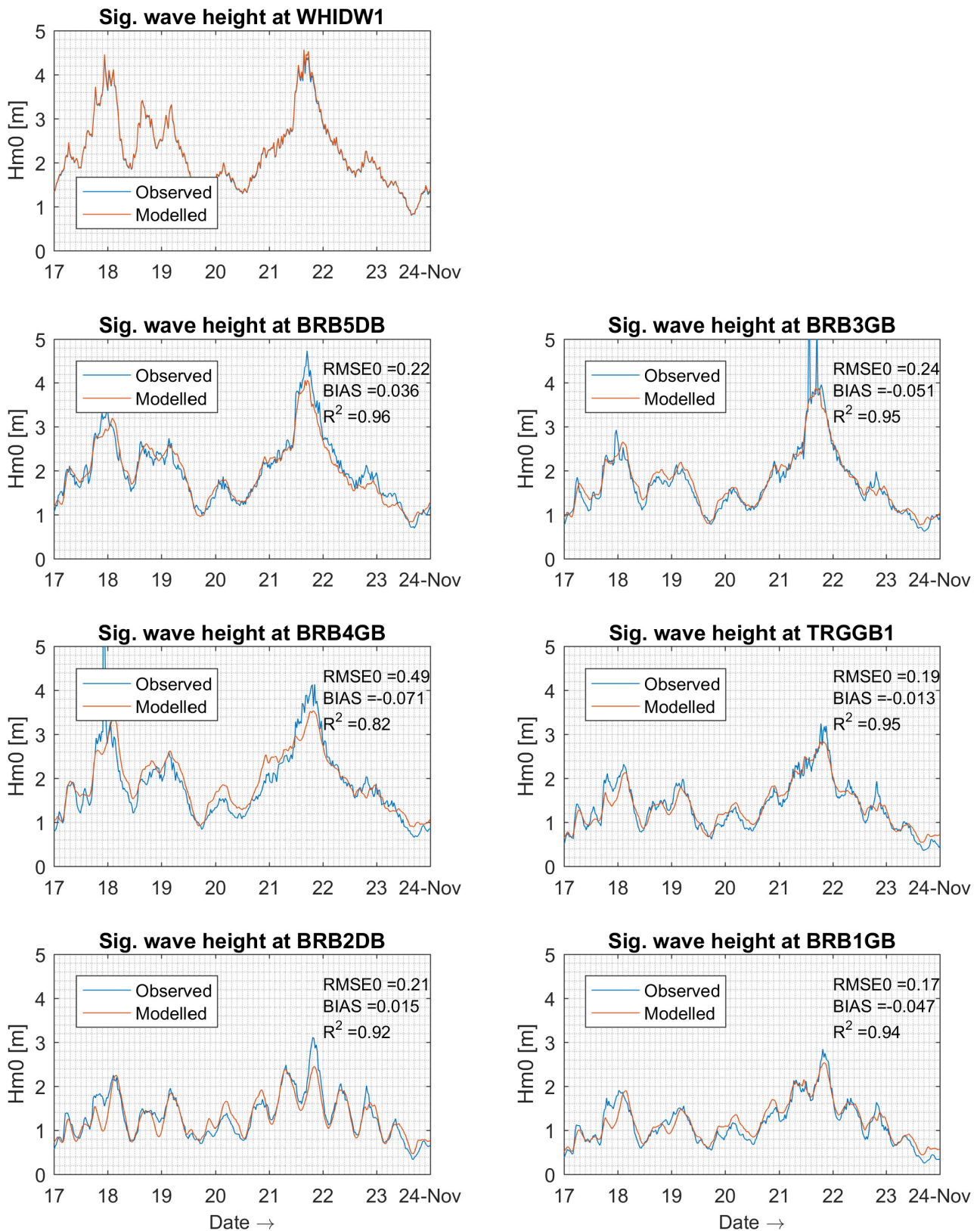


Figure 28 – Comparison of peak wave period between the observed data and modelled results (T009c5) at measurement stations, with WAM cycle 3 formula for WIND GENERATION, and Komen et al. (1984) and Janssen (1991) for WHITE CAPPING DISSIPATION

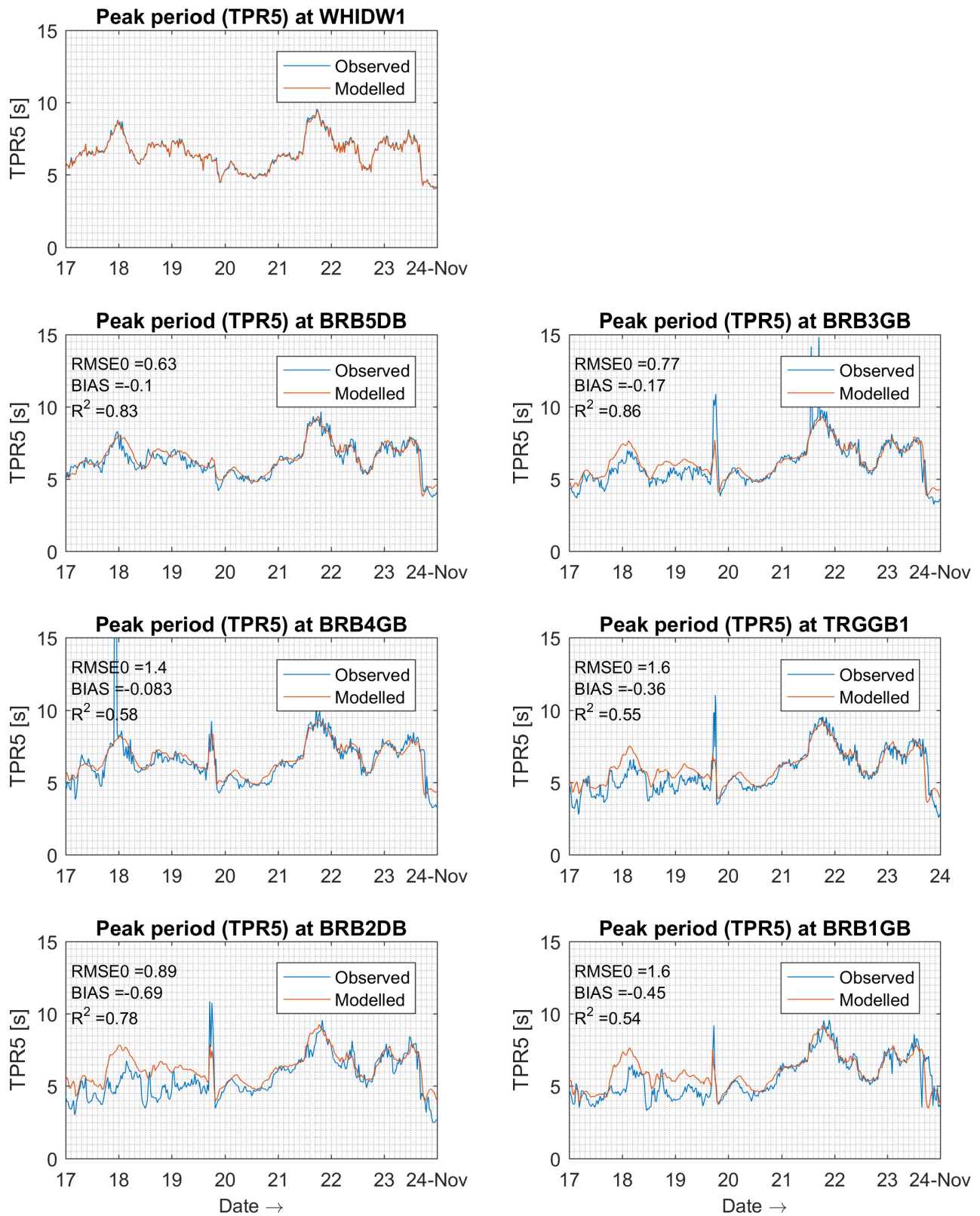
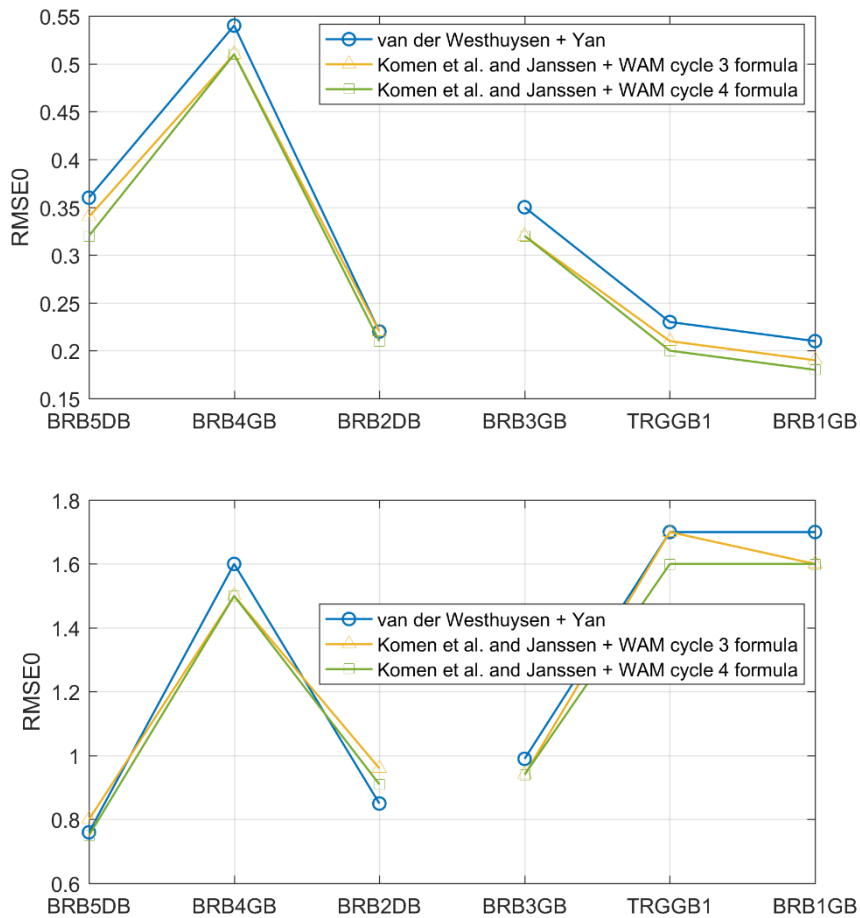


Figure 29 – RMSE0 of different combination for WIND GENERATION and WHITE CAPPING DISSIPATION at measurement stations, upper: significant wave height, lower: peak wave period.



### 4.3 Computation time and parallelization performance

The parallelization performance of the TOMAWAC model has been investigated in this section. Five test wave simulations were performed on 1, 12, 24, 48 and 96 cores respectively (one serial and four parallel simulations). The computational time versus the number of utilized cores is shown in Figure . Two metrics for the evaluation of the parallelization performance are the following:

- Speedup index ( $S_p$ ), which is defined as the ratio between the computational time of the serial run (1 core) and the computational time of a parallel run;
- Performance ( $\alpha_p$ ), which is defined as the ratio between the Speedup and the number of the cores ( $S_p/n_{cpu}$ ).

The Speedup and the Performance versus the number of cores are presented in Figure . A theoretically perfect parallelization would give  $S_p$  values on the black line of the left figure. However, in practice the Speedup values decrease evidently when the number of cores becomes very high (96 cores). The decrease seems to be linear within 24 cores.

Although the value of  $\alpha_p$  drops quite fast when the number of cores exceeds 24, the absolute computational time can be still reduced by half when the number of cores is increased to 96. Compared to the hydrodynamical TELEMAC2D model, the wave model shows a better parallel performance (G. Kolokythas *et al.*, 2021a). Apart from the fact that the wave model here has a different resolution and domain, this can also

be attributed to the spectral nature of the wave propagation model, i.e. a lot more computational load on nodal base. This is advantageous for the morphodynamic modelling where typically the wave module is the bottleneck with respect to computation time in long term morphodynamic modelling.

Figure 30 – Computational time versus the number of cores utilized for the parallel test runs.

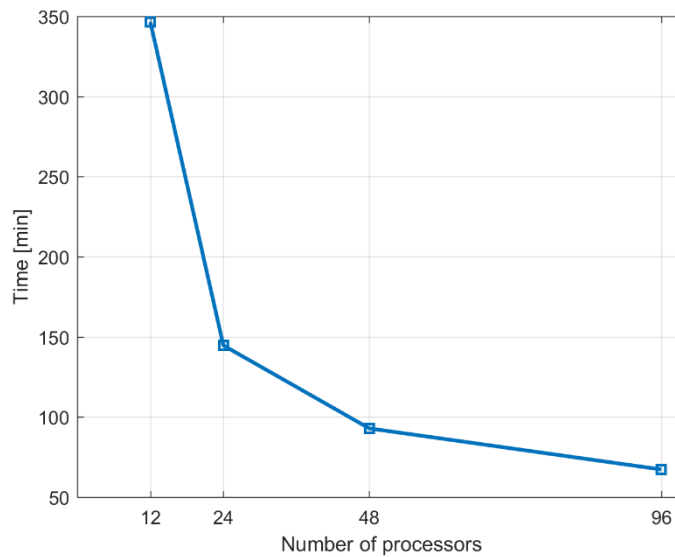
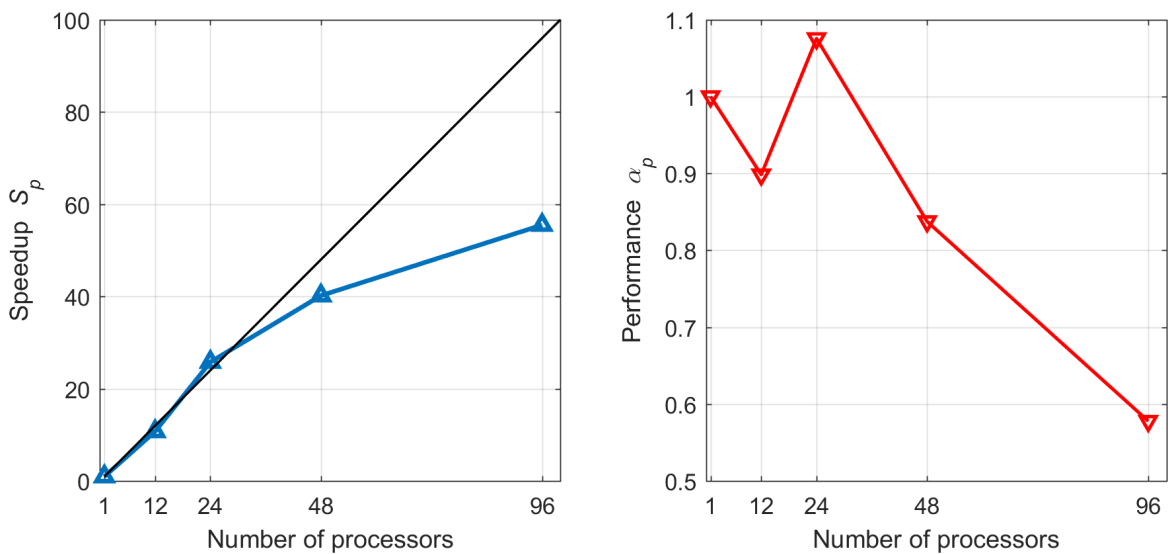


Figure 31 – Speedup ( $S_p$ ) versus the number of cores (left figure) and Performance ( $\alpha_p$ ) versus the number of cores utilized for the parallel test runs.



## 4.4 Coupled simulation of TELEMAC2D and TOMAWAC

In view of the validation against observed data, the stand-alone TOMAWAC model has shown satisfactory results when tidal variation of the water level was taken into account. In order to earn better insights on how the coupling can possibly influence the wave simulation, the TOMAWAC model was firstly coupled with only water level computed by the TELEMAC2D hydrodynamic model, and further coupled with both water level and current velocity computed by TELEMAC2D.

### 4.4.1 Coupled with water level only

The coupled model was set up with influence of only water level on waves. The feedback of waves to hydrodynamics (i.e. wave setup and wave driven current) was always considered during the coupled simulation. The comparison of significant wave height between the simulation and observation is presented in Figure 32. It can be observed that the RMSE0 at the two nearshore stations BRB2DB and BRB1GB reaches 0.25 and 0.26, which are a little higher than 0.21 and 0.18 from the stand-alone wave simulation (Figure 33). The peaks of the significant wave height are overestimated in particular by the coupled simulation.

In order to explore such differences, a number of test runs have been carried out (results are not shown here). The variable  $dH/dt$  as water depth derivative with respect to time is found to be exaggerated very much by a wrong code in the routine *cormar.f* of TOMAWAC model when the coupled simulation was carried out (Figure 34 vs. Figure 35). After the fixing the bug, the variable  $dH/dt$  displays a good agreement between the coupled and stand-alone simulations, and the modelled significant wave height also becomes almost identical to that from the stand-alone simulation (Figure 36).

Figure 32 – Comparison of significant wave height between the observed data and modelled results (HSW005g) at measurement stations, coupled with water level only.

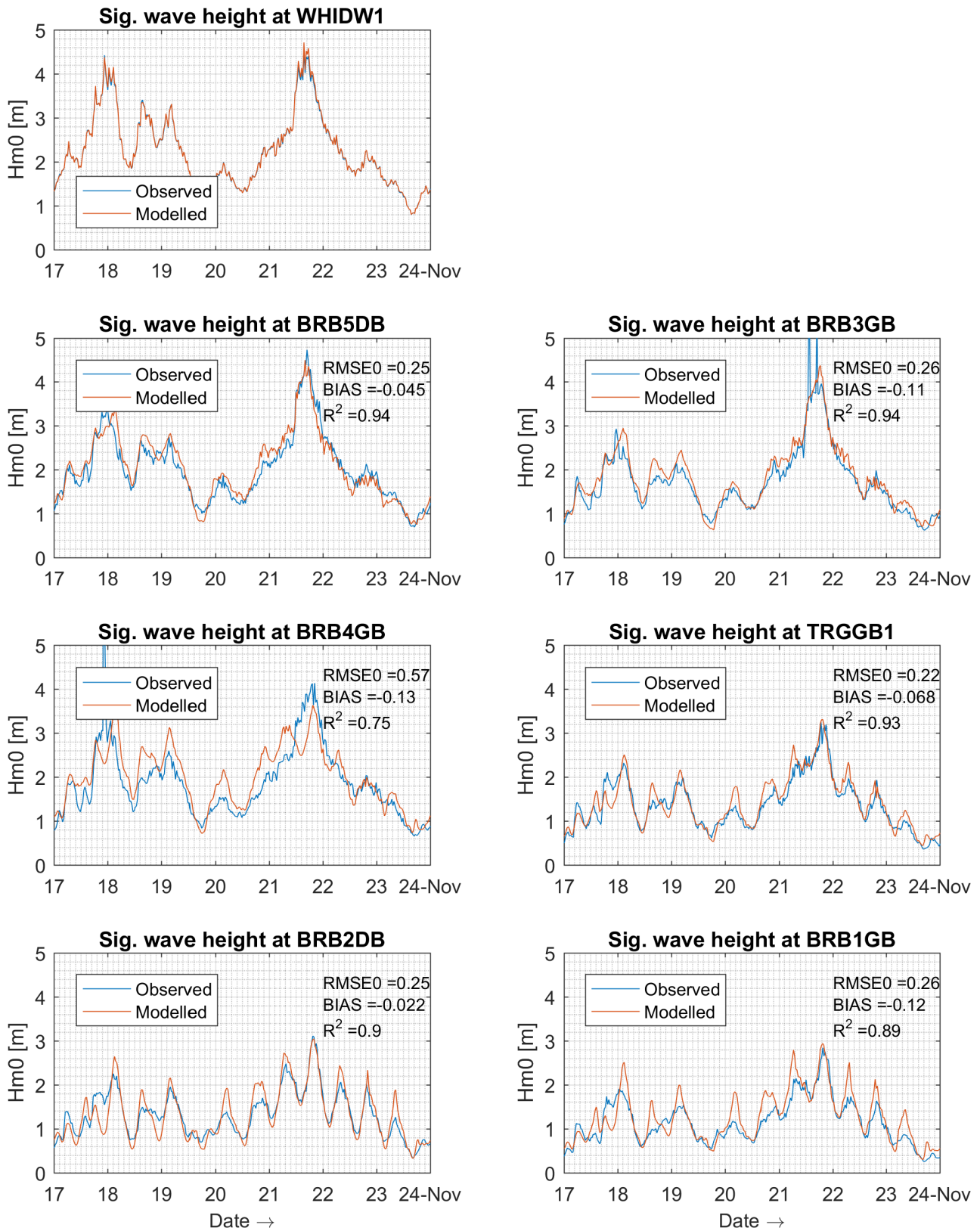


Figure 33 – Comparison of significant wave height between the observed data and modelled results (W002b) at measurement stations, stand-alone wave model with water level inputs

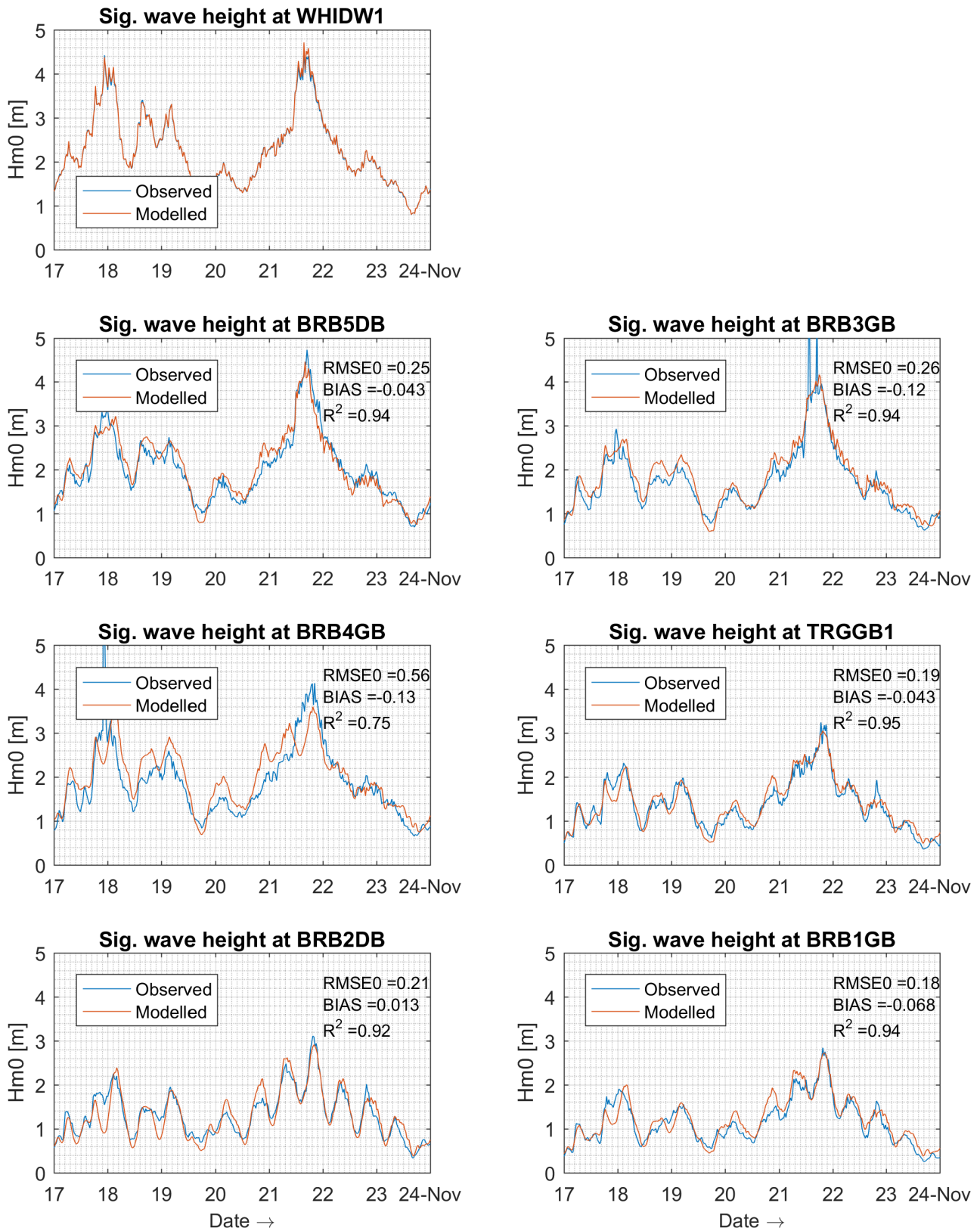


Figure 34 – Comparison of water depth derivative respect to time between the coupled and stand-alone simulations, with original wrong code in the routine cormar.f for coupled simulation.

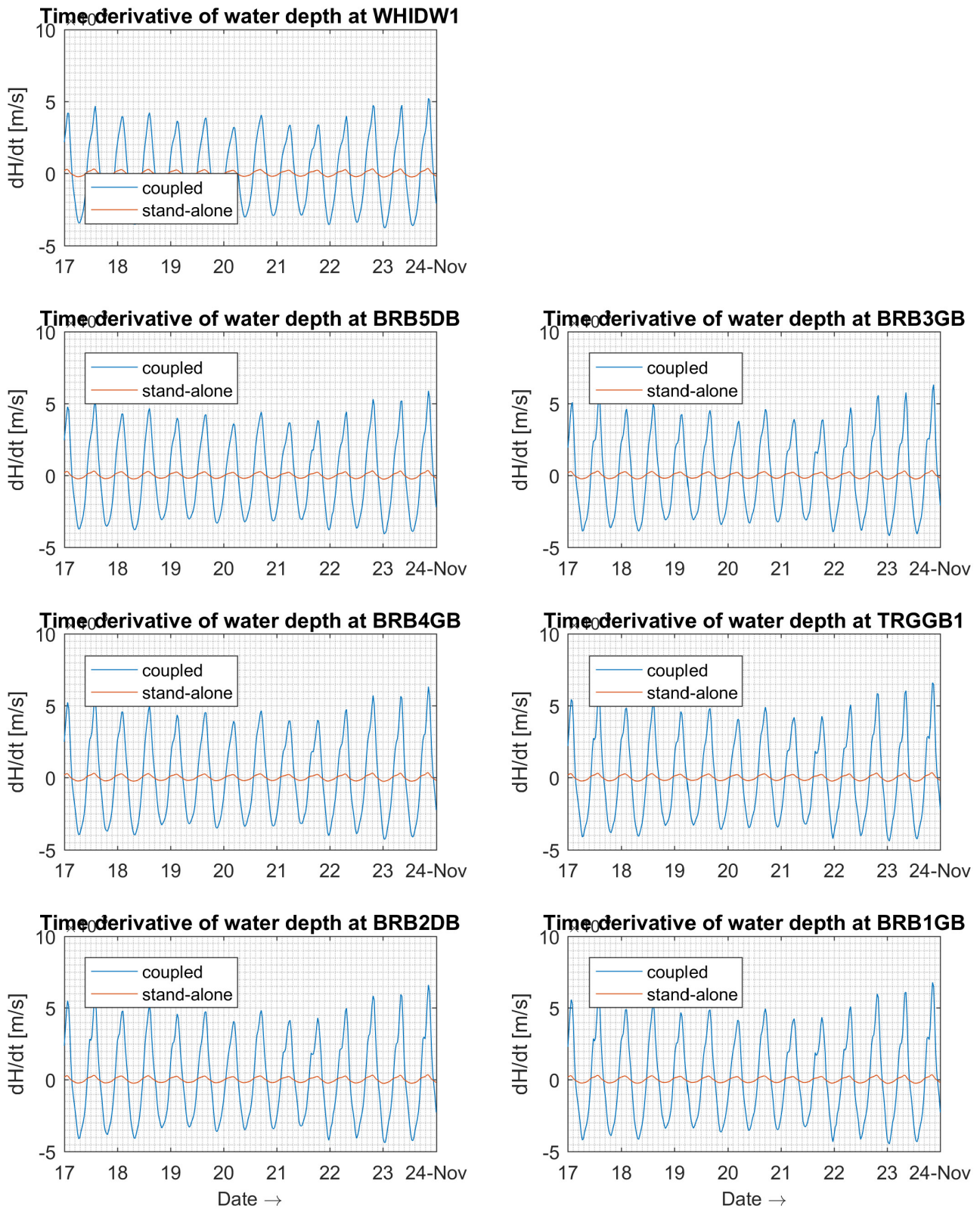


Figure 35 – Comparison of water depth derivative respect to time between the coupled and stand-alone simulations, with fixed code in the routine cormar.f for coupled simulation.

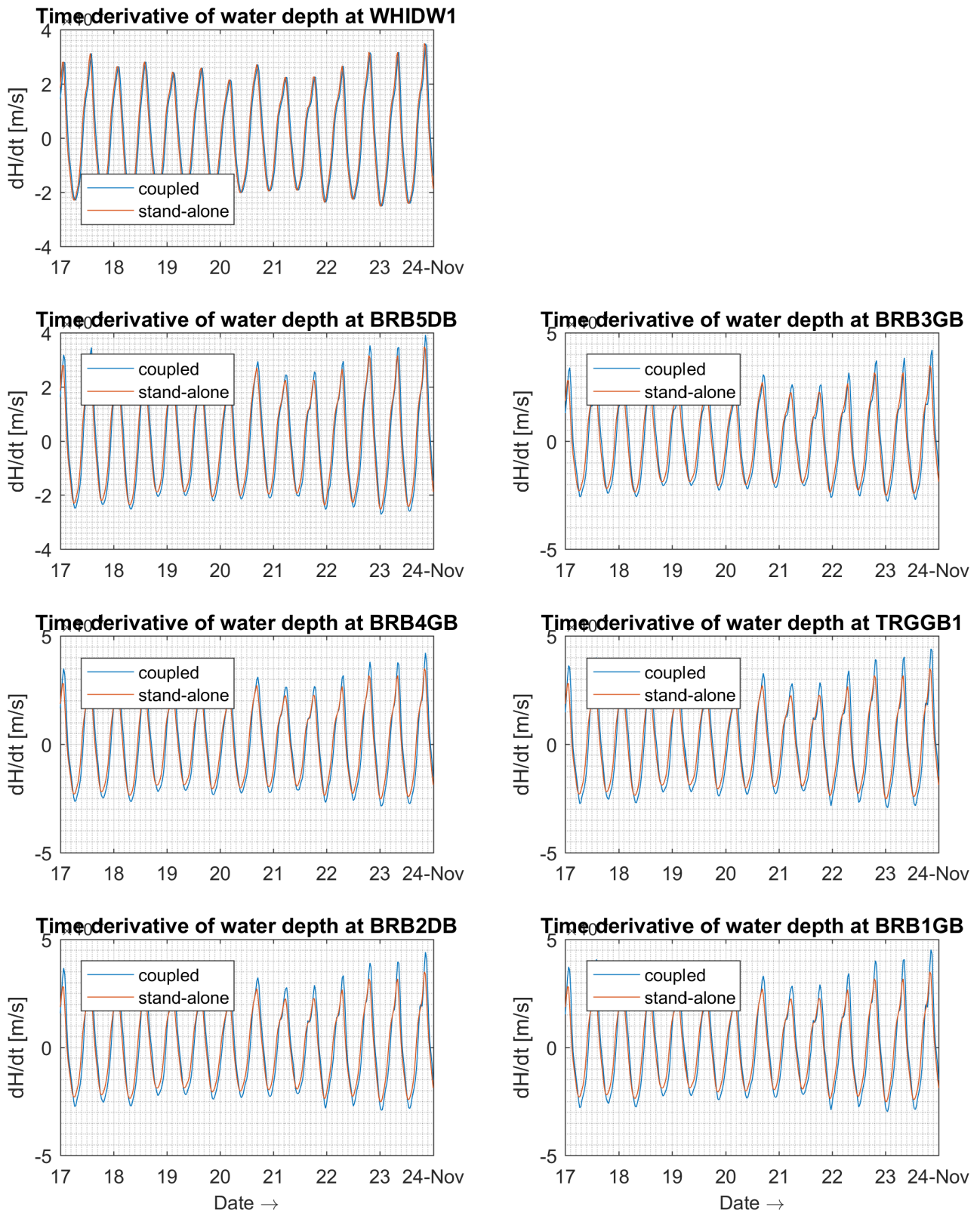
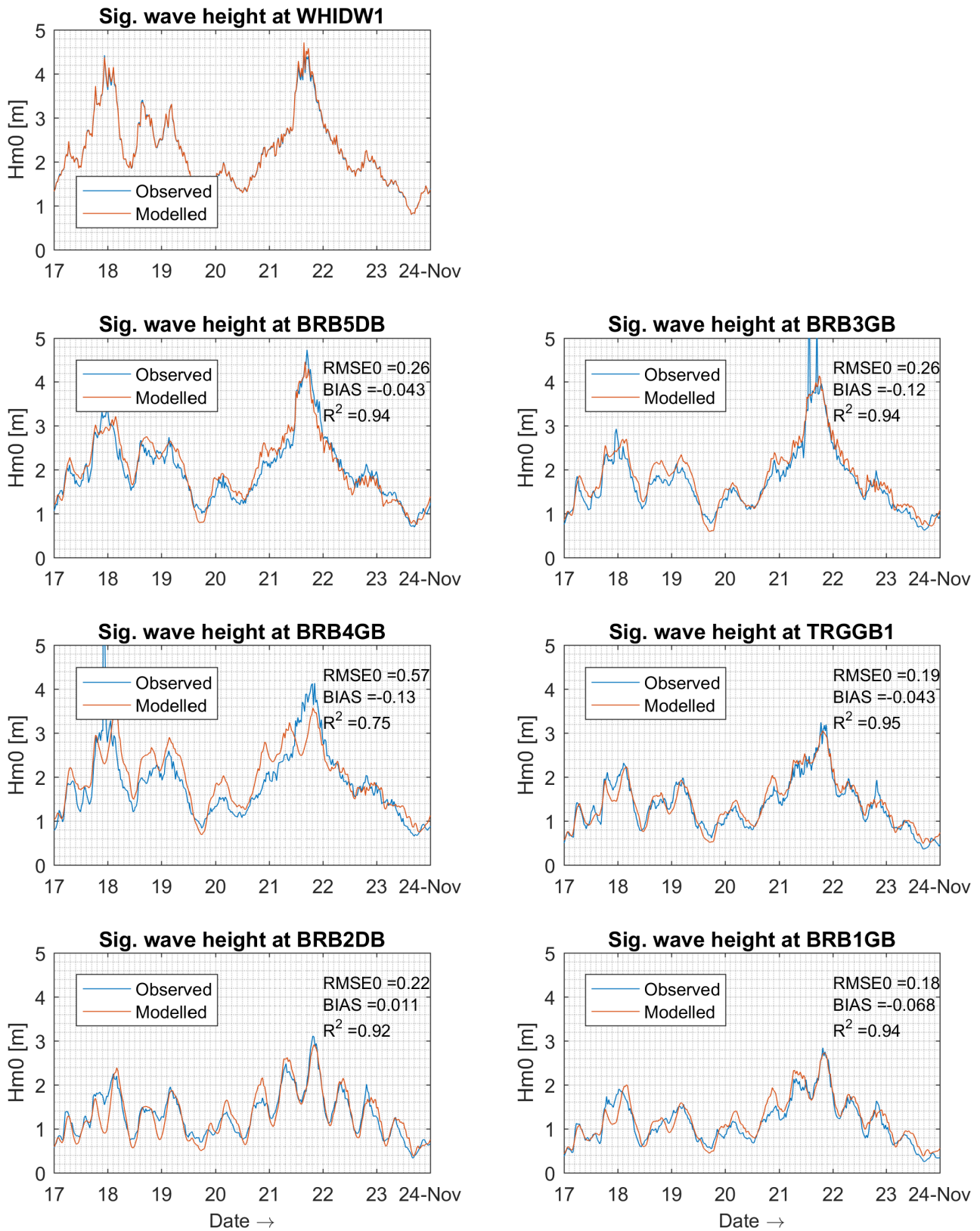


Figure 36 – Comparison of significant wave height between the observed data and modelled results (HSW005s) at measurement stations, with fixed code in the routine cormar.f for coupled simulation.



#### 4.4.2 Coupled with water level and current velocity both

In addition to the influence of water level on waves, the influence of current velocity on waves was also introduced to the coupled model with the correct code fixed for computation of the variable  $dH/dt$  during the coupled simulation.

Figure 37 displays the modelled significant wave height from the coupled simulation. Compared with the last coupled simulation in which only the influence of water level is considered, the RMSE0 at the two nearshore stations BRB2DB and BRB1GB increases evidently (0.30 vs. 0.22, 0.29 vs. 0.18). In order to find out the reason for the poorer performance of the coupled model with influence of water level and current velocity both, many test runs were carried out and special attention was also given to relevant literature.

Linear wave theory shows that there is an extra term for transport of energy to different frequencies in the equations due to accelerating or decelerating currents (Holthuijsen, 2007). If this term is included, the model gives substantially worse results in comparison with the observed data. However, the reason is not clear. A schematic test has been designed to check the implementation of this term in the code. The result shows a good agreement with the theory. Then the implementation of this term does not seem to be a bug in the model. One possible reason may be associated with non-conservation of mass in the aspect of numerical computation, which needs a further investigation. In the current model the terms associated to  $\partial \vec{U} / \partial n$  and  $\partial \vec{U} / \partial s$  are ignored in the the modified routine *conw4d.f*.

Figure 37 – Comparison of significant wave height between the observed data and modelled results (HSW009f) at measurement stations, coupled with water level and current velocity both.

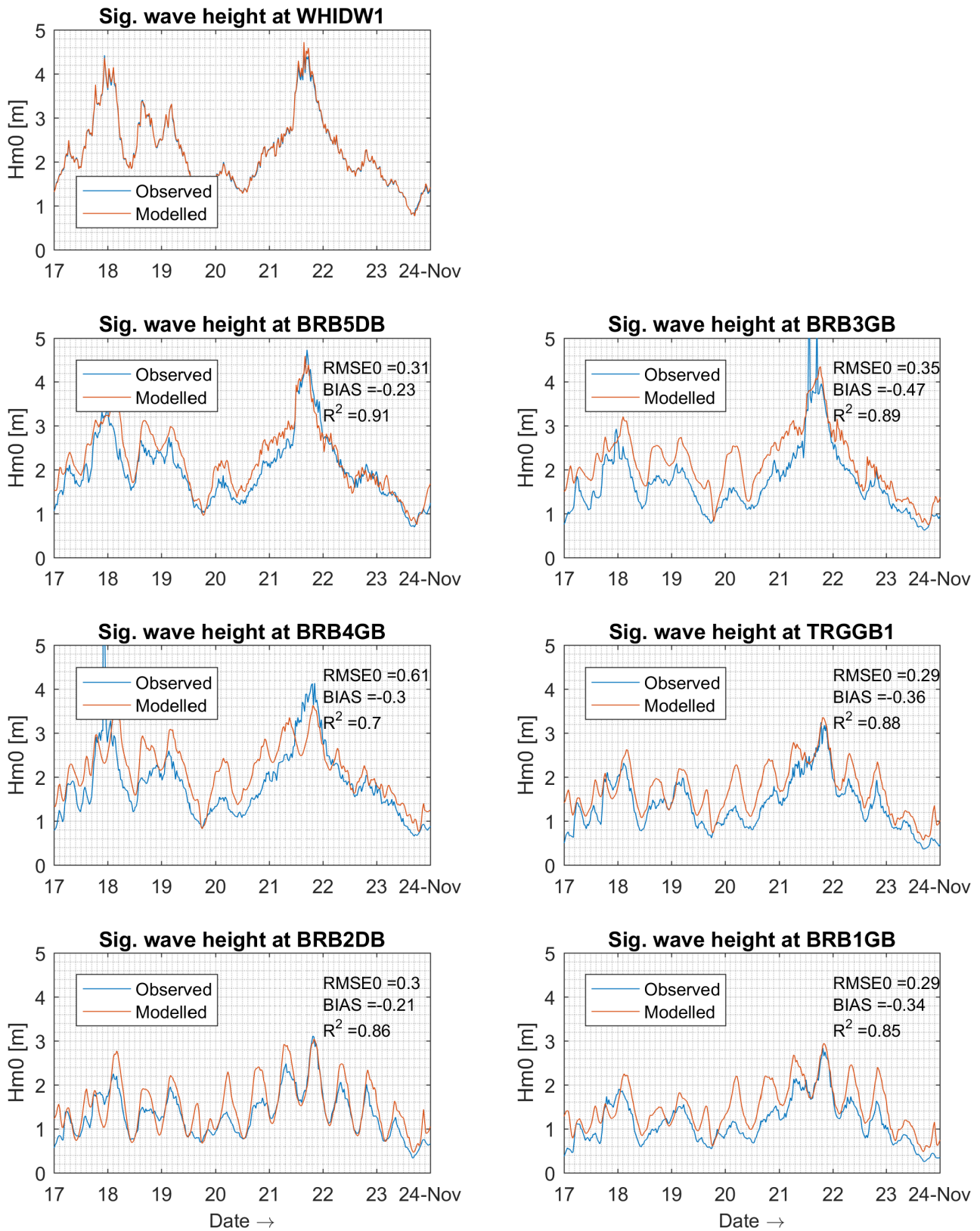


Figure 38 – Comparison of significant wave height between the observed data and modelled results (HSW009I) at measurement stations, coupled with water level and current velocity both but without consideration of energy transfer between frequencies due to accelerating and decelerating currents.

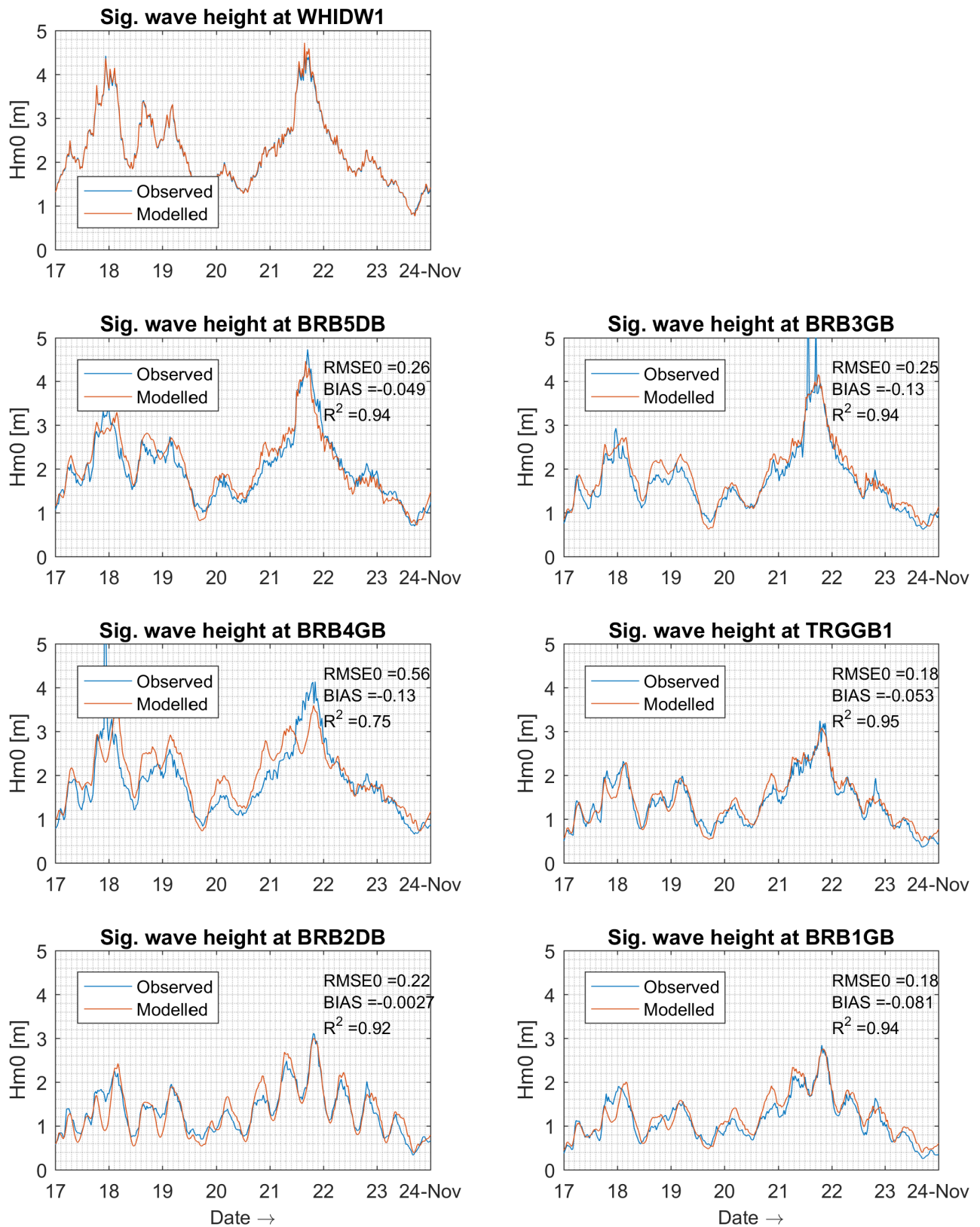
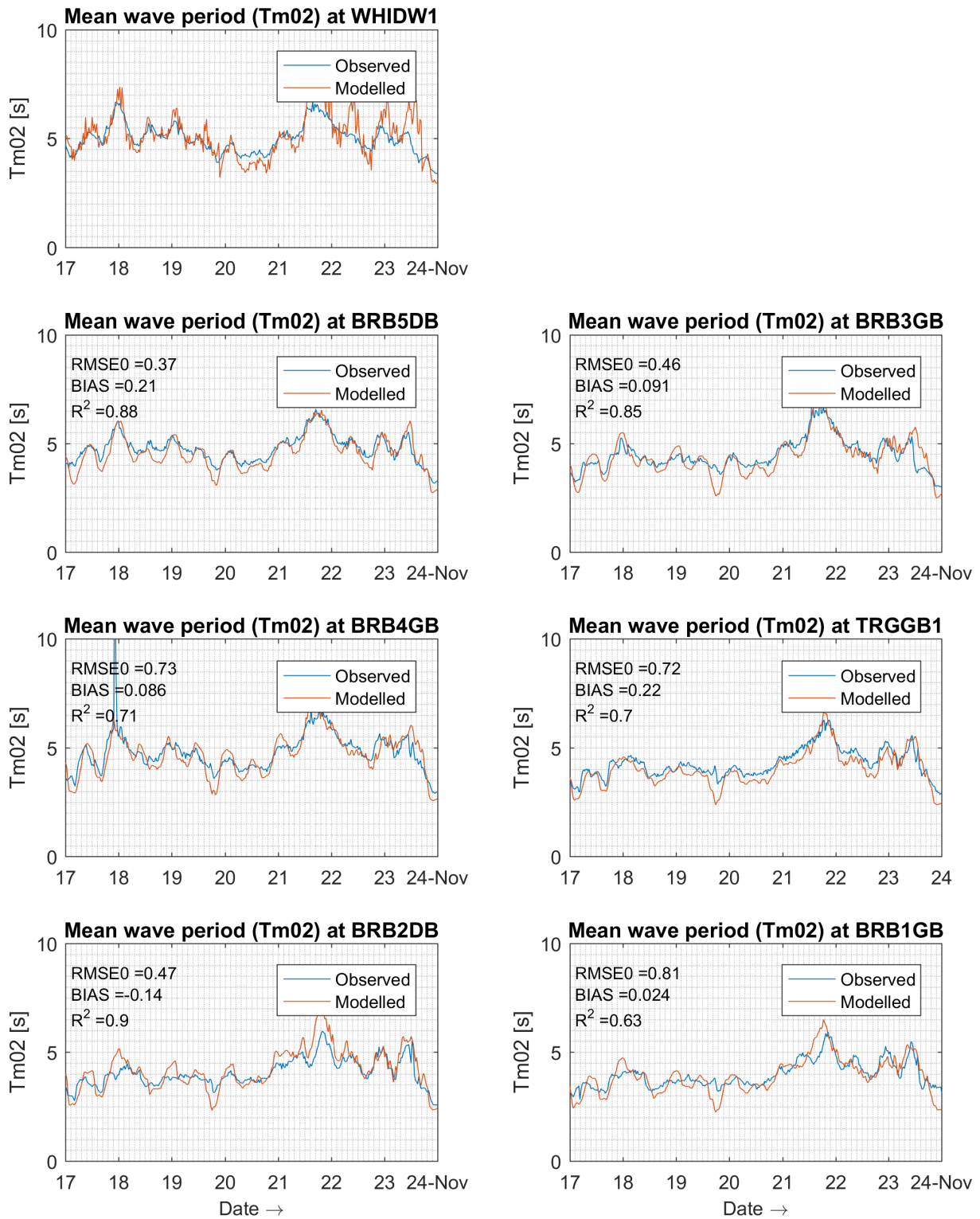


Figure 39 – Comparison of mean wave period between the observed data and modelled results (HSW009I) at measurement stations, coupled with water level and current velocity both but without consideration of energy transfer between frequencies due to accelerating and decelerating currents.



## 5 TEL2TOM

It was mentioned before that the wave transport model and the hydrodynamical model do not require the same quality requirements with respect to the mesh generation. Also, due to the spectral nature of the wave propagation model, it is desirable to be able to reduce the resolution or even to withdraw parts of the domains where the waves will have limited impact on currents and morphology, or when the wave propagation in this part of the domain has no impact on the wave-current interaction in the actual domain of interest. Therefore, it was decided to build a new module that would allow to couple the 2D hydrodynamics model to the wave propagation model, when the models have different meshes.

### 5.1 Method

The module is presented in detail on the Telemac User Conference 2019 (Breugem *et al.*, 2019). A copy of the extended conference paper is added to Appendix A. A brief comprehensive description is given here:

The communication between TELEMAC2D and TOMAWAC goes by exchanging the following variables:

- Water depth, u velocity and v velocity from TELEMAC2D to TOMAWAC
- Significant wave height, peak period, wave force (in x and y direction), wind velocity (in x and y direction), orbital velocity and mean wave direction from TOMAWAC to TELEMAC2D.

In the standard TELEMAC2D – TOMAWAC coupling, both models share the same mesh. Therefore, the coupling is one to one on a nodal base. In the TEL2TOM version, the user has to define for each node of the TOMAWAC model from which node(s) of the TELEMAC2D model the node will receive water depth and velocity components and which weights the nodes get in the summation. The same holds for the communication from the TOMAWAC model back to the TELEMAC2D model. Since the nodes and coefficients are not predefined, this allows for maximum flexibility in the choice of interpolation: e.g. nearest point, linear, inverse distance, ...

For the Scaldis-Coast model a linear interpolation will be used. In this case for the communication from the TELEMAC2D grid to the TOMAWAC grid, for each node of the TOMAWAC grid, the coupling nodes are the three vertices of the enclosing triangle in the TELEMAC2D mesh that contains the TOMAWAC node and the corresponding weights are the barycentric coordinates of the TOMAWAC point related to this TELEMAC2D triangle. The same holds for the communication back from the TOMAWAC grid to the TELEMAC2D grid.

This is illustrated in the figure below with a zoom of the locally high resolution TELEMAC2D grid in blue and the coarser TOMAWAC grid in red, Figure 40. When communication will be sent from TELEMAC2D to TOMAWAC, for node **40230**, the corresponding TELEMAC2D nodes are the vertices of the enclosing triangle: **83223**, **135704** and **226536** (the enclosing triangle is marked in bold blue as well in the figure). The corresponding weights are the barycentric coordinates of point 40230 with respect to the enclosing triangle. The barycentric coordinates  $(\lambda_1, \lambda_2, \lambda_3)$  of any point  $(x, y)$  with respect to any triangle are calculated by:

$$\lambda_1 = \frac{(y_2 - y_3)(x - x_3) + (x_3 - x_2)(y - y_3)}{(y_2 - y_3)(x_1 - x_3) + (x_3 - x_2)(y_1 - y_3)}$$

$$\lambda_2 = \frac{(y_3 - y_1)(x - x_3) + (x_1 - x_3)(y - y_3)}{(y_2 - y_3)(x_1 - x_3) + (x_3 - x_2)(y_1 - y_3)}$$

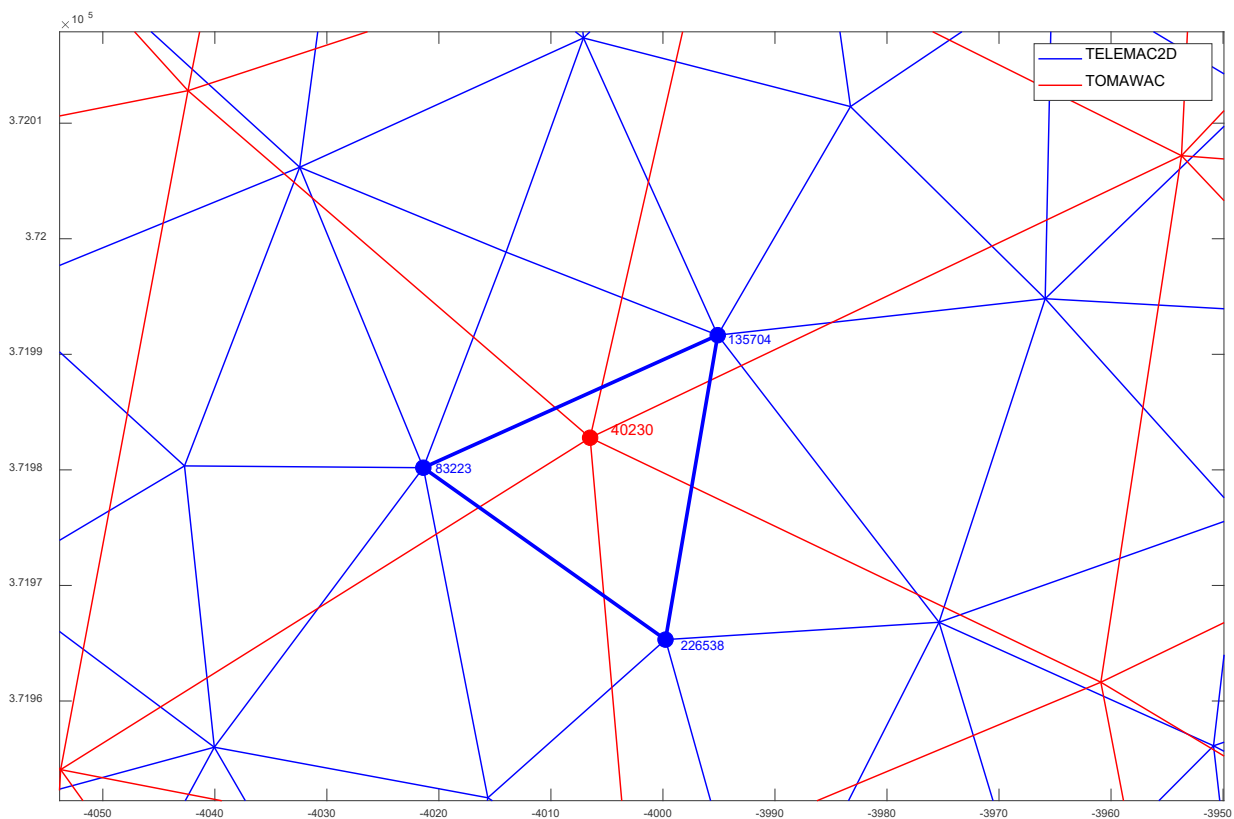
$$\lambda_3 = 1 - \lambda_1 - \lambda_2$$

where the indices 1 to 3 refer to the vertices of the triangle. Finally, in the example below, when communicating a variable from the TELEMAC2D grid to the TOMAWAC grid, for node 40230 this makes:

$$VAR_{40230} = 0.41 VAR_{83223} + 0.43 VAR_{13704} + 0.16 VAR_{226538}$$

The node index numbers and the corresponding weights have to be calculated by the user and stored in the TELEMAC2D and TOMAWAC geo-files as additional parameters, see Appendix A. In Matlab® the function `pointLocation` can be used to find the enclosing triangle and to calculate the corresponding barycentric coordinates. A new Matlab® function, `Telemac_TEL2TOM_coupling.m`, is added to `Telemac_WL_toolbox` on the FHR SVN<sup>2</sup> repository to extend the input Seraphin files of TELEMAC2D and TOMAWAC with the TEL2TOM coupling variables.

Figure 40 – Zoom of the TELEMAC2D and TOMAWAC gid with local node numbers



## 5.2 Schematised coastal model testcase

To test the functionality of the TEL2TOM application, it has been implemented in schematized coastal model for the Belgian coast around Wenduine, Figure 41. A TOMAWAC domain has been considered by offsetting the open boundaries of the TELEMAC2D domain by ~5.0 km. Three different cases have been considered including coarse meshes (minimum grid size 50 m) for TELEMAC2D and TOMAWAC (C1), fine meshes (minimum grid size 25 m) for TELEMAC2D and TOMAWAC (C2), and one case with fine TELEMAC2D mesh and coarse TOMAWAC mesh (C3) as shown in Figure 41. The bathymetry of the schematized case and

<sup>2</sup> [https://wl-subversion.vlaanderen.be/#!/#repoSpNumMod/view/head/Matlab/Telemac\\_WL\\_toolbox/](https://wl-subversion.vlaanderen.be/#!/#repoSpNumMod/view/head/Matlab/Telemac_WL_toolbox/)

the coarse meshes are shown in Figure 41. In the testcases C1 and C2 although the models have a different stretch for the wave and hydrodynamics, inside the boundaries of the TELEMAC-2D model, the grid nodes of the two models coincide. In the C3 testcase, both grids are completely independent.

Table 4 – Simulation cases of the idealized model using the TEL2TOM functionality.

Test case	TELEMAC2D min grid size (m)	TOMAWAC min grid size (m)	TELEMAC2D num. of nodes	TOMAWAC num. of nodes	Simulation time (hours)
C1	50	50	7161	11650	3.35
C2	25	25	24332	33251	10.87
C3	25	50	24332	11650	3.08

The tidal data occurred from assigning a sinusoidal tide along the offshore boundary of the TELEMAC2D domain (indicated with black line in Figure 41). The wave data for TOMAWAC occurred by considering waves with significant wave height equal to 2 m and peak wave period equal to 6.32 s coming from north. In addition, constant wind has also been considered from north with wind velocity  $V_y = -12.24$  m/s. The total simulation time was equal to ~13 days.

Figure 41 – TOMAWAC domain and mesh for test case C1. TELEMAC2D domain area is indicated with black solid line.

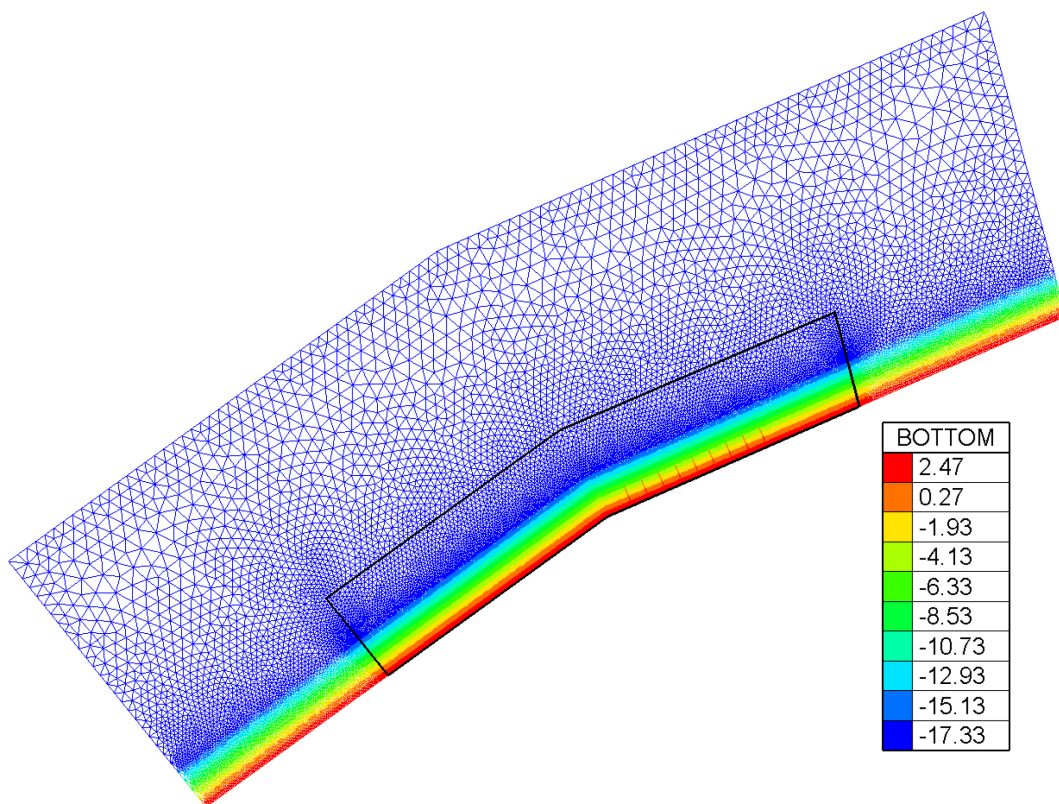


Figure 42 – Snapshot of the velocity magnitude after 12d 16.5h of full simulation of tides and waves for test case C3. Black line corresponds to the cross-shore section considered for comparing the hydrodynamic data for each test case.

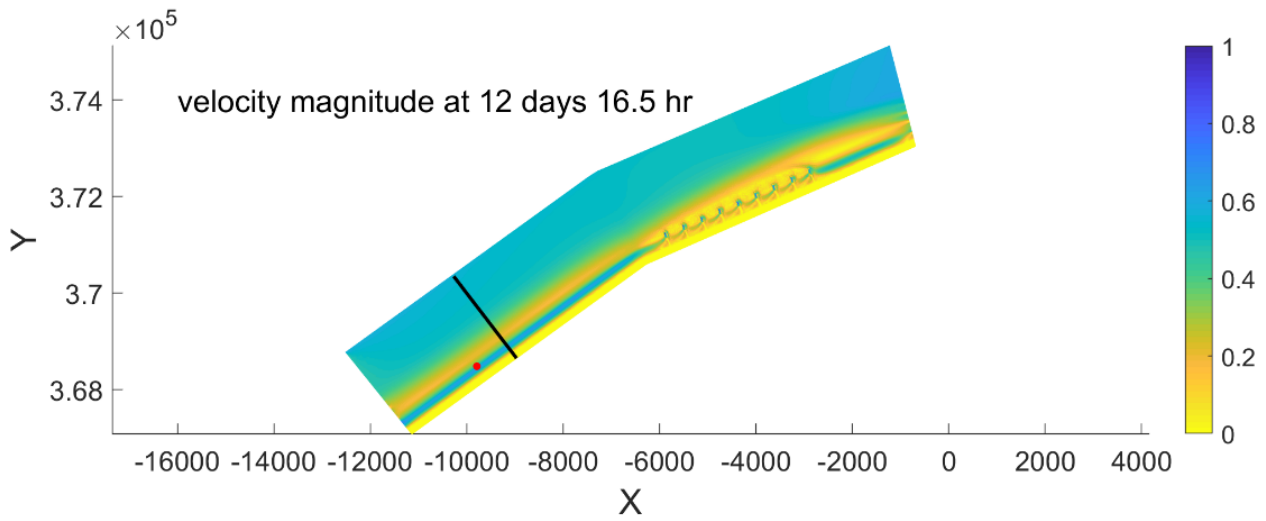
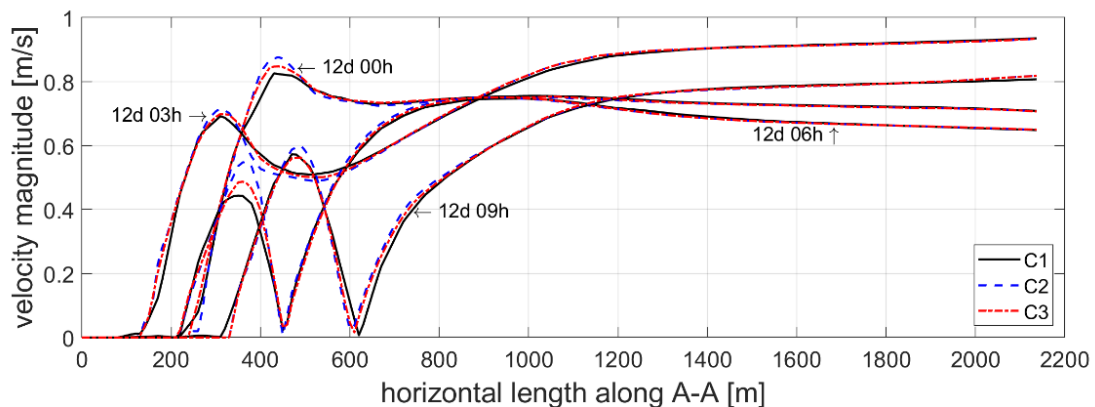


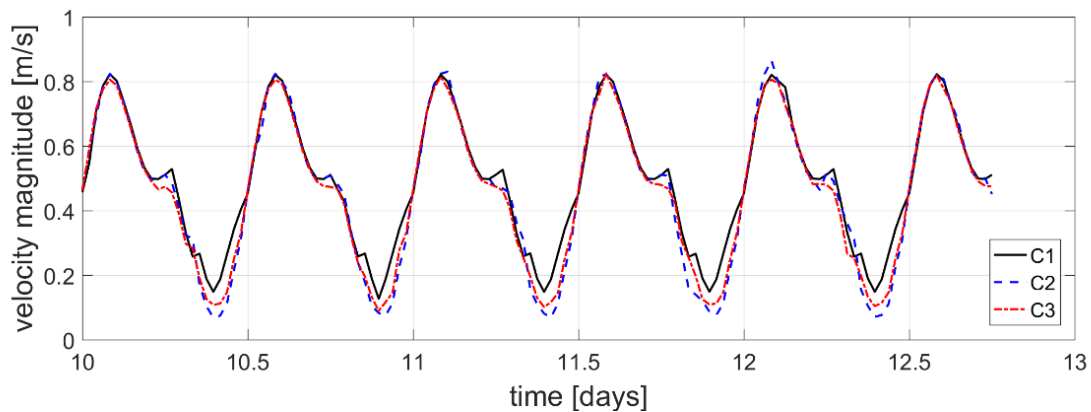
Figure 42 depicts a snapshot of the velocity magnitude in the TELEMAC2D domain. In addition Figure 43 gives cross-shore profiles of the velocity magnitude for test cases C1 (coarse meshes for TELEMAC2D and TOMAWAC), C2 (fine meshes for TELEMAC2D and TOMAWAC) and C3 (fine mesh for TELEMAC2D and coarse mesh for TOMAWAC). It can be concluded that the results occurring with case C3 demonstrate discrepancies smaller than 5% with those of case C2. In this case we can conclude that TEL2TOM functionality works properly and that it can accurately reproduce velocity magnitudes in the nearshore region and thus, the occurring wave-driven currents.

Figure 43 – Cross-shore profiles (section indicated with black solid line in Figure 42) of the velocity magnitude within fractions of one tidal cycle for test cases C1 (black solid line), C2 (blue dashed line) and C3 (red dash-dotted line).



Moreover, based on the above-mentioned profiles, we have taken timeseries of the velocity magnitude in one point of the cross-shore section located 370 m far from the coastal boundary of the TELEMAC2D domain. The results shown in Figure 44 and we can see that TEL2TOM configuration results (case C3) demonstrate much smaller discrepancies with the case C2 of the fine meshes, especially in capturing the troughs and the second harmonic of the timeseries. The bars are clearly captured with almost zero discrepancy.

Figure 44 – Timeseries of velocity magnitude at a specific location 370 m far from the coastal boundary of TELEMAC2D domain) for test cases C1 (black solid line), C2 (blue dashed line) and C3 (red dash-dotted line).



From the above-mentioned analysis, it can be safely concluded that the TEL2TOM functionality can provide accuracy in the hydrodynamic results (wave-driven currents) by considering a much coarser TOMAWAC domain. This can also contribute in significant level of computational speed up (see Table 4). It can be observed that the required time for simulating case C3 is even smaller than the time for case C1. This can be contributed to the fact the CPU time is dependent on the occupancy rate of the used HPC machines, but also with the coarse TOMAWAC grid and the accurate hydrodynamic input of TELEMAC2D, the required number of iterations for the source terms per timestep is low at the same level for the two test cases.

### 5.3 Implementation of TEL2TOM in the Scaldis-Coast model

In Section 4.4.2 the TOMWAC wave model was successfully coupled to the TELEMAC2D model. The models were running on the same mesh, i.e. the high resolution TELEMAC2D model, see Figure 7. In this section, the TEL2TOM module is applied to the Scaldis-Coast model. By omitting the Western and Eastern Scheldt estuary, and locally reducing the grid resolution in the nearshore from 25 m to 50 m, the total number of nodes is reduced from 273 000 to 138 000 nodes and the number of triangular elements from more than 500 000 to nearly 260 000.

In Figure 45 and Figure 46 the coupled Scaldis-Coast modelled significant wave height and mean wave period with and without the use of TEL2TOM are compared. Applying the TEL2TOM approach has no effect on the wave propagation at the measurement stations. However, the computational cost in this case has been reduced by a factor two. Notice that in the offshore parts of the domain, although both grids are not identical, still the resolution is still comparable, see Figure 9 and Figure 10 on page 13. Only at nearshore stations TRGGBG1, BRB2DB and BRB1GB the TELEMAC2D model has a higher resolution than the wave propagation model. Since the application of TEL2TOM has no significant impact on none of the station, one might consider also reduce the grid resolution in the rest of the domain as well. However, this has not been further investigated.

Figure 45 – Comparison of significant wave height for the fully coupled TELEMAC2D-TOMWAC model with (A003) and without TEL2TOM (HSW009)

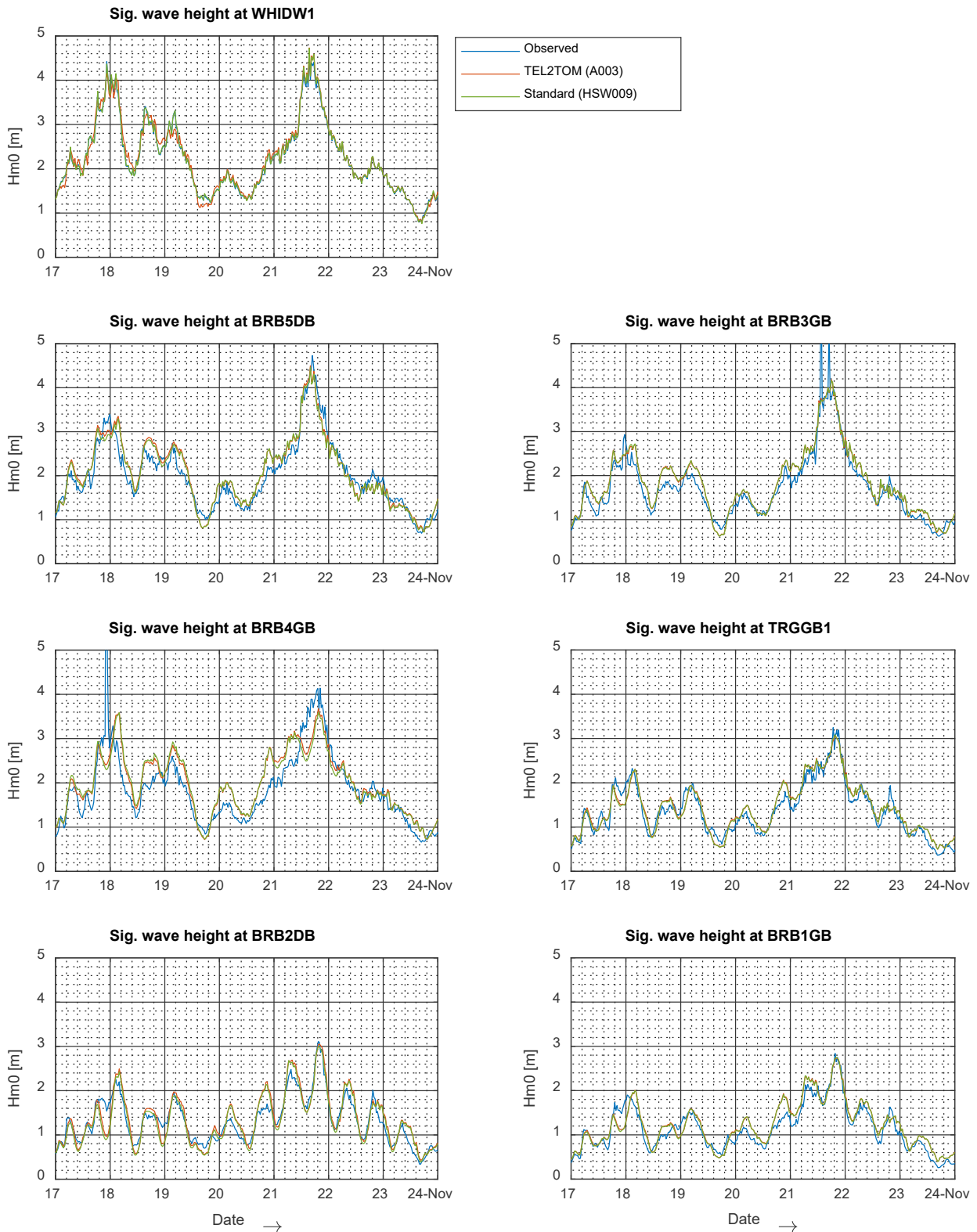
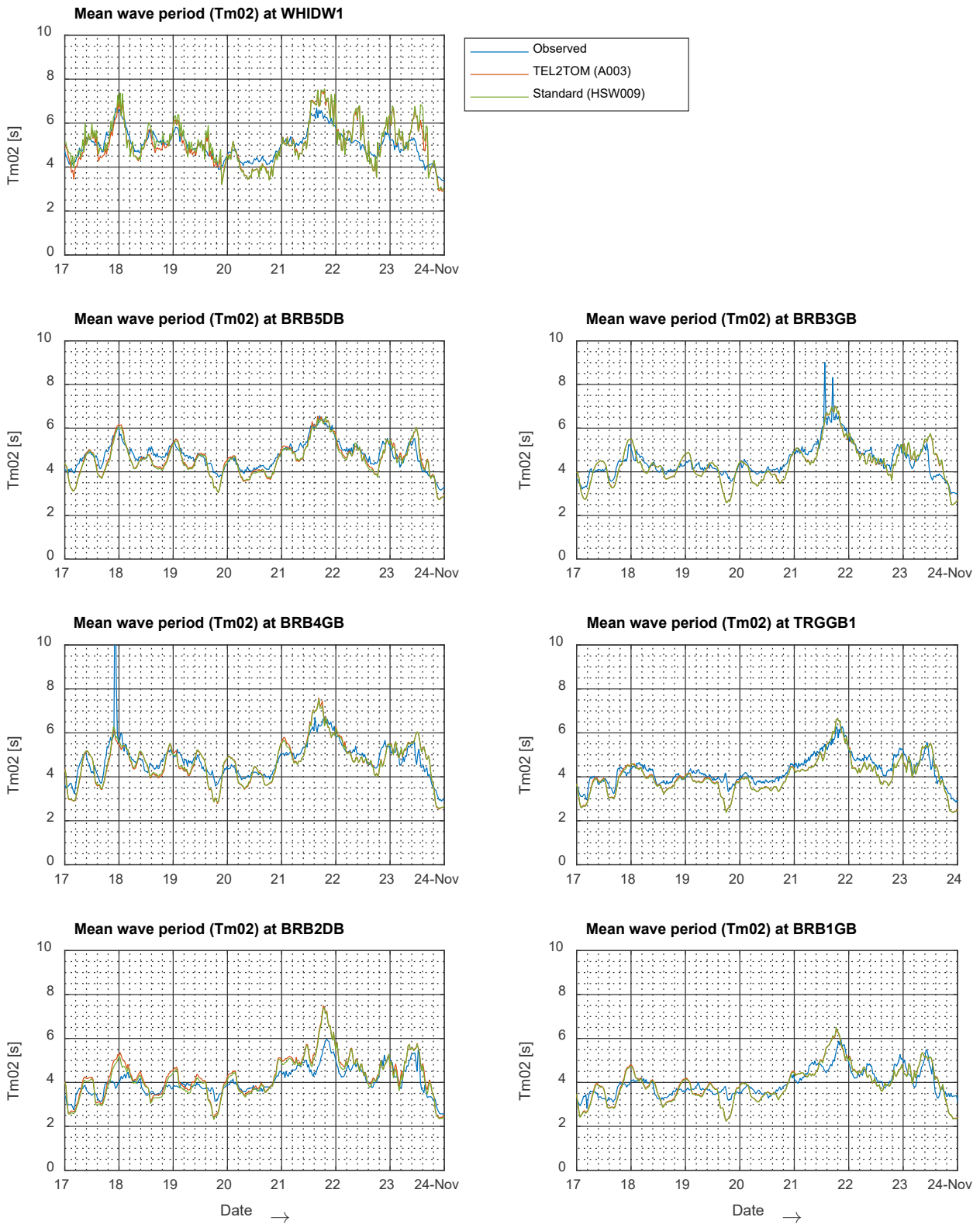


Figure 46 – Comparison of mean wave period for the fully coupled TELEMAC2D-TOMWAC model with (A003) and without TEL2TOM (HSW009). In blue is the observed mean wave period



## 6 Conclusions

An individual TOMAWAC wave model has been developed to simulate waves in the Belgian coastal zone. This model was firstly imposed with wave and wind boundary conditions which were provided both by the Westhinder fixed observation station and ERA5 data respectively and were compared. The space-uniform and space-varying boundary conditions and forcing terms generated quite comparable model results. Due to the relatively higher temporal resolution of the Westhinder station, some observed peaks can be captured by the model more accurately. From the viewpoint of the long-term morphological model a JONSWAP spectrum based on significant wave height, peak wave period and wave direction is preferred. It has been tested and a JONSWAP with boundary direction spreading of two (which is a typical value for a local wind sea) was selected as preferred boundary condition settings.

Besides, the water level is found to be a very important input for TOMAWAC to properly simulate waves in the coastal zone. Therefore, an accurate simulation of waves requires correct water level information which is provided by the hydrodynamic model. The coupling is a two-way coupling, in which the wave model allows the hydrodynamic model to calculate the wave setup and wave induced currents. However, due to some concerns regarding to the results, the influence of the current acceleration on the propagation in frequency space has been ignored.

In the sensitivity tests other options for DEPTH-INDUCED BREAKING DISSIPATION are not observed to give better agreement with observed significant wave height as the original one. Another combined options for WHITE CAPPING DISSIPATION and WIND INPUT shows comparable results.

A new module for coupling the wave and tidal model on non-uniform grids, TEL2TOM, has been developed and successfully applied to the Scaldis-Coast model. The module allows to reduce the grid resolution of the wave model and to exclude those parts of the domain that don't experience significant waves or that don't contribute to the wave propagation in the zone of interest, in this case these are the Eastern Scheldt and the Western Scheldt estuary. By reducing the grid, the computational cost of the coupled model could be reduced up to a factor two. A further optimization is might still be possible by reducing the resolution also in the offshore parts of the domain, but this has not been further investigated so far.

The final versions of the stand-alone and coupled Scaldis-Coast wave propagation models are archived in the Flanders Haudraulics Research SVN repository:

[https://wl-subversion.vlaanderen.be/#!/#repoSpNumMod/view/head/TELEMAC/Scaldis-Kust/15\\_068%20Complex%20Model%20Kustvisie%202021/2\\_WAVEMODELS](https://wl-subversion.vlaanderen.be/#!/#repoSpNumMod/view/head/TELEMAC/Scaldis-Kust/15_068%20Complex%20Model%20Kustvisie%202021/2_WAVEMODELS)  
[https://wl-subversion.vlaanderen.be/#!/#repoSpNumMod/view/head/TELEMAC/Scaldis-Kust/15\\_068%20Complex%20Model%20Kustvisie%202021/2\\_WAVEMODELS](https://wl-subversion.vlaanderen.be/#!/#repoSpNumMod/view/head/TELEMAC/Scaldis-Kust/15_068%20Complex%20Model%20Kustvisie%202021/2_WAVEMODELS).

Three versions of the model are available:

- **TOMAWAC\_W001** – Stand alone TOMAWAC model with spatially uniform water levels, variable in time. One-year run: *representative year* 28/11/2015 - 02/12/2016
- **TOMAWAC-TELEMAC\_A003** – Coupled wave-current interaction model with TEL2TOM coupling, for the validation period 16/11/2015 - 24/11/2015
- **TOMAWAC-TELEMAC\_B002** – Coupled TEL2TOM model for the *representative year* 28/11/2015 - 02/12/2016

The latter one will eventually be coupled to the sediment transport and bed-update model. The meaning of the *representative year* is extensively discussed in the next report (G. Kolokythas *et al.*, 2021b).

## References

**Breugem, W.A.; Fonias, E.; Wang, L.; Bolle, A.; Kolokythas, G.; De Maerschallck, B.** (2019). TEL2TOM: coupling TELEMAC2D and TOMAWAC on arbitrary meshes, *in*: (2019). *XXVIth Telemac-Mascaret User Conference, 15-17 October, Toulouse: proceedings*

**Geuzaine, C.; Remacle, J.-F.** (2009). Gmsh: a three-dimensional finite element mesh generator with built-in pre-and post-processing facilities. *Int. J. Numer. Methods Eng.* 79(11). ISBN 1097-0207 0: 1309–1331. doi:10.1002/nme.2579

**Kolokythas, G.; Fonias, S.; Wang, L.; De Maerschallck, B.; Vanlede, J.; Mostaert, F.** (2021a). Modelling Belgian Coastal zone and Scheldt mouth area: Sub report 12: Scaldis-Coast model - Model setup and validation of the 2D hydrodynamic model. *FHR Reports, 15\_068\_12*. Flanders Hydraulics Research: Antwerp. 113 pp.

**Kolokythas, G.; Fonias, S.; Wang, L.; De Maerschallck, B.; Vanlede, J.; Mostaert, F.** (2021b). Modelling Belgian Coastal zone and Scheldt mouth area: Sub report 14: Scaldis-Coast model - Model setup and validation of the morphodynamic model. *FHR Series, 15\_068\_14*. Flanders Hydraulics Research: Antwerp

**Kolokythas, G.K.; Wang, L.; Fonias, S.; De Maerschallck, B.; Vanlede, J.; Mostaert, F.** (2018). Modelling Belgian Coastal zone and Scheldt mouth area: sub report 6 – Progress report 2. Evaluation of numerical modelling tools and model developments. Version3.0. *FHR reports, 15\_068\_6*. Flanders Hydraulics Research: Antwerp

**Komijani, H.; Ortega, H.; Zhang, Q.** (2016). Opstellen van een hydrodynamische modellen suite TELEMAC-TOMAWAC voor de Broersbank: Leuven



# Appendix A. Paper presented at the TELEMAC User Conference 2019 (TUC 2019)

## TEL2TOM: coupling TELEMAC and TOMAWAC on arbitrary meshes

WA Breugem<sup>1</sup>, E Fonias<sup>1,2</sup>, L Wang<sup>1,2</sup>, A Bolle<sup>1</sup>  
<sup>1</sup>International Marine and Dredging Consultants  
Antwerp, Belgium  
[abr@imdc.be](mailto:abr@imdc.be)

G Kolokythas<sup>2</sup>, B De Maerschalck<sup>2</sup>  
<sup>2</sup>Flanders Hydraulics Research  
Antwerp, Belgium

*Abstract*— In this paper, a novel approach is presented to perform coupled simulations of TELEMAC and TOMAWAC. In this approach different meshes are considered: a dense mesh for TELEMAC in order to manage fast and accurate resolution of the flow and a much coarser for TOMAWAC in order to exclude bays or rivers and increase the computational speed of the wave model. The communication of flow variables is implemented by means of linear interpolation. Two applications are presented utilizing the TEL2TOM functionality: a schematic case through the Littoral tutorial and a real world application in the Belgian coast. The simulation of wave-current interaction in the Belgian coast application using TEL2TOM functionality was approximately 2 times faster compared to a simulation using the same mesh for TELEMAC and TOMAWAC, without losing model accuracy in the regions of interest.

### Introduction

Currently, TELEMAC and TOMAWAC use the same computational meshes for performing coupled simulations of waves and currents. However, it would be advantageous to be able to use different meshes in TELEMAC and TOMAWAC. Then it would be possible to use a different spatial resolution in each models, which could lead to a substantial speed up in case a coarser mesh is used in TOMAWAC than in TELEMAC. Additionally it would be possible to use domains with different spatial extents. This could for example be used to exclude bays or rivers from TOMAWAC, where little wave action is expected. Another use would be to use a larger domain for TOMAWAC than for TELEMAC, in order to have a smoothly varying wave field at the boundary of the TELEMAC domain, which is beneficial when performing simulations of wave-current interaction. The preceding examples show that a more flexible coupling method is needed, that permits the use of interpolation as well as extrapolation. Moreover, in order to have fast calculation times, the coupling should be fully parallel and have little computational overhead.

The objective of the present paper is to present a novel, flexible module coupling framework developed within TELEMAC, which is applied for the coupling of TELEMAC2D and TOMAWAC on arbitrary grids. To this end, examples of the application of this framework in a simplified and a real world test case are presented.

## Description of the code development

### Model coupling framework

Presently, already some module coupling frameworks exist such as MCT [1] or OASIS, which served as inspiration for the present code development. However, it was chosen to use a custom module coupler, specially designed for TELEMAC, rather than a general purpose model coupler. In this way maximum advantage of TELEMAC could be taken, while minimizing the changes needed to the code.

The coupling module consists of a main module, `couple_mod.F`, whose objectives is to exchange data in parallel between two models, which may have different meshes as well as different domain compositions (though both are using the same number of processors). The module is intended to be as flexible as possible, allowing the communication of a varying number of variables between both models. Also, the module is designed to allow interpolation and extrapolation of variables in a flexible way, based on weight factors and matching node numbers specified by the user in the geometry files of each coupled model. In this way different interpolation methods can easily be defined. For example:

- Nearest neighbour interpolation can be defined, by using a single node number of the closest node, with a weight factor of one. This type of interpolation can also be used for extrapolation (for data on nodes outside of the mesh).
- Bilinear interpolation (on a triangular mesh), can be obtained using the three nodes of a triangle in the mesh of the sender with the weights for the three points determined according to the distance of the node to the three other nodes.
- Other forms of interpolation (e.g. inverse distance interpolation or conservative interpolation) can be used using a larger number of nodes from which information is received.

It was chosen to let the user provide the information about interpolation and extrapolation in order to allow maximum flexibility. Many optimized routines are available in for example Python or Matlab to determine these coefficients efficiently during pre-processing.

The general methodology of the coupling is as follows:

- In a model receiving information, the following information is defined for each node of the mesh:
  - Global node number(s) in the sending model from which information is received at a point. The number of nodes from which information is received can be varied, but should be identical for all points in the mesh. Hence one can specify for example to use information from three nodes (e.g for linear interpolation) when sending information from TELEMAC to TOMAWAC, but only use information from one node (for nearest neighbour interpolation), when sending information back from TOMAWAC to TELEMAC. However in this example, each node in TOMAWAC needs to receive information from three different nodes in TOMAWAC. In case one wants to use information from less nodes for some specific locations (e.g. to mix nearest neighbour and linear interpolation), one has to specify some dummy node numbers, in combination with a weighting factor (described below) of zero. In case a node does not receive any information from the sending model, the number of the node from which information is received is set to zero. In that case, a default value (typically zero) is applied as received information.
  - Weighting factors need to be defined for each nodes of the sending model that transfer information to a node of the receiving model. The sum of these weights should be one, which is checked by the code. In nearest neighbour interpolation the weighting factor is one, in a linear interpolation the weighting factors are the barycentric coordinates (in Matlab the function 'pointLocation' can be called to calculate the node numbers and barycentric coordinates).

- The information of the nodes from which information is received and their corresponding weights is used to determine the parallel communication pattern between the two models.
- Each coupling step, information is exchanged in parallel between the two models using the weighting factors in order to do the user defined interpolation.

The module consists of the following subroutines:

**INIT\_COUPLE:** Initialisation of the coupling module, which allocates memory for the data structures used in the coupling.

**ADD\_SENDER:** Every model that sends information to another module calls this routine once, in order to let the coupler know that it will send information to another model. In this routine, some memory allocations are done, and the list of global node numbers of the sender is send to all processes of the receiving model.

**ADD\_RECEIVER:** Every model that receives information will call this module once. First the list of global node numbers is received from the sending model. Then, the node numbers of the sending model from which information is expected are read from the geometry file (in a separate subroutine **READ\_RECV**). Also the weighting factors related to these are read. The list of node numbers from which information is expected, in combination with the received global node numbers of the sending model are used to determine how to communicate data from the sender to the receiver by making lists of data to send, and data to receive, i.e. a mapping between the sender and the receiver. The lists of node numbers from which information is expected, is communicated to the right processor of the sender model.

**SEND\_COUPLE:** Every coupling time step, this routine is called by the sender. This routine sends the necessary variables to the correct process of the receiver, using the mapping defined in **ADD\_RECEIVER**.

**RECEIVE\_COUPLE:** Every coupling time step, this routine is called by the receiver. It receives the data send by **SEND\_COUPLE**, and performs the interpolation using the stored weights.

**END\_COUPLE:** Deallocation of the memory used for the coupling.

### Application for coupling TELEMAC and TOMAWAC

The implementation is made in the cookiecuttershark branch, which is based on TELEMAC v7p2r1. In order to apply the coupling routine for coupling TELEMAC and TOMAWAC, the following modifications of the code are made:

Two new variables are added (type `bief_obj`; object of objects), called **TEL2TOM** and **TOM2TEL**, which contain pointers to the coupled variables. These pointers are set using the subroutine **ADD\_BLO**, in the subroutines **POINT\_TELEMAC2D** and **POINT\_TOMAWAC**. The number of variables being communicated is stored in the variables **NVARTOM2TEL** and **NVARTEL2TOM**.

The variables that can currently be communicated are:

- Water depth, u velocity and v velocity (from TELEMAC to TOMAWAC)
- Significant wave height, peak period, wave force (in x and y direction), wind velocity (in x and y direction), orbital velocity and mean wave direction (from TOMAWAC to TELEMAC).

The variables that are communicated (for example water depth), need to be defined separately in both TELEMAC and TOMAWAC, as they now are on different meshes.

Each model (TELEMAC and TOMAWAC) already had a separate variable defining the mesh (defined respectively in `declarations_telemac2d.f` and `declarations_tomawac.f`). Only in the subroutine `homere_telemac2d.f`, where both variables are used, it was necessary to define an alias for the TOMAWAC mesh. However, there is one variable related to the mesh in parallel, which is not in the variable **MESH**, which is the variable **NPTIR**. Therefore, it is necessary to update this variable by calling the subroutine **GET\_MESH\_NPTIR** in the subroutines **WAC** and **TELEMAC2D**.

Note also that PARTEL splits by default each geometry file, separately into different subdomains. Hence no changes to PARTEL or the PYTHON scripts were necessary for the coupling of TELEMAC and TOMAWAC with different meshes. Also GRETEL correctly merges the meshes in case different meshes are used. Hence changes to GRETEL were also not needed.

Some function calls to the coupling routines need to be made. The routines ADD\_SENDER and ADD\_RECEIVER are called twice in HOMERE\_TELEMAC2D, once for sending information from TELEMAC to TOMAWAC and once for sending information from TOMAWAC to TELEMAC. The functions SEND\_COUPLE and RECEIVE\_COUPLE are used to exchange data between the modules during the initialisation and during every coupling time step.

Finally, some default values were needed in the initialisation (for example the radiation stress was set to zero in the initialisation).

## Limitations

Presently there are some limitations, when using the coupling:

- The coupling only works in parallel (using more than one processor for each coupled model).
- The number of processors needs to be the same for each coupled model.
- No special treatment of dry nodes is currently implemented.
- No special interpolation method is used for interpolating wave directions.

The coupling is currently only implemented between TELEMAC2D and TOMAWAC, not yet between TELEMAC3D and TOMAWAC. In principle, this extension to TELEMAC3D is straightforward, especially when the exchange is limited to two-dimensional variables (as is the case in TELEMAC v7p2). In that case, the changes that need to be made are limited to a number of function calls to the coupling routines within TOMAWAC-3D, and the definition of some separate variables in TELEMAC3D for the coupling. However, the flexibility of the coupling module, also allows three-dimensional information to be send, for example by specifying each vertical layer as a separate two-dimensional variable, defined as a pointer to a part of a three-dimensional variable.

## Test Cases

### Schematic test (Littoral)

In order to test the TEL2TOM functionality, an existing TELEMAC test (*littoral*) was executed. In this test case, three-way coupling between TELEMAC2D, TOMAWAC and SISYPHE is tested. The test case describes a beach with a slope of 1:5, on which waves (significant wave height 1.0 m, peak period 8.0 s, wave direction 30<sup>o</sup>) propagate toward the coast. The waves generate a longshore current in the breaker zone, which on its turn generates sediment transport (calculated using the equation of Bijker), which can lead to changes in the bed elevation. Note hereby that SISYPHE uses the same mesh as TELEMAC2D. Further note that the water depth is communicated from TELEMAC2D to TOMAWAC. Any change in the bed level calculated in SISYPHE is implicitly included in this variable.

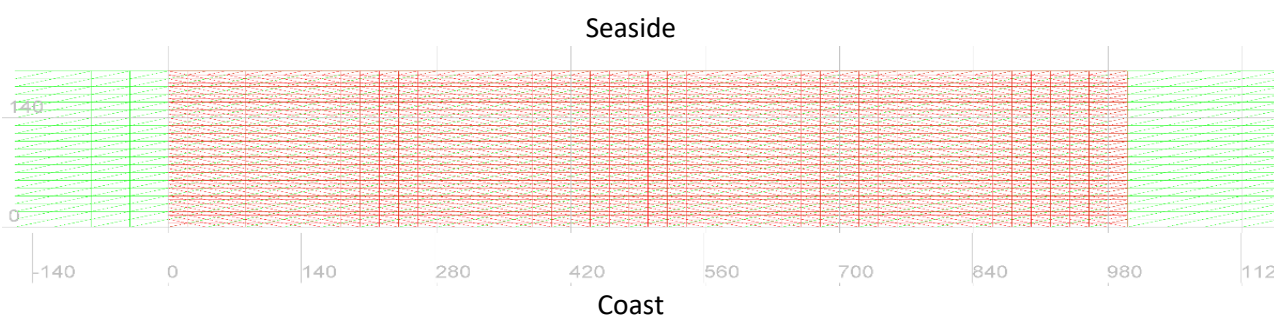
On the lateral boundaries of the TELEMAC model, a custom FORTRAN code is used to calculate the lateral velocity from the radiation stresses calculated in TOMAWAC (the technique is described below). Note that in principle, it would have been possible to use the Neumann boundary conditions developed by Breugem et al (2018) [2] to calculate the velocity at the boundary, but it was chosen to keep the test case as close as possible to the original one. For the test case, two different setups were tested (Figure 47):

- Settings comparable to the original test case setup (further referred to as *fine*). The same mesh is used for TELEMAC as for TOMAWAC. In order to have a fully developed wave profile, in this case,

the wave spectra at the centreline of the model are applied to the lateral boundaries using a custom FORTRAN subroutine. The settings for TEL2TOM were set such that data was directly applied at each node in the other model.

- A setup with different meshes (further referred to as *coarse*). The mesh for TELEMAC and SISYPHE was kept the same as in the original test case. However, the mesh for TOMAWAC was coarsened by a factor 2. Further, the TOMAWAC domain was extended laterally (Figure 47). On the lateral boundaries, wave boundary conditions with a wave height of 1.0 m were applied. The part of the TOMAWAC outside the TELEMAC mesh was used, to make sure that a correctly developed wave profile forms at the lateral boundary of the TELEMAC model. Hence the custom FORTRAN code for transferring wave conditions from the centre to the boundary was not used any longer. The weights for information of exchange were set such that linear interpolation was used to exchange information between the two meshes. In the part of the TOMAWAC domain outside of the TELEMAC domain, extrapolation was used using the nearest neighbour method for flow velocities and water depths.

Figure 47 – Mesh for TELEMAC and SIYPHE (red) and TOMAWAC (green) for the littoral drift test case (tutorial test case).



Each case was run on two parallel processors (the minimum for TEL2TOM). The results of the first case (same mesh for TELEMAC and TOMAWAC) were first compared with the results of the original test case in TELEMAC v7p3. The results at the end of the case were similar between the case in v7p3 and the case using TEL2TOM (not shown), but some small changes existed in the spin-up period, because of changes in the application of the boundary conditions in TOMAWAC between v7p2 and v7p3. Note that the comparison was done using v7p3 rather than v7p2, because this version contains some important bugfixes for three-way coupling. These bugfixes are also applied in the TEL2TOM code.

The results of the *fine* and the *coarse* setups (using TEL2TOM) are shown in Figure 48 to Figure 50 for the wave height, velocity profile and free surface elevation on a profile perpendicular to the beach in the centre of the domain. In general the results are very similar. The wave height has the same maximum in both cases, but the profile is slightly different around the breaker zone, due to the differences in mesh resolution for TOMAWAC. This leads to a wave driven current, with a slightly broader profile (but the same peak velocity) as in the case with the same meshes. Also the calculated wave setup is very similar between the two models. With respect to the calculation time, the coarse case with two different meshes is about two times faster than the original case.

Hence this test case shows that using TEL2TOM, similar results are obtained as using the same mesh for TELEMAC and TOMAWAC, but that substantial calculation time, as well as storage space for output can be saved. Also this test case shows that using extrapolation, a more flexible modelling approach is possible, which can be for example advantageous in determining boundary conditions for TOMAWAC on the boundary of a TELEMAC domain.

Figure 48 – Calculated significant wave height on a transect perpendicular to the beach for the fine and the coarse model.

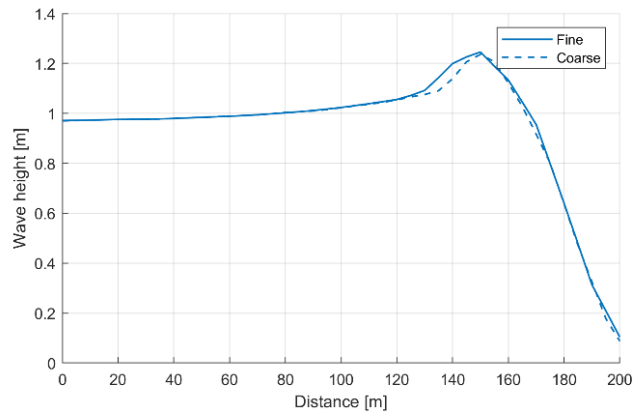


Figure 49 – Calculated velocity profile on a transect perpendicular to the beach for the fine and the coarse model.

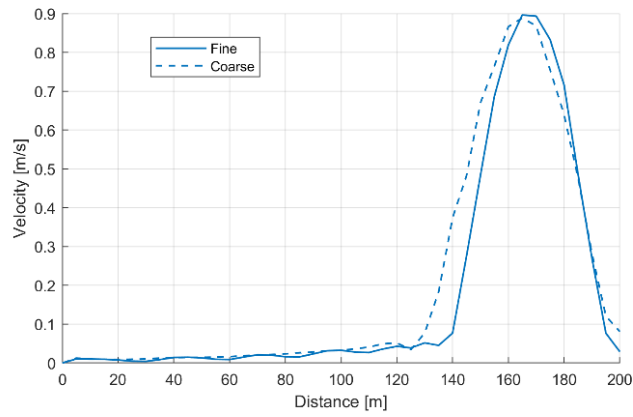
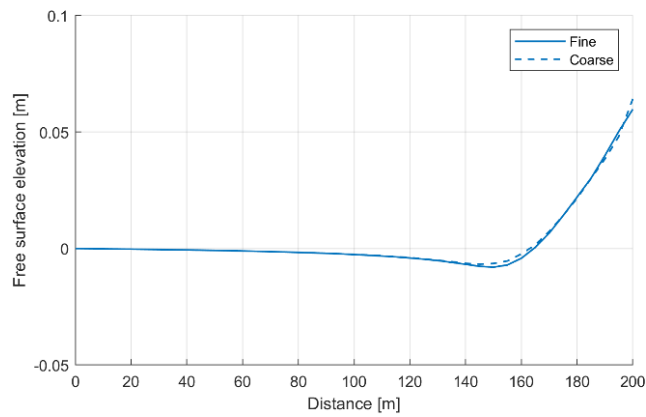


Figure 50 – Calculated elevation of the free surface on a transect perpendicular to the beach for the fine and the coarse model.

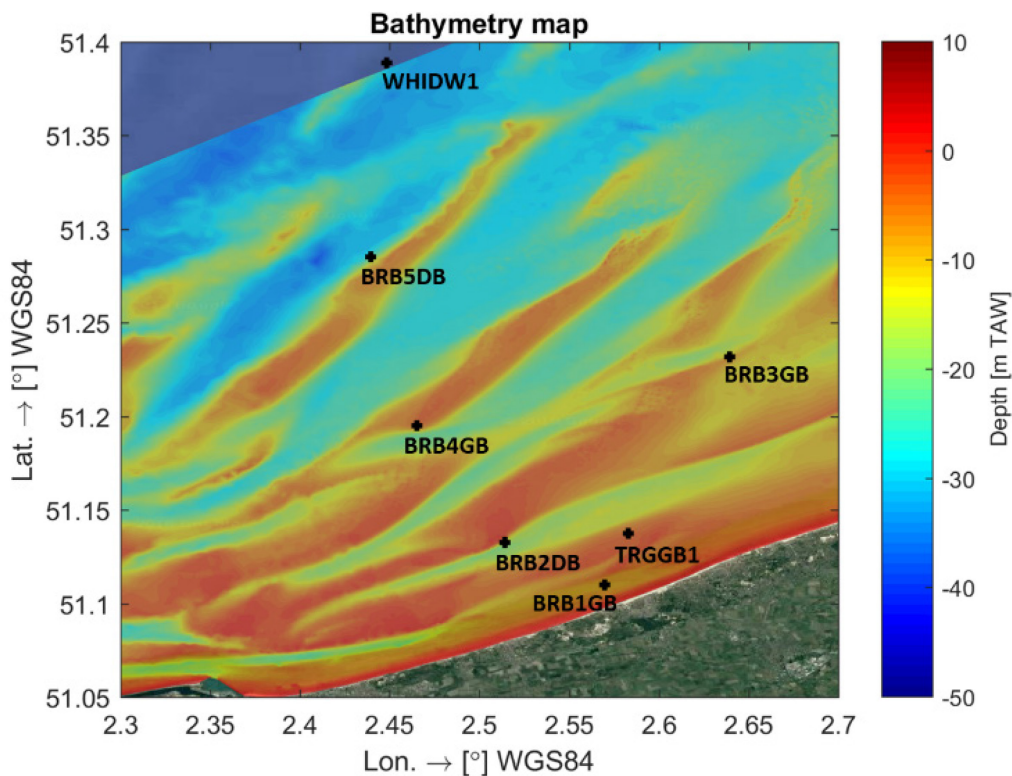


### Real world case (Belgian coast)

The TEL2TOM functionality has also been implemented within the Scaldis-Coast model for simulating tidal flow, wave flow and sediment transport within the Belgian coast. The computational meshes for TELEMAC2D and TOMAWAC are presented in Figure 52. In this application, both TELEMAC2D and TOMAWAC have the same offshore boundary, but within the TOMAWAC domain the inner ports and the Eastern Scheldt and Western Scheldt regions have been excluded in order to reduce number of triangles. Furthermore, the minimum resolution of TOMAWAC is substantially coarser (using elements of 50 m in the coast) than the resolution of the TELEMAC2D mesh (using elements of 25 m in the coastal zone). This resulted in the reduction of the number of nodes for TOMAWAC down to 137,752 from the initial number of 258,390 (46.6% reduction). Linear interpolation is used for exchanging information between TELEMAC and TOMAWAC. The reduction of the number of nodes in TOMAWAC was desired, because TOMAWAC is the bottle neck with respect to the calculation time. Reducing the calculation time, long term morphodynamic calculations become feasible.

The coupled model has been simulated for a period of 8 days starting from 16 Nov 2015 and the boundary conditions for the waves came from Westhinder station (code name WHIDW1, Figure 51). The model results are compared with the dataset collected at stationary measurement points in the Broersbank project (Komijani *et al.* [3]).

Figure 51 – Locations of the field measurement stations of the Broersbank project (Komijani *et al.* [3]).



The TEL2TOM model results are given in Figure 53 and Figure 54 in terms of significant wave height and mean period, respectively. The results demonstrate a very good agreement with the observations (comparable as the results obtained using the same mesh for TELEMAC and TOMAWAC, not shown). However, the simulation time is reduced significantly, more or less by a factor 2.

Figure 52 – Computational domains and meshes for TOMAWAC (upper figure) and TELEMAC2D (lower figure) for the TEL2TOM simulation of the Scaldis-Coast model.

---

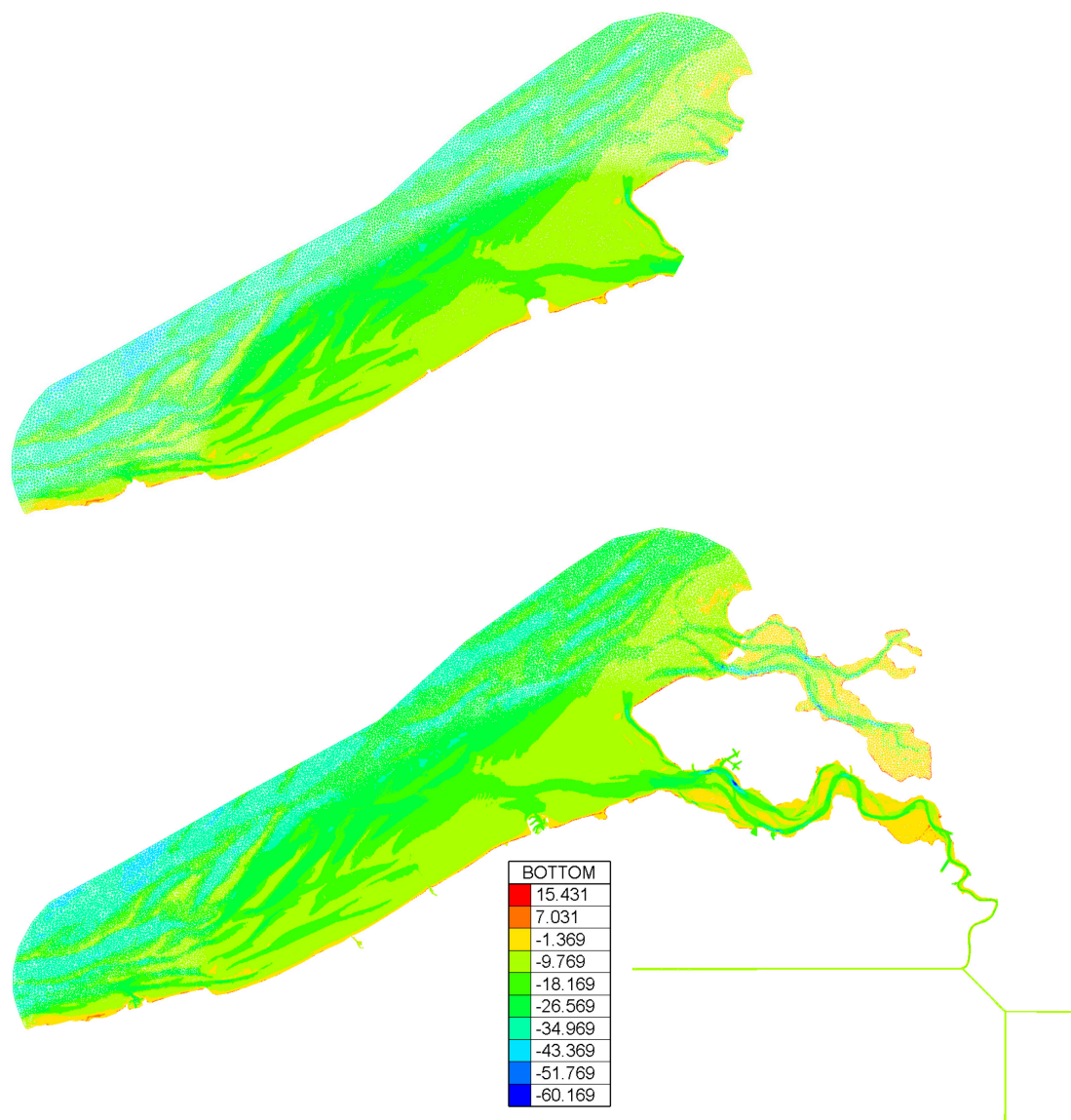


Figure 53 – Comparison of significant wave height between the observed data and modelled results at measurement stations, for a coupled TELEMAC2D-TOMAWAC case using TEL2TOM with a coarser TOMAWAC mesh.

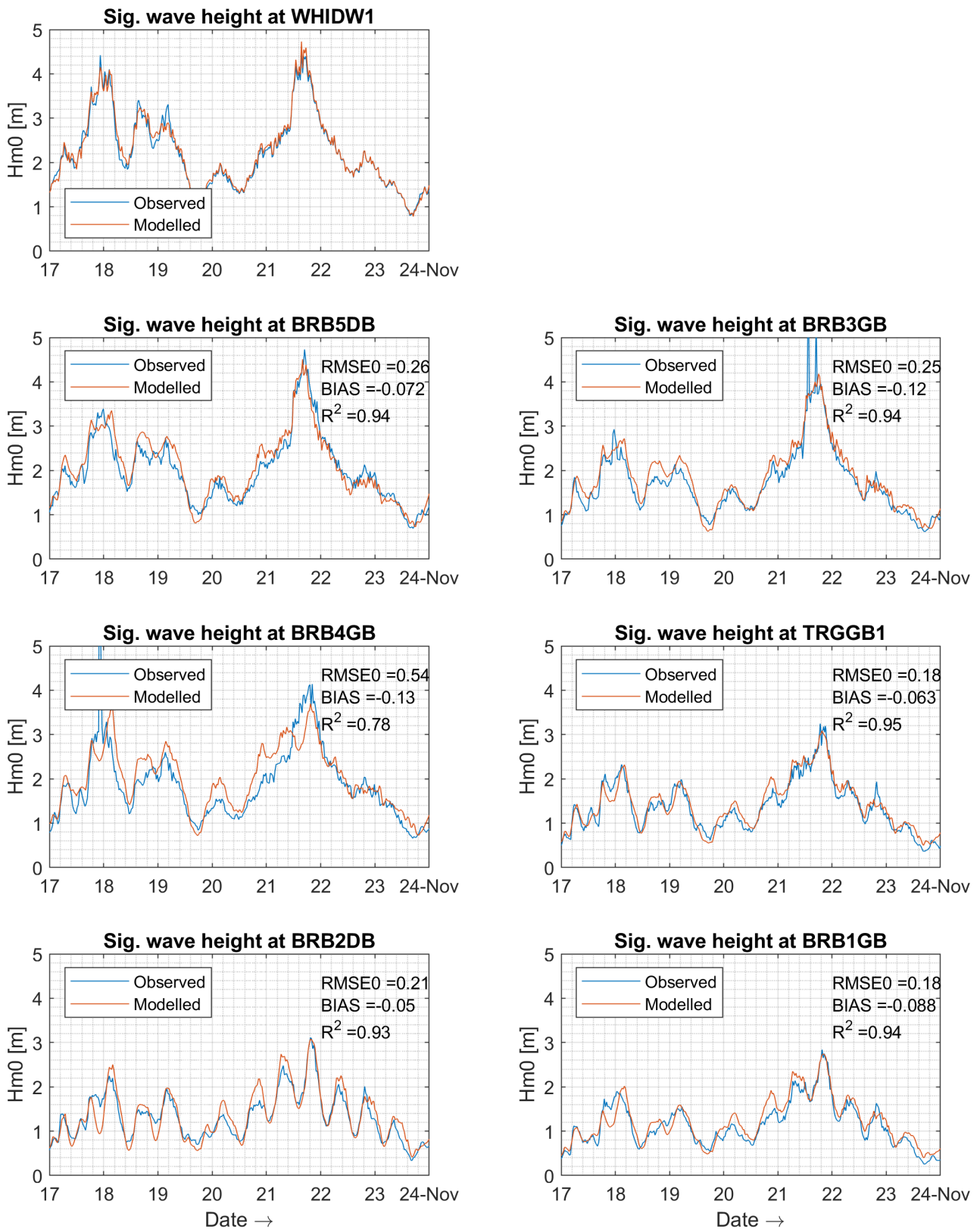
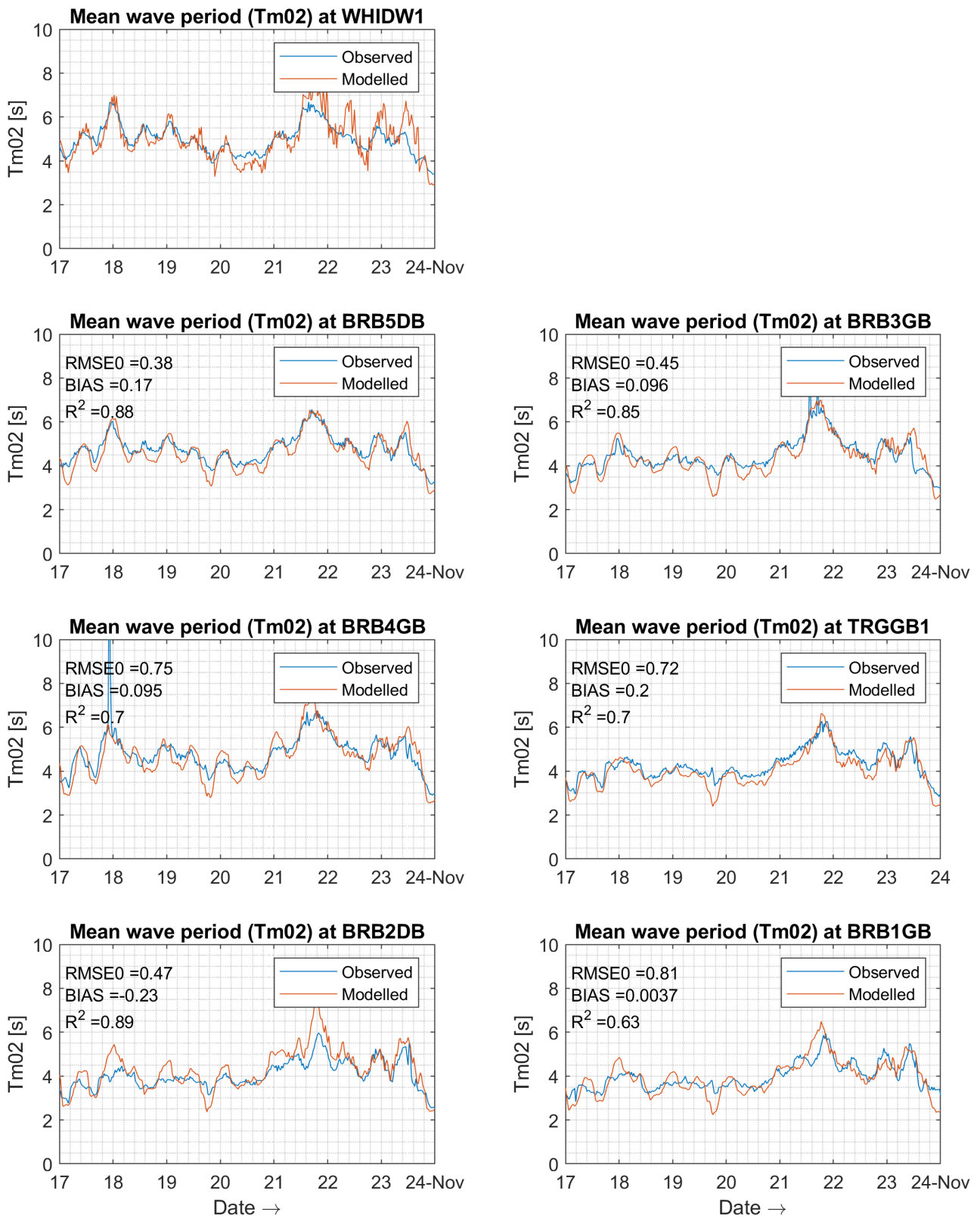


Figure 54 – Comparison of mean wave period between the observed data and modelled results at measurement stations, for coupled a TELEMAC2D-TOMAWAC case using TEL2TOM with a coarser TOMAWAC mesh.



## User Manual

In order to use different meshes for TELEMAC and TOMAWAC do the following:

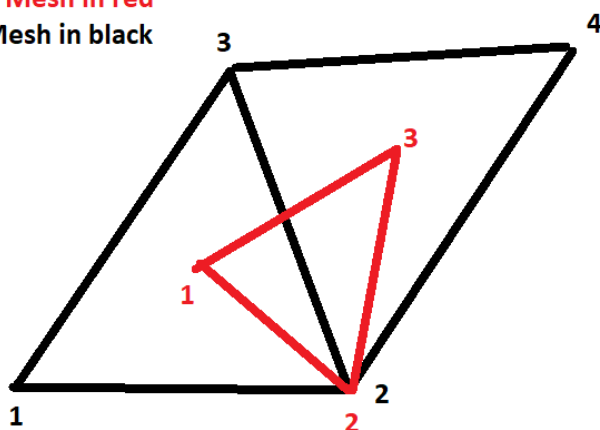
- 1.) Make separate GEOMETRY FILES for TELEMAC and TOMAWAC (with a different mesh). Add these to the .cas files of TELEMAC and TOMAWAC.
- 2.) Add to the GEOMETRY file for TOMAWAC the following variables:
  - a. TEL2TOM01: This variable contains for each node in the TOMAWAC mesh the number of the first node in TELEMAC from which TOMAWAC receives information. In case the node does not need to receive information, set this number to zero.
  - b. TEL2TOMWTS01. The weight factor applied to the information received from the node specified in TEL2TOM01.
  - c. Optionally add information from additional nodes in variables TEL2TOM02 to TEL2TOMNN, where NN is the number of nodes from which information is received.
  - d. For each of these additional variables TEL2TOM02 to TEL2TOMNN add the corresponding weights TEL2TOMWTS02 to TEL2TOMWTSNN. For each receiving node, the sum of the weights of the sending nodes must be equal to one.

A schematic example of this procedure, for a simple mesh consisting of one TOMAWAC element and two TELEMAC elements, is shown in Figure 55.

- 3.) Add the following variables to the GEOMETRY file for TELEMAC:
  - a. TOM2TEL01 to TOM2TELNN: with the node number of the node in TOMAWAC from which TELEMAC receives information, for each TELEMAC node. The working is similar as for TEL2TOM, as explained above.
  - b. TOM2TELWTS01 to TOM2TELWTSNN: the corresponding weights for sending information from TOMAWAC to TELEMAC.
- 4.) Specify the keyword PARALLEL PROCESSORS in the .cas files for TELEMAC and TOMAWAC. Use the same number of processors in both models. The minimum number of processors that can be used is currently 2.

Figure 55 – Example showing the numbering convention for linear interpolation on a simple mesh when sending information from TELEMAC to TOMAWAC.

**TOMAWAC Mesh in red**  
**TELEMAC Mesh in black**



**TEL2TOM01 = 1,1,2**  
**TEL2TOM02 = 2,2,3**  
**TEL2TOM03 = 3,3,4**  
**TEL2TOM01WTS = 0.33,0.33,0.34**  
**TEL2TOM02WTS = 0.00,1.00,0.00**  
**TEL2TOM03WTS = 0.33,0.33,0.34**

The TOMAWAC mesh is shown in red, the TELEMAC mesh in black. Linear interpolation is used, using three nodes in TELEMAC to get information for one node in TOMAWAC. The variables added to the TOMAWAC are shown in red for each different node. In this example, node 1 in TOMAWAC received information from node 1, 2 and 3 in TELEMAC. The weights are each approximately 0.33 (as the TOMAWAC node is in the centre of the TELEMAC node). Node 2 in TOMAWAC also receives information from node 1, 2 and 3 in TELEMAC. However, because this node coincides with node 2 in TELEMAC, the node for this weight is 1.0, whereas the weight for information coming from the other nodes is 0.0.

## Summary and Conclusions

In this paper, the TEL2TOM functionality has been presented. Through this novel approach, TELEMAC and TOMAWAC meshes and domains can be different and TOMAWAC mesh can be coarser. The TEL2TOM has been firstly applied in a schematic case through the Littoral tutorial and then in a real world application within the Belgian coast using the Scaldis-Coast model for tidal flow and waves. The use of TEL2TOM resulted in significant computational speed-up (to a factor of 2) while showing similar accuracy against field measurements for wave in the Belgian coast.

## References

Larson, Jay, Robert Jacob, and Everest Ong. "The model coupling toolkit: a new Fortran90 toolkit for building multiphysics parallel coupled models." *The International Journal of High Performance Computing Applications* 19.3 (2005): 277-292.

Breugem, Alexander, Efstratios Fonias, Li Wang, Annelies Bolle, Gerasimos Kolokythas, and Bart De Maerschalck. "Neumann (Water Level Gradient) Boundaries in TELEMAC 2D and Their Application to Wave-Current Interaction," 111–16. Norwich, United Kingdom, 2018. <https://doi.org/10.14465/2018.tucxxv.nrw>.

H. Komijani, H. Ortega and Q. Zhang, "Opstellen van een hydrodynamische modellen suite TELEMAC-TOMAWAC voor de Broersbank: Leuven", 2016

DEPARTMENT **MOBILITY & PUBLIC WORKS**  
Flanders hydraulics Research

Berchemlei 115, 2140 Antwerp

T +32 (0)3 224 60 35

F +32 (0)3 224 60 36

[waterbouwkundiglabo@vlaanderen.be](mailto:waterbouwkundiglabo@vlaanderen.be)

[www.flandershydraulicsresearch.be](http://www.flandershydraulicsresearch.be)